Title

Dynamic Analysis of Large Linear Structure-Foundation Systems with Local Nonlinearities

Permalink

Author

Ibrahimbegovic, Adnan

Publication Date

1989-06-01

DYNAMIC ANALYSIS OF LARGE LINEAR STRUCTURE-FOUNDATION SYSTEMS WITH LOCAL NONLINEARITIES

By:

ADNAN IBRAHIMBEGOVIC

Faculty Investigator:

EDWARD L. WILSON

Dynamic Analysis of Large Linear Structure-Foundation Systems with Local Nonlinearities

Abstract

The general framework for dynamic analysis of the structure-foundation systems with inelastic constitutive equations is presented in this work. The analysis is based on added motion approach, which is justified by the small displacement gradient theory we are confined to. Motivated by the sound earthquake-resistant design philosophy, the general formulation is specialized to account for local, predetermined nonlinearities in large linear structural systems.

A new model for dynamic frictional contact analysis is fitted within the proposed framework as a model problem for local nonlinearity. As opposed to the existing models for the dynamic frictional contact, here presented model accommodates both dynamic and quasi-static problems.

The consistent reduced representation of the linear part of the complete structure-foundation system is obtained by utilizing a dynamic substructuring method. This is in sharp contrast with the vast majority of ad-hoc simplified models used for the same purpose. Modal truncation within each substructure (with adequate spectral content truncation criteria) is used to enhance computational efficiency.

The non-proportional damping, which arises due to the local paraxial approximation of radiation condition, is accommodated by efficient iterative procedure within the real Ritz vector subspace. It was demonstrated that the proposed approach is far more efficient than the adequate one that utilizes the complex Ritz vector subspace.

A consistent formulation for the kinematic interaction problem, i.e. the deconvolution analysis of free-field motion is also presented. The analysis is performed without a priori imposing assumption on wave pattern. In addition, the models used for the kinematic interaction are completely consistent with the ones later used for the inertial interaction, which provides the direct recovery of the total stress field in the foundation substructure.

ACKNOWLEDGMENTS

Table of Contents

Chapter 1
Introduction

1.1 Objectives of the Study

Considerable research has been conducted on the dynamic analysis of structure-foundation systems, but the state-of-the-art today remains limited to linear analysis. The primary reason for that, beside tradition, is the wide spread use of the frequency domain analysis techniques employed to facilitate the modeling of the foundation as semi-infinite domain. The main objective of this study is to expand the analysis practice to nonlinear problems. Accordingly, the general formulation of the structure-foundation model with inelastic constitutive equations, opposite to standard practice, is given in the time domain. Motivated by a sound design philosophy for the maximum credible earthquake, it was of interest to further specialize the general formulation to account for localized nonlinearities at a predetermined location in a large linear system. Various base isolation systems fit naturally in that context. In particular, local nonlinearity at the structure-foundation interface in the form of dynamic frictional contact is studied.

The versatility of the dynamic substructuring concept and modal truncation to reduce the linear part of the total system to an easily manageable form prior to the nonlinear response computation, is also evaluated. As a by-product of this work, a general setting for linear analysis of structure-foundation systems is furnished. Consistency of the approach to a reduced model generation is obtained by representing the linear part of the complete system by a reduced Ritz subspace, as opposed to the vast majority of ad-hoc simplified models used for the study of the structure-foundation interaction.

The main application of the derived approach is to earthquake engineering analysis, hence the discussion is primary concerned with transient excitation. However, some consideration is also given to the harmonic excitation and associated steady-state response. An iterative procedure is provided to accommodate the non-proportional damping, that characterizes structure-foundation interaction problems, within the real Ritz vector subspace representation of the linear part. The proposed methodology is demonstrated to be more efficient than the adequate one that utilizes the complex Ritz vector subspace representations of the linear part.

1.2. Outline

After this outline, a short review of the existing methodology for the linear dynamic analysis of structure-foundation systems is given, which concludes Chapter 1. The advantages and the disadvantages of two existing approaches, continuum and discretized, are discussed.

In Chapter 2 the added motion approach which makes direct use of free-field motion (i.e. the motion obtained in the site either by measurements or an independent study of the site amplification) is formulated. The formulation is specialized for linear viscoelastic constitutive equations and a discretization procedure that utilizes the finite element method. Time domain analysis is used throughout. This inevitably implies an approximation in enforcing the radiation condition in the semi-infinite foundation domain. Different ways for approximate modeling of radiation condition are hence discussed.

A short parametric study of structure-foundation effect is presented in Chapter 3. The analysis is performed on linear models of buildings and dams, to indicate a class of problems where interaction effect is significant.

The coordinate reduction schemes are studied in Chapter 4, with an aim to select the set of optimal coordinates for the response computation. The principles of static correction (or the mode acceleration) and the combination of the exact particular and the approximate homogeneous solution are reevaluated with respect to the spectral content of excitation. The load dependent Lanczos vector algorithm with the spectral content truncation criterion is

crucial in this development. The direct application of the optimal subspace is further used for the dynamic substructuring method. An efficient method that accommodates non-proportional damping which arises in the discretized model is also discussed as an alternative to complex vector subspace generated by Lanczos vector algorithm with an indefinite inner-product.

The general formulation for the nonlinear structure-foundation dynamic analysis is presented in Chapter 5. We also point out the ill-posedness of the kinematic interaction problem, which is an unavoidable part of general formulation. The specialization of the general formulation to a linear viscoelastic foundation constitutive model is further considered. Finally, the specialization to inelastic constitutive equations for the interface only, with the rest of the complete system being linear, is furnished.

The inelastic interface constitutive equations are given in the form of a generalized Coulomb law (that holds locally) for dynamic frictional contact, as discussed in Chapter 6. The problem is first cast in the form of a variational inequality, and then, by a regularization procedure, recast into a variational equality. The elastic compliance for the normal interface is given in the form of the power law. The dissipation of energy in an impact reflected by the coefficient of the restitution is accounted for by the local dissipative model of the nonlinear viscoelastic form. The numerical procedures, the finite element discretization and the step-by-step integration techniques are also discussed. A 2D-isoparametric 6-noded dynamic frictional contact element is described. The element is limited to small displacement (linearized kinematics), since the large sliding is not likely to cause only limited nonlinearities. The proposed formulation of the dynamic frictional contact can be expanded to accommodate large sliding of one body over another. To facilitate that, a 2D segment element is developed.

Some closing remarks and possible future work directions are given in Chapter 7.

1.3. Short Review of Existing Methodology

The structure-foundation interaction effect is one of the most active research areas in the engineering community. Consequently, the list of references and more or less significant

contributions to the present state-of-the-art would be too extensive for the scope of this work. Instead, we limit ourselves to a short discussion of some prominent features of the dynamic analysis of structure-foundation systems. For a more extensive, quite recent review we refer to Ibrahimbegovic [1988].

There are two main modeling techniques, with a variety of minor modifications : the continuum model and the discretized model. The modeling distinction relates to the foundation component of the complete (structure-foundation) system. The common features of both techniques are discussed first, and the advantages and the disadvantages of each of them are examined later.

First, one has to point out that structure-foundation interaction is not the *site effect* or *soil amplification*. The soil amplification denotes the transformation of an earthquake motion field from the source (rupture) to the *free-field* motion (motion experienced by the foundation without any structure on it). The soil amplification depends on the mechanical properties of the foundation material, or on the constitutive model used to represent the foundation material. The term amplification is somewhat misleading, since there is amplification over the certain range of frequencies and decay over the others. Despite the fact that in some cases the site amplification has a primary role in the dynamic response of the structure-foundation system (e.g. 1985 Mexico City earthquake), its analysis is not carried out in this study. For one reason, once the earthquake motion at the rupture is "known", the site amplification analysis can be carried out in a straight-forward manner as for any dynamic system under the forced vibrations.

Structure-foundation interaction denotes the influence that the presence of a structure has on the change of the free-field motion. Namely, the free-field earthquake motion as registered at a certain point will generally be different from the motion experienced by the base of the structure, even for the structures with negligible mass. The difference consists, in general, of a filtering of translational motion and the occurrence of rotational components. Since this effect, for given free-field motion, depends only on geometry (kinematics) of the structural basis shape, it is commonly called *kinematic interaction*. The free-field motion is usually specified at a single point in the site (*control point*), hence kinematic

interaction actually represents deconvolution problem. Kinematic interaction is not present only in the case of surface supported structures under vertically propagating seismic waves. For the structures with non-negligible mass, the inertial forces on the structure will also contribute to the change of free-field motion through structural deformation. This effect is called the *inertial interaction*.

From the identification of kinematic interaction as a deconvolution problem, it immediately follows that the linear constitutive model of the foundation has to be assumed in order to make its solution possible. In addition, for the total stress recovery, the model used for the solution of the kinematic interaction has to be consistent with the model used for the solution of the inertial interaction. Very often this requirement is violated and the kinematic interaction is carried out on the simplified foundation models. The consistent formulation of the kinematic interaction is discussed shortly in Chapter 5 and the main part of this work concentrates on the inertial interaction procedure.

Flexibly supported structures differ from the rigidly supported ones (the model resulting from neglecting structure-foundation interaction effect) mainly in two aspects :

(1)   the foundation motion is generally different from the free-field motion (as discussed for the kinematic and the inertial interaction)

(2)   part of the vibrating structure energy is dissipated through the radiation of the waves in a semi-infinite foundation medium.

Two main modeling techniques, the continuum and the discretized, differ in the way in which the modeling of the foundation is performed and the radiation condition is enforced.

Continuum Model

The early approach to the structure-foundation interaction effect has favored continuum model for the foundation. The structural model was oversimplified as a one-dimensional (1D) 'stick' model with a rigid surface foundation. *Impedance* (complex stiffness) was obtained for various simple shapes of the rigid foundation and for the linear elastic constitutive equations for the foundations under harmonic excitation, The boundary

element method generalized the same approach to the flexible foundations. The boundary element method can be recognized as a generalization of Treftz method for an approximate solution of the governing partial differential equations (just as the finite element method is the generalization of Ritz method). For the application of the boundary element method, the shape functions are assumed to satisfy the governing partial differential equations throughout the domain and the weighted residual approach is applied to enforce the boundary conditions. The boundary element method has gone a long way from the first systematic engineering exposure (Brebbia [1978]) to the rigorous mathematical treatment (Herrera [1987]). However, its application is still limited to restrictive, highly idealized foundation models (at most viscoelastic layered foundations). The main reason for that is the restrictive availability of the proper shape function that would satisfy all field equations throughout the domain, i.e. Green's function (see Stakgold [1979]). In particular, only a linear constitutive law for the foundation material is allowed. On the other hand, the *radiation condition* which represents dissipation of the energy through the wave propagation in the semi-infinite foundation media, is automatically satisfied by virtue of the Green's function. Once a foundation impedance is obtained, dynamic analysis of the structure-foundation system is performed utilizing the substructure method, which is based on enforcing compatibility and equilibrium conditions along the structure-foundation interface. The analysis is completely performed in the frequency domain which is dictated by the form of Green's function. Some recent modifications of this method are turned to an approximation of Green's function so that the analysis can be performed in the time domain. It should be stated that since utilizing the boundary element method discretization process is performed, the name continuum method is somewhat misleading (really reminiscent of the first approach).

Discretized Model

The essential characteristic of this model is that the governing partial differential equations are solved approximately by the assumed shape functions which are not Green's function of the problem. Hence, the field equations are not satisfied exactly, but by the weighted

residual approach (in projection to the chosen subspace), while the boundary conditions (essential boundary conditions) are (within the shape functions representation). Thus, the method faces no difficulties in handling the inelastic constitutive equations for the foundation material, as well as anisotropy, non-homogeneity etc. However, the radiation condition is not automatically enforced any more. *Transmitting boundaries* (or quiet boundaries) are used for an approximate modeling of the radiation conditions. Different possibilities exist for this purpose, as discussed in the next chapter. It should be pointed out that the perfect absorption results of the transmitting boundaries are encountered only in a special case (for incident wave perpendicular to the boundary). In the case of inelastic constitutive equations, as the main interest of this study, one can expect that the dissipation of energy due to the inelasticity should compensate and diminish the effect of the approximation of the radiation condition.

Chapter 2

Linear Dynamic Analysis : Structure-Foundation
Systems with Linear Viscoelastic Constitutive Equations

In this chapter, the preferred approach to the dynamic analysis of the structure-foundation system is thoroughly discussed. The analysis is concerned with the linear viscoelastic constitutive model that provides a *consistent* definition of the damping matrix in discretized model. The analysis is limited to linearized kinematics. The added motion approach is followed, as first suggested by Clough&Penzien [1975].

2.1. Boundary Value Problem in Elastodynamics

We start with the general considerations of the initial-boundary value problem in elastodynamics. The governing partial differential equations (yet referred as field equations) hold throughout the domain Ω which occupies the body reference configuration. Since we limit ourselves to the linearized kinematics, small displacement gradient theory, the difference between the deformed (current) configuration and the reference configuration can be neglected. Also, as a consequence of the linearized kinematics, Cauchy stress measure and infinitesimal strain measure can be used throughout. The stress principle $t_i = \sigma_{ij} \, n_j$ holds as a consequence of the linear momentum balance and the symmetry of stress tensor $\sigma_{ij} = \sigma_{ji}$ as a consequence of the angular momentum balance (standard summation convention on repeated indices is used throughout).

The field equations that follow from our assumptions are th .

-linearized kinematics

$$\varepsilon_{ij} = \frac{1}{2} \left(u_{i,j} + u_{j,i} \right) \, ... \quad \text{for } x \in \Omega, \, t \in (0,T] \qquad (2.1.1)$$

where $(\ )_{,i}$ is a partial derivative with respect to coordinate x_i, i.e. $(\ )_{,i} = \dfrac{\partial}{\partial x_i}(\ )$, and ε_{ij} are the strain tensor components.

-equilibrium equations

$$\sigma_{ij,j} + \rho b_i - \rho \ddot{u}_i = 0 \ \ \ldots\ \ \text{for } \mathbf{x} \in \Omega,\ t \in (0,T] \tag{2.1.2}$$

where the symmetry of the stress tensor is utilized.

-constitutive equations

$$\sigma_{ij} = D_{0\,ijkl}\ \varepsilon_{kl} + D_{1\,ijkl}\ \dot{\varepsilon}_{kl} + \sigma_{0\,ij} \ \ \ldots\ \ \text{for } \mathbf{x} \in \Omega,\ t \in (0,T] \tag{2.1.3}$$

where the first part represents the elastic stress contribution and the second part defines a viscous stress contribution, while the third part is the initial stress. The usual assumption of ellipticity (positive definiteness) for the elasticity tensor is $D_{0\,ijkl}\ \varepsilon_{ij}\ \varepsilon_{kl} \geq \alpha\ \varepsilon_{ij}\ \varepsilon_{kl}$ ($\alpha > 0$), and the symmetry condition $D_{0\,ijkl} = D_{0\,jilk} = D_{0\,klij}$. For isotropic linear elasticity the constitutive tensor has the form $D_{0\,ijkl} = \lambda\delta_{ij}\delta_{kl} + \mu(\delta_{ik}\delta_{jl}+\delta_{il}\delta_{jk})$. From thermodynamic considerations (the second law of thermodynamics and Kelvin dissipative inequality, see Lubliner [1989]) it can be shown that $D_{1\,ijkl}\ \varepsilon_{ij}\ \varepsilon_{kl} \geq \beta\ \varepsilon_{ij}\ \varepsilon_{kl}$. These constitutive equations correspond to what is called linear viscoelasticity or a viscoelastic material with short memory (see Duvaut&Lions [1976]), since the state of the stress at the moment t depends only on the deformation at the instant t and at the immediately preceding instant. For isotropic material, the tensorial form of $\mathbf{D}_1$ is analogous to that of the elastic moduli, i.e. $D_{1\,ijkl}(t) = \beta_0(t)\delta_{ij}\delta_{kl} + \beta_1(t)(\delta_{ik}\delta_{jl}+\delta_{il}\delta_{jk})$. For a viscoelastic material with long memory, the state of stress at the instant t depends on the deformation at the instant t and also on the deformation at the times preceding t. Hence, the constitutive equations can be stated as

$$\sigma_{ij} = D_{0\,ijkl}\ \varepsilon_{kl} + \int_0^t D_{1\,ijkl}(\mathbf{x},t-\tau)\ \frac{\partial \varepsilon_{kl}}{\partial \tau}\ d\tau + \sigma_{0\,ij} \ \ldots \text{for } \mathbf{x} \in \Omega,\ t \in (0,T] \tag{2.1.4}$$

These equations complicate the semidiscrete equations of motion to the form of the integro-differential rather than the differential equations, as will be shown in the next

section.

The boundary conditions can be divided into the prescribed displacement boundary Γ_u and the prescribed traction boundary Γ_σ:

$$u_i = \bar{u}_i \quad ..... \quad \text{for } \mathbf{x} \in \Gamma_u, \; t \in (0,T] \qquad (2.1.5)$$

$$t_i = \sigma_{ij} \, n_j = \bar{t}_i \quad ..... \quad \text{for } \mathbf{x} \in \Gamma_\sigma, \; t \in (0,T]$$

where the Cauchy stress principle is used.

For the boundary conditions given completely on Γ_u one solves the Dirichlet boundary value problem and in opposite, for the boundary conditions specified on Γ_σ completely one has to solve the Von Neumann boundary value problem. For the general problem we consider mixed boundary conditions such that $\Gamma = \Gamma_u \cup \Gamma_\sigma$

Initial conditions for the set of equilibrium field equations which are second order in time are given as:

$$u_i = u_{0i} \quad ..... \quad \text{for } \mathbf{x} \in \Omega, \; t = 0 \qquad (2.1.6)$$

$$\dot{u}_i = \dot{u}_{0i} \quad ..... \quad \text{for } \mathbf{x} \in \Omega, \; t = 0$$

The solution of the initial-boundary value problem, defined by (2.1.1) to (2.1.6), is displacement, strain and stress fields $\mathbf{u}$, $\boldsymbol{\varepsilon}$ and $\boldsymbol{\sigma}$, that satisfy all equations. For the proof of existence and uniqueness of its solution, one would have to be precise about the nature of the functional space where the solution is defined. Instead, we derive a formally equivalent variational problem and concentrate on the spaces where the solution of that problem lives (formal equivalence relates to not specifying functional spaces in which the solution is defined). The uniqueness of the solution to the stated initial-boundary value problem is further discussed in Chapter 5.

Variational Problem

Starting with the equilibrium equation (2.1.2) we will get the weak form of the differential equation by the weighted residual approach, which is defined by

$$\int_\Omega \left(\sigma_{ij,j} + \rho b_i - \rho \ddot{u}_i \right) w_i \, d\Omega = 0 \qquad (2.1.7)$$

We want to rewrite the first of the three terms in the last equation utilizing the Gauss divergence theorem (see Duvaut&Lions [1976] or Hughes [1987]):

$$\int_\Omega \sigma_{ij,j} \, w_i \, d\Omega = - \int_\Omega \sigma_{ij} \, w_{i,j} \, d\Omega + \int_\Omega \left(\sigma_{ij} \, w_i \right)_{,j} d\Omega \qquad (2.1.8)$$

By the divergence theorem the second term on the right hand side in (2.1.8) becomes:

$$\int_\Omega \left(\sigma_{ij} \, w_i \right)_{,j} d\Omega = \int_\Gamma \sigma_{ij} \, n_j \, w_i \, d\Gamma = \int_\Gamma t_i \, w_i \, d\Gamma \qquad (2.1.9)$$

where the last term is obtained by utilizing the stress principle.

The first term on the right hand side of (2.1.8) can be split into

$$- \int_\Omega \sigma_{ij} \, \frac{1}{2} \, (\, w_{i,j} + w_{j,i} \,) \, d\Omega - \int_\Omega \sigma_{ij} \, \frac{1}{2} \, (\, w_{i,j} - w_{j,i} \,) \, d\Omega \qquad (2.1.10)$$

and further utilizing the well known tensor algebra result (e.g. Chadwick [1976]) that the trace of product of symmetric (σ_{ij}) and antisymmetric ($\frac{1}{2} \, (w_{i,j} - w_{j,i})$) tensor has to be zero, only the first term of the equation (2.1.10) remains. Hence the weak form of (2.1.7) can be rewritten as

$$\int_\Omega \rho \ddot{u}_i \, w_i \, d\Omega + \int_\Omega \sigma_{ij} \, \frac{1}{2} \, (\, w_{i,j} + w_{j,i} \,) \, d\Omega = \int_\Gamma t_i \, w_i \, d\Gamma + \int_\Omega \rho b_i \, w_i \, d\Omega \qquad (2.1.11)$$

Until now, nothing has been assumed about the function w_i (except integrability) and it is conventional that at this point one impose the condition that $w_i = 0$ on Γ_u, so that, in variational interpretation of the weak form, function ($u_i + w_i$) belongs again to the same functional space, i.e. it satisfies the essential boundary conditions. After this, the first term

on the right hand side of (2.1.11) can be split into two parts.

$$\int_\Gamma t_i \ w_i \ d\Omega = \int_{\Gamma_u} t_i \ w_i \ d\Omega + \int_{\Gamma_\sigma} t_i \ w_i \ d\Omega = 0 + \int_{\Gamma_\sigma} \bar{t}_i \ w_i \ d\Omega \qquad (2.1.12)$$

We can also recognize that $\varepsilon_{ij}^w = \dfrac{1}{2} \ (w_{i,j} + w_{j,i})$ by utilizing (2.1.1). By enforcing that the constitutive equations (2.1.3) hold locally (at each point) we obtain the final weak form of equilibrium equations:

$$\int_\Omega \rho \ddot{u}_i \ w_i \ d\Omega + \int_\Omega D_{1 \ ijkl} \ \dot{\varepsilon}_{kl} \varepsilon_{ij}^w \ d\Omega + \int_\Omega D_{0 \ ijkl} \ \varepsilon_{kl} \varepsilon_{ij}^w \ d\Omega =$$

$$\int_{\Gamma_\sigma} \bar{t}_i \ w_i \ d\Gamma + \int_\Omega \rho b_i \ w_i \ d\Omega - \int_\Omega \sigma_{0 \ ij} \ \varepsilon_{ij}^w \ d\Omega \qquad (2.1.13)$$

The examination of (2.1.13), where the highest derivative which appears is of order one, shows that the functional spaces where the solution of (2.1.13) should be sought are Sobolev spaces H^1 (spaces of finite energy) (see Lions&Magenes [1972])

Remark 2.1.1. The requirement that $w_i = 0$ *on* Γ_u can be reformulated by imposing the restriction that w_i lives in the same space as u_i (i.e. that $w_i = \bar{u}$ *on* Γ_u) but then the variation w_i has to be substituted by $(w_i - u_i)$. Hence, we define the virtual displacement as the difference of two kinematically admissible displacement fields. This form has some advantages once we go to nonlinear analysis in the later chapters, where the solution space is the convex set rather than the differentiable manifold (see Stakgold [1979]).

Remark 2.1.2. For the special cases of an incompressible material model for the foundation component, the weak form (2.1.13) must be modified by the weak form of constitutive equations (2.1.3), which is further generalization towards the 3-field variational principle (Washizu [1982]). In that $\iota^{\,\cdots}$ nstitutive equations (2.1.3) must be substituted by $\varepsilon_{ij} = C_{0 \ ijkl} \ \sigma_{kl} + C_{1 \ ijkl} \ \dot{\sigma}_{kl} + \varepsilon_{0 \ ij}.$

2.2. Discretization

The finite element method is the generalization of the Ritz method, where the basis for the functional space in which the solution is sought is constructed by patching together shape functions defined over a part of reference configuration Ω called the finite element and denoted Ω_e. It is a natural requirement that $\Omega = \cup \, \Omega_e$ should be satisfied, but for an irregular shape of boundary Γ, that is not always the case. Instead, one has defined $\Omega^h = \cup \, \Omega_e$ as an approximation to the real domain Ω. This represents a discretization error which is usually disregarded in numerical computations. The variational problem (2.1.13) in elastodynamics, within the finite element context, is solved by a semidiscretization procedure. Namely, the governing partial differential equations are first discretized in space and transferred into a set of ordinary differential equations in time. A variety of techniques from a rich mathematics literature on the subject can then be exercised to solve the set of second order differential equations.

The semidiscretization procedure can be thought of as a restriction (projection) of the complete functional space V where the solution of the boundary value problem lives onto a space of functions V^h spanned by chosen finite element polynomial shape functions, such that $V^h \subset V$. Any constraint imposed on the functions in V (e.g. incompressibility $div \, \mathbf{u} = 0$) must be preserved in V^h.

Hence, we have a fundamental relationship (note that we extended summation convention over repeated indices for the semidiscrete quantities as well):

$$u_i(\mathbf{x},t) = \sum_e u_{il}^h(t) \, N_l(\mathbf{x}) \quad \ldots\ldots \quad i=1,2,3 \tag{2.2.1}$$

and by its differentiation with respect to time we get

$$\dot{u}_i(\mathbf{x},t) = \sum_e \dot{u}_{il}^h(t) \, N_l(\mathbf{x}) \quad \ldots\ldots \quad i=1,2,3$$

$$\ddot{u}_i(\mathbf{x},t) = \sum_e \ddot{u}_{il}^h(t) \, N_l(\mathbf{x}) \quad \ldots\ldots \quad i=1,2,3$$

where u_i ($\dot{u}_i, \ddot{u}_i$) are the components of the displacement (velocity, acceleration) at any point

$\mathbf{x} \in \Omega$; $N_I(\mathbf{x})$ are the chosen shape functions at the node I and u_{iI}^h ($\dot{u}_{iI}^h, \ddot{u}_{iI}^h$) are the nodal values of the displacement (velocity, acceleration) in the semidiscretized model. To simplify notation, we further drop the superscript h (reminder of semidiscretization procedure). To avoid possible confusion in notation, all semidiscretized quantities carry upper case subscript (e.g. $(\ )_I$).

The displacement vector for general 3D case is

$$\mathbf{u}(\mathbf{x},t) = \begin{pmatrix} u_1(\mathbf{x},t) \\ u_2(\mathbf{x},t) \\ u_3(\mathbf{x},t) \end{pmatrix} \tag{2.2.2}$$

while the finite element nodal displacements are

$$\mathbf{u}_I(t) = \begin{pmatrix} u_{1I}(t) \\ u_{2I}(t) \\ u_{3I}(t) \end{pmatrix} \tag{2.2.3}$$

The equations (2.2.2) and (2.2.3) are used to define the matrix notation for (2.2.1) as

$$\mathbf{u}(\mathbf{x},t) = \mathbf{A}_I(\mathbf{x})\,\mathbf{u}_I(t) \quad \ldots\ldots \quad \text{for } I = 1,2,\ldots,N_{np} \tag{2.2.4}$$

where the summation index I goes over all the nodes (N_{np}) and $\mathbf{A}_I(\mathbf{x})$ takes the form

$$\mathbf{A}_I(\mathbf{x}) = N_I(\mathbf{x})\,\mathbf{I} \tag{2.2.5}$$

with $\mathbf{I}$ being the (3×3) identity matrix.

For the adequate discretization of the stress divergence term in (2.1.13), we define the mapping of the strain tensor (with 6 independent components) to a vector (6×1). The order of the components is arbitrary and we choose

$$\boldsymbol{\varepsilon} = \begin{bmatrix} \varepsilon_{11} & \varepsilon_{12} & \\ \varepsilon_{21} & \varepsilon_{22} & \varepsilon_{23} \\ \varepsilon_{31} & \varepsilon_{32} & \varepsilon_{33} \end{bmatrix} \quad \rightarrow \quad \boldsymbol{\varepsilon} = \left(\varepsilon_{11}\ \varepsilon_{22}\ \varepsilon_{33}\ 2\varepsilon_{12}\ 2\varepsilon_{23}\ 2\varepsilon_{31} \right)^T \tag{2.2.6}$$

This automatically defines the map of the stress tensor from the requirement of energy conjugate quantities.

$$\sigma = \begin{bmatrix} \sigma_{11} & \sigma_{12} & \sigma_{13} \\ \sigma_{21} & \sigma_{22} & \sigma_{23} \\ \sigma_{31} & \sigma_{32} & \sigma_{33} \end{bmatrix} \quad \rightarrow \quad \sigma = \left(\sigma_{11} \; \sigma_{22} \; \sigma_{33} \; \sigma_{12} \; \sigma_{23} \; \sigma_{31} \right)^T \tag{2.2.7}$$

By utilizing (2.2.6) and (2.2.5), the mechanical part of the internal energy density in the tensor representation $1/2 \; tr \; (\sigma \; \varepsilon) = 1/2 \; \sigma_{ij}\varepsilon_{ij}$ has a matrix representation counterpart as $1/2 \; \sigma^T \; \varepsilon = 1/2 \; \sigma_i \varepsilon_i$.

The strain displacement relationship can be presented in matrix notation as

$$\varepsilon = \mathbf{B}_I \; \mathbf{u}_I = \begin{bmatrix} N_{I,1} & 0 & 0 \\ 0 & N_{I,2} & 0 \\ 0 & 0 & N_{I,3} \\ N_{I,2} & N_{I,1} & 0 \\ 0 & N_{I,3} & N_{I,2} \\ N_{I,3} & 0 & N_{I,1} \end{bmatrix} \begin{pmatrix} u_{1I}(t) \\ u_{2I}(t) \\ u_{3I}(t) \end{pmatrix} \tag{2.2.8}$$

and the constitutive fourth order tensors (in (2.1.3)) are mapped into (6 × 6) matrices with the general form

$$\mathbf{D} = \begin{bmatrix} D_{1111} & D_{1122} & D_{1133} & D_{1112} & D_{1123} & D_{1131} \\ & D_{2222} & D_{2233} & D_{2212} & D_{2223} & D_{2231} \\ & & D_{3333} & D_{3312} & D_{3323} & D_{3331} \\ & & & D_{1212} & D_{1223} & D_{1231} \\ & symm. & & & D_{2323} & D_{2331} \\ & & & & & D_{3131} \end{bmatrix} \tag{2.2.9}$$

Since we utilize the Galerkin method, the functional space of the variations coincides with the space in which the solution is sought (in discretized form it is the space V^h). Hence all the equations (2.2.1) through (2.2.8) directly apply, with $\mathbf{u}_I(t)$ substituted by $\mathbf{w}_I(t)$. Some other choice for the projection subspace is also possible (e.g. Petrov-Galerkin method).

Hence, the semidiscrete weak form (2.1.13) can be rewritten in the matrix notation as

$$\mathbf{w}_I^T(t) \left\{ \int\limits_\Omega \mathbf{I} \, \rho \, N_I \, N_J \, d\Omega \, \ddot{\mathbf{u}}_J(t) + \int\limits_\Omega \mathbf{B}_I^T \mathbf{D}_1 \, \mathbf{B}_J \, d\Omega \, \dot{\mathbf{u}}_J(t) + \int\limits_\Omega \mathbf{B}_I^T \mathbf{D}_0 \, \mathbf{B}_J \, d\Omega \, \mathbf{u}_J(t) \right\} =$$

$$\mathbf{w}_I^T(t) \left\{ \int\limits_{\Gamma_*} \mathbf{A}_I^T \bar{\mathbf{t}} \, d\Gamma + \int\limits_\Omega \mathbf{A}_I^T \rho \, \mathbf{b} \, d\Omega - \int\limits_\Omega \mathbf{B}_I^T \sigma_0 \, d\Omega \right\} \qquad (2.2.10)$$

where indices $I,J = 1,2,...,N_{np}$.

In (2.2.10) above, we denote the mass matrix by

$$\mathbf{M}_{IJ} = \int\limits_\Omega \mathbf{I} \, \rho \, N_I \, N_J \, d\Omega \qquad (2.2.11)$$

the damping matrix

$$\mathbf{C}_{IJ} = \int\limits_\Omega \mathbf{B}_I^T \mathbf{D}_1 \, \mathbf{B}_J \, d\Omega \qquad (2.2.12)$$

the stiffness matrix

$$\mathbf{K}_{IJ} = \int\limits_\Omega \mathbf{B}_I^T \mathbf{D}_0 \, \mathbf{B}_J \, d\Omega \qquad (2.2.13)$$

the load vector

$$\mathbf{f}_I(t) = \int\limits_{\Gamma_*} \mathbf{A}_I^T \bar{\mathbf{t}} \, d\Gamma + \int\limits_\Omega \mathbf{A}_I^T \rho \, \mathbf{b} \, d\Omega - \int\limits_\Omega \mathbf{B}_I^T \sigma_0 \, d\Omega \qquad (2.2.14)$$

and collect all nodal displacement vectors (same for velocities and accelerations)

$$\mathbf{u}(t) = \left(u_{11} u_{21} u_{31} .. u_{1I} u_{2I} u_{3I} .. u_{1N_{np}} u_{2N_{np}} u_{3N_{np}} \right)^T \qquad (2.2.15)$$

For the independent values of arbitrary components of $\mathbf{w}(t)$, we can then conclude that

$$\mathbf{M} \, \ddot{\mathbf{u}}(t) + \mathbf{C} \, \dot{\mathbf{u}}(t) + \mathbf{K} \, \mathbf{u}(t) = \mathbf{f}(t) \qquad (2.2.16)$$

which is a set of the semidiscrete equations of motion.

Remark 2.2.1. For the constitutive equations of the linear viscoelastic material (or viscoelastic material with short memory) one has a *consistent* way to determine the damping

matrix from the material constitutive parameters, which are known a priori. However, a common practice in structural engineering is to determine the damping properties from experiments on the complete structural system and then to furnish the particular form of the damping matrix that uncouples the equations of motion (e.g. Rayleigh damping or Caughey series, see Caughey [1960]). This defines the so called *proportional damping* matrix C. The proportional form of C can be directly computed from specified modal damping ratios as shown by Wilson&Penzien [1972]. For many systems (we will deal with) a consistent definition of damping does not lead to proportional damping, i.e. we have systems with *non-proportional* damping.

Remark 2.2.2. For the constitutive equations (2.1.4) of the viscoelastic material with the long memory, one would obtain a set of integro-differential equations of motion in the form

$$\mathbf{M} \ddot{\mathbf{u}}(t) + \int_0^t \mathbf{C}(t-\tau) \frac{d\mathbf{u}(\tau)}{dt} d\tau + \mathbf{K} \mathbf{u}(t) = \mathbf{f}(t)$$

Step-by-step Integration Techniques

The extensive consideration of the different possibilities for the solution of the semidiscrete equations (2.2.16) is given in Wilson [1977]. For loading of short duration (impulse loading) step-by-step numerical procedures are usually the most effective. However, for loading of long duration (such as earthquake loading) mode superposition is the appropriate numerical method.

Further discussion of different numerical procedures and the ways to enhance their efficiency is left for later chapter. Here we limit ourselves to a short discussion of Newmark-Wilson unified algorithms to solve a set of semidiscrete equations (2.2.16) for the general form of loading f(t). For a more thorough discussion we refer to Bathe&Wilson [1976] or Belytcshko&Hughes [1983]. The main purpose of this discussion is to serve as the logical closure to a full discretization of the equations of motion. Newmark algorithms are a 2-parameter (conventional β and γ) family given by

$$\mathbf{u}_k = \mathbf{u}_{k-1} + \Delta t \,\dot{\mathbf{u}}_{k-1} + \frac{\Delta t^2}{2} \,[\,(1-2\beta)\,\ddot{\mathbf{u}}_{k-1} + 2\beta\,\ddot{\mathbf{u}}_k)]$$

$$\dot{\mathbf{u}}_k = \dot{\mathbf{u}}_{k-1} + \Delta t \,[(1-\gamma)\,\ddot{\mathbf{u}}_{k-1} + \gamma\,\ddot{\mathbf{u}}_k)] \qquad\qquad (2.2.17)$$

$$\mathbf{M}\,\ddot{\mathbf{u}}_k + \mathbf{C}\,\dot{\mathbf{u}}_k + \mathbf{K}\,\mathbf{u}_k = \mathbf{f}_k$$

where $\mathbf{u}_k$, $\dot{\mathbf{u}}_k$ and $\ddot{\mathbf{u}}_k$ are approximations for $\mathbf{u}(t_k)$, $\dot{\mathbf{u}}(t_k)$ and $\ddot{\mathbf{u}}(t_k)$, respectively. Equation $(2.2.17^3)$ is simply the equation of motion in terms of the approximate solution. The Wilson-θ algorithm is related to the 2-parameter Newmark family by a special choice of the parameter θ, which can be identified in the equation

$$\mathbf{M}\,\ddot{\mathbf{u}}_{k+\theta} + \mathbf{C}\,\dot{\mathbf{u}}_{k+\theta} + \mathbf{K}\,\mathbf{u}_{k+\theta} = \mathbf{f}_{k+\theta} \qquad\qquad (2.2.18)$$

where $\mathbf{u}_{k+\theta}$, $\dot{\mathbf{u}}_{k+\theta}$ and $\ddot{\mathbf{u}}_{k+\theta}$ are approximation for $\mathbf{u}(t_k+\theta\Delta t)$, $\dot{\mathbf{u}}(t_k+\theta\Delta t)$ and $\ddot{\mathbf{u}}(t_k+\theta\Delta t)$ respectively.

For the special choice of parameters $\beta=1/4$ and $\gamma=1/2$, the Newmark algorithm is equivalent to trapezoidal rule for the corresponding first order system (see Hughes [1987]). By the celebrated Dahlquist theorem (see Gears [1971]) the trapezoidal rule is the highest order (second order) A-stable linear multi-step method. Hence, one can do no better than that. However, some improvements of the dissipative properties over higher frequencies are in some cases desirable, since the trapezoidal rule has spectral radii equal to one over all frequencies. Different suggestions have appeared in the literature, but the dissipation properties (at the expense of reducing order) can be achieved by different selections of the parameters β and γ than for the trapezoidal rule (average acceleration method). In that case, one has to worry about proper selection of parameters β and γ to preserve the stability property with:

unconditional stability

$$2\beta \geq \gamma \geq \frac{1}{2}$$

-conditional stability

$$\gamma \geq \frac{1}{2}$$

$$\beta < \frac{1}{2}\gamma$$

$$\omega \leq \omega_{cr} = \frac{\xi\,(\gamma - 1/2) + [(\gamma/2 - \beta) + \xi^2\,(\gamma - 1/2)^2]^{1/2}}{(\gamma/2 - \beta)\Delta t}$$

where the conditional stability criterion is given for one (modal) equation with frequency ω

and damping ratio $\xi = \dfrac{\omega}{\sqrt{2mk}}$.

If we utilize equations (2.2.17), the discretization process of the equations of motion can be completed. For convenience, the discretized set of equations and the complete algorithm are summarized in Table 2.2.1.

Table 2.2.1. Unified Newmark/Wilson step-by-step algorithm

A. Initial Computations

1.   Form stiffness matrix $\mathbf{K}$, mass matrix $\mathbf{M}$ and damping matrix $\mathbf{C}$

2.   Initialize $\mathbf{u}_0$, $\dot{\mathbf{u}}_0$ and $\ddot{\mathbf{u}}_0$

3.   Select step size Δt and parameters β, γ and θ, and compute integration constants

$$a_0 = \frac{1}{\beta(\theta\Delta t)^2} \qquad\qquad a_5 = 0.5\,\theta\,\Delta t\,\left(\frac{\gamma}{\beta} - 2\right)$$

$$a_1 = \frac{\gamma}{\beta\theta\Delta t} \qquad\qquad a_6 = \Delta t\,(1 - \gamma)$$

$$a_2 = \frac{1}{\beta\theta\Delta t} \qquad\qquad a_7 = \Delta t\,\gamma$$

$$a_3 = \frac{0.5}{\beta} - 1 \qquad\qquad a_8 = (0.5 - \beta)\,\Delta t^2$$

$$a_4 = \frac{\gamma}{\beta} - 1 \qquad\qquad a_9 = \beta\,\Delta t^2$$

4. Form effective stiffness matrix : $\hat{\mathbf{K}} = \mathbf{K} + a_0\mathbf{M} + a_1\mathbf{C}$

5. Triangularize $\hat{\mathbf{K}} = \mathbf{L}\,\mathbf{D}\,\mathbf{L}^T$

B. For Each Time Step

1. Calculate effective load at time $t_{k+\theta} = t_{k-1} + \theta\,\Delta t$

$$\hat{\mathbf{f}}_{k+\theta} = \mathbf{f}_{k-1} + \theta\,(\mathbf{f}_k - \mathbf{f}_{k-1}) + \mathbf{M}\,(a_0\mathbf{u}_{k-1} + a_2\dot{\mathbf{u}}_{k-1} + a_3\ddot{\mathbf{u}}_{k-1}) +$$

$$\mathbf{C}\,(a_1\mathbf{u}_{k-1} + a_4\dot{\mathbf{u}}_{k-1} + a_5\ddot{\mathbf{u}}_{k-1})$$

2. Solve for displacements at time $t_{k+\theta} = t_{k-1} + \theta\,\Delta t$

$$\mathbf{L}\,\mathbf{D}\,\mathbf{L}^T\,\mathbf{u}_{k+\theta} = \hat{\mathbf{f}}_{k+\theta}$$

3. Calculate acceleration, velocity and displacement at time $t_k = t_{k-1} + \Delta t$

$$\mathbf{temp}_1 = a_0\,(\mathbf{u}_{k+\theta} - \mathbf{u}_{k-1}) - a_2\,\dot{\mathbf{u}}_{k-1} - a_3\,\ddot{\mathbf{u}}_{k-1}$$

$$\mathbf{temp}_2 = \frac{(\mathbf{temp}_1 - \ddot{\mathbf{u}}_{k-1})}{\theta}$$

$$\mathbf{temp}_1 = \mathbf{temp}_2 + \ddot{\mathbf{u}}_{k-1}$$

$$\ddot{\mathbf{u}}_k = \mathbf{temp}_1$$

$$\dot{\mathbf{u}}_k = \dot{\mathbf{u}}_{k-1} + a_6\ddot{\mathbf{u}}_{k-1} + a_7\mathbf{temp}_1$$

$$\mathbf{u}_k = \mathbf{u}_{k-1} + \Delta t\,\dot{\mathbf{u}}_{k-1} + a_8\ddot{\mathbf{u}}_{k-1} + a_9\mathbf{temp}_1$$

2.3 Added Motion Approach

The added motion method for the dynamic analysis of structure-foundation systems is based on the additive split of the total motion field into two motion fields : the free-field motion (motion of the foundation with no structure on it) and the added motion field (due to addition of a structure). The additive split of the total motion field is justified by the linearized kinematics (small displacement gradient theory) we consider in this work. The evaluation of the structural component behavior within the added motion approach is still straightforward, since for the structural component of structure-foundation system the added motion is the same as the total motion. On the other hand, the evaluation of the foundation component behavior becomes more complicated. However, the deconvolution analysis in kinematic interaction is greatly simplified.

For the derivation of the added motion approach, we refer to system presented on Figure 2.3.1. By definition, the free-field motion is determined considering the foundation part by itself. The semidiscrete equations of motion (utilizing notation from previous section) are then

$$\mathbf{M}_f \, \ddot{\mathbf{v}}(t) + \mathbf{C}_f \, \dot{\mathbf{v}}(t) + \mathbf{K}_f \, \mathbf{v}(t) = \mathbf{f}_{ff}(t) \tag{2.3.1}$$

where $\mathbf{M}_f$, $\mathbf{C}_f$ and $\mathbf{K}_f$ are mass, damping and stiffness matrices of the semidiscretized foundation model; $\mathbf{v}(t)$, $\dot{\mathbf{v}}(t)$ and $\ddot{\mathbf{v}}(t)$ are free-field displacement, velocity and acceleration vectors, and $\mathbf{f}_{ff}(t)$ is far-field boundary loading (due to earthquake ground motion).

By addition of a structure to the foundation component, a complete structure-foundation system is formed. The equations of motion for the complete system to the same far-field boundary loading $\mathbf{f}_{ff}(t)$ can be stated as

$$\left[\mathbf{M}_s + \mathbf{M}_f \right] \left(\ddot{\mathbf{v}}(t) + \ddot{\mathbf{u}}(t) \right) + \left[\mathbf{C}_s + \mathbf{C}_f \right] \left(\dot{\mathbf{v}}(t) + \dot{\mathbf{u}}(t) \right) +$$
$$\left[\mathbf{K}_s + \mathbf{K}_f \right] \left(\mathbf{v}(t) + \mathbf{u}(t) \right) = \mathbf{f}_{ff}(t) \tag{2.3.2}$$

where $\mathbf{u}(t)$, $\dot{\mathbf{u}}(t)$ and $\ddot{\mathbf{u}}(t)$ are added motion displacement, velocity and acceleration vectors, and $\mathbf{M}_s$, $\mathbf{C}_s$ and $\mathbf{K}_s$ are structural mass, damping and stiffness. The rest of the matrices and vectors are the same as in (2.3.1). Note that in the equation (2.3.2), the brackets stand for

the matrix assembly process, while the braces stand for vector addition. To clarify further the structure of equation (2.3.2), we present a partitioned form for all the matrices and vectors with a remark that the structure degrees of freedom (dofs) carry subscript s, foundations dofs subscript f, while interface dofs (dofs common to both structure and foundation) carry subscript i.

-free-field motion :   -added motion :   -far-field boundary loading :

$$
\mathbf{v}(t) = \begin{pmatrix} \mathbf{0} \\ \mathbf{v}_i(t) \\ \mathbf{v}_f(t) \end{pmatrix}
\qquad
\mathbf{u}(t) = \begin{pmatrix} \mathbf{u}_s(t) \\ \mathbf{u}_i(t) \\ \mathbf{u}_f(t) \end{pmatrix}
\qquad
\mathbf{f}_{ff}(t) = \begin{pmatrix} \mathbf{0} \\ \mathbf{0} \\ \mathbf{f}_f(t) \end{pmatrix}
$$

-structure mass matrix :   -foundation mass matrix :

$$
\mathbf{M}_s = \begin{bmatrix} \mathbf{M}_{ss} & \mathbf{M}_{si} & \mathbf{0} \\ \mathbf{M}_{is} & \mathbf{M}_{ii}^s & \mathbf{0} \\ \mathbf{0} & \mathbf{0} & \mathbf{0} \end{bmatrix}
\qquad
\mathbf{M}_f = \begin{bmatrix} \mathbf{0} & \mathbf{0} & \mathbf{0} \\ \mathbf{0} & \mathbf{M}_{ii}^f & \mathbf{M}_{if} \\ \mathbf{0} & \mathbf{M}_{fi} & \mathbf{M}_{ff} \end{bmatrix}
\qquad (2.3.3)
$$

-structure damping matrix :   -foundation damping matrix :

$$
\mathbf{C}_s = \begin{bmatrix} \mathbf{C}_{ss} & \mathbf{C}_{si} & \mathbf{0} \\ \mathbf{C}_{is} & \mathbf{C}_{ii}^s & \mathbf{0} \\ \mathbf{0} & \mathbf{0} & \mathbf{0} \end{bmatrix}
\qquad
\mathbf{C}_f = \begin{bmatrix} \mathbf{0} & \mathbf{0} & \mathbf{0} \\ \mathbf{0} & \mathbf{C}_{ii}^f & \mathbf{C}_{if} \\ \mathbf{0} & \mathbf{C}_{fi} & \mathbf{C}_{ff} \end{bmatrix}
$$

-structure stiffness matrix :   -foundation stiffness matrix :

$$
\mathbf{K}_s = \begin{bmatrix} \mathbf{K}_{ss} & \mathbf{K}_{si} & \mathbf{0} \\ \mathbf{K}_{is} & \mathbf{K}_{ii}^s & \mathbf{0} \\ \mathbf{0} & \mathbf{0} & \mathbf{0} \end{bmatrix}
\qquad
\mathbf{K}_f = \begin{bmatrix} \mathbf{0} & \mathbf{0} & \mathbf{0} \\ \mathbf{0} & \mathbf{K}_{ii}^f & \mathbf{K}_{if} \\ \mathbf{0} & \mathbf{K}_{fi} & \mathbf{K}_{ff} \end{bmatrix}
$$

Combining equations (2.3.1) and (2.3.2) we get

$$
\left[\mathbf{M}_s + \mathbf{M}_f \right] \left(\ddot{\mathbf{v}}(t) + \ddot{\mathbf{u}}(t) \right) + \left[\mathbf{C}_s + \mathbf{C}_f \right] \left(\dot{\mathbf{v}}(t) + \dot{\mathbf{u}}(t) \right) +
$$

$$
\left[\mathbf{K}_s + \mathbf{K}_f \right] \left(\mathbf{v}(t) + \mathbf{u}(t) \right) = \mathbf{M}_f \, \ddot{\mathbf{v}}(t) + \mathbf{C}_f \, \dot{\mathbf{v}}(t) + \mathbf{K}_f \, \mathbf{v}(t) \qquad (2.3.4)
$$

and after cancellation we get

$$\left[\, \mathbf{M}_s + \mathbf{M}_f \,\right] \ddot{\mathbf{u}}(t) + \left[\, \mathbf{C}_s + \mathbf{C}_f \,\right] \dot{\mathbf{u}}(t) + \left[\, \mathbf{K}_s + \mathbf{K}_f \,\right] \mathbf{u}(t) =$$

$$-\mathbf{M}_s \, \ddot{\mathbf{v}}(t) - \mathbf{C}_s \, \dot{\mathbf{v}}(t) - \mathbf{K}_s \, \mathbf{v}(t) \qquad\qquad (2.3.5)$$

If we denote the mass, damping and stiffness of the complete interacting system as $\mathbf{M}$, $\mathbf{C}$ and $\mathbf{K}$ respectively, and take advantage of the sparsity in the partitioned matrix quantities of (2.3.3), the equation (2.3.5) can be rewritten as

$$\mathbf{M}\,\ddot{\mathbf{u}}(t) + \mathbf{C}\,\dot{\mathbf{u}}(t) + \mathbf{K}\,\mathbf{u}(t) = - \begin{bmatrix} \mathbf{M}_{si} \\ \mathbf{M}_{ii}^s \\ \mathbf{0} \end{bmatrix} \ddot{\mathbf{v}}_i(t) - \begin{bmatrix} \mathbf{C}_{si} \\ \mathbf{C}_{ii}^s \\ \mathbf{0} \end{bmatrix} \dot{\mathbf{v}}_i(t) - \begin{bmatrix} \mathbf{K}_{si} \\ \mathbf{K}_{ii}^s \\ \mathbf{0} \end{bmatrix} \mathbf{v}_i(t)\,(2.3.6)$$

Note that by the solution of the equations (2.3.6), only the added motion field will be obtained. For the structure, the added motion field represents the total motion field (see partitioned equations (2.3.3)); hence the added motion formulation in the form (2.3.6) is amiable to dynamic analysis of structure-foundation systems with the nonlinear constitutive equations for the structural component as will be elaborated in later chapters. The important advantage of the formulation (2.3.6) is that the excitation is directly specified as the free-field motion i.e. the motion measured at the control point. For surface supported structures, this has the additional advantage of eliminating the need for the deconvolution phase in the structure-foundation dynamic analysis. The formulation (2.3.6) does not place any limitation upon the choice of interface, and any of the possibilities presented on Figure 2.3.2. is eligible. For embedded structures with the interface specified as either a rigid or a flexible boundary, the free-field interface motion has to be determined from the specified motion at the control point to account for the kinematic interaction. In order to eliminate the scattering problem related to this approach, partitioning of the system in the manner of so-called *volume meth* . ..., be used (see Lysmer [1978] or Bayo&Wilson [1984]). The same approach can be extended to the formulation of the structure-foundation model presented herein. The structure matrices in (2.3.6) for the interface dofs are then formulated from the difference of the physical properties of the structure and the foundation for the embedded part.

If the equations (2.3.6) are to be used for structure-foundation dynamic analysis, the free-field velocities and displacements have to be obtained by integrating given acceleration record. For linear systems (and as shown in later chapters for systems with inelastic interface only), this inconvenience can be avoided by further separating the added motion field into its dynamic and pseudo-static components:

$$\mathbf{u}(t) = \mathbf{u}_d(t) + \mathbf{u}_{ps}(t) \tag{2.3.7}$$

The pseudo-static motion represents the motion of the complete system produced by the free-field displacements imposed at the interface dofs, when the dynamic effects are neglected. By definition it can be computed from the equations (2.3.6)

$$\mathbf{K}\,\mathbf{u}_{ps}(t) = - \begin{bmatrix} \mathbf{K}_{si} \\ \mathbf{K}_{ii}^s \\ 0 \end{bmatrix} \mathbf{v}_i(t)$$

$$\mathbf{u}_{ps}(t) = \mathbf{R}\,\mathbf{v}_i(t) \tag{2.3.8}$$

$$\mathbf{R} = - \mathbf{K}^{-1} \begin{bmatrix} \mathbf{K}_{si} \\ \mathbf{K}_{ii}^s \\ 0 \end{bmatrix}$$

where $\mathbf{R}$ is referred to as the influence coefficient matrix.

If we introduce (2.3.7) and (2.3.8) into the added motion formulation (2.3.6) (and neglect the damping proportional forcing function), the new formulation is furnished

$$\mathbf{M}\,\ddot{\mathbf{u}}_d(t) + \mathbf{C}\,\dot{\mathbf{u}}_d(t) + \mathbf{K}\,\mathbf{u}_d(t) = - \left\{ \mathbf{M}\,\mathbf{R} + \begin{bmatrix} \mathbf{M}_{si} \\ \mathbf{M}_{ii}^s \\ 0 \end{bmatrix} \right\} \mathbf{v}_i(t) \tag{2.3.9}$$

For both embedded structures and structures supported at the ground surface, the assumption of the free-field motion of the same value at each interface nodal point, further simplifies the equations of motion (2.3.9). In this case, the pseudo-static displacements of the structure due to unit displacement at the interface dofs ($2.3.8^2$) are rigid body displacements. Hence, one recovers the standard form of the equations of motion for the rigid base earthquake ground motion :

$$M \ddot{u}_d(t) + C \dot{u}_d(t) + K u_d(t) = - M_s R_{rb} v_i(t)$$ (2.3.10)

where M_s is the structure mass matrix given by (2.3.3^2) and R_{rb} is the rigid body transformation matrix (a set of rigid body displacements for unit displacement at the structure basis).

To recapitulate, the added motion approach in the form (2.3.10) separates the total motion field into the dynamic and pseudo-static added motion for the structure and into the dynamic, pseudo-static and free-field motion for the foundation component. However, the assumption on the constant free-field motion over all interface dofs simplifies the stress recovery in the structure, i.e. the solution of the equation (2.3.10) is sufficient for that purposes.

2.4. Transmitting Boundaries

To demonstrate the conceptual principle of the local transmitting boundaries, we can first concentrate on the scalar wave equation in the half-space domain:

$$\frac{\partial^2 w}{\partial t^2} - \frac{\partial^2 w}{\partial x^2} - \frac{\partial^2 w}{\partial y^2} = 0 \quad , \text{ for } x \geq 0$$ (2.4.1)

The general solution of (2.4.1) has the form

$$w = W \, e^{i \, (\xi \, x + \eta \, y + \omega \, t)}$$ (2.4.2)

where (x,y,t) and (ξ,η,ω) are dual variables.

After substitution of (2.4.2) into (2.4.1) we obtain characteristic equation

$$(-\omega^2 + \xi^2 + \eta^2) \, W = 0$$ (2.4.3)

which can be factorized into

$$(\xi - \sqrt{\omega^2 - \eta^2}) (\xi + \sqrt{\omega^2 - \eta^2}) \, W = 0$$ (2.4.4)

Hence, from (2.4.4), the special families of solutions to the wave equation (2.4.1) representing the waves traveling to the left are given by the plane waves

$$w = W \ e^{i \ (\sqrt{\omega^2-\eta^2} \ x \ + \ \omega \ t \ + \ \eta \ y)} \ , \qquad with \ \omega^2 - \eta^2 > 0, \quad \omega > 0 \tag{2.4.5}$$

If the pair (η,ω) is held fixed (one wave), one first order differential boundary condition which annihilates w on the boundary $x = 0$ has the form

$$\left(\frac{d}{dx} - i \ \sqrt{\omega^2 - \eta^2} \right) \ w_{|x=0} = 0 \tag{2.4.6}$$

More generally, the wave trains traveling to the left can be represented by

$$w(x,y,t) = \int \int e^{i \ (\sqrt{\omega^2-\eta^2} \ x \ + \ \omega \ t \ + \ \eta \ y)} \ W(0,\eta,\omega) \ d\eta d\omega \tag{2.4.7}$$

where $W(0,\eta,\omega)$ is Fourier transform in the (y,t) variables. We note that, by the Fourier inversion formula, $w(0,y,t)$ is given by the inverse Fourier transform of the amplitude function $W(0,\eta,\omega)$. By superposition of the calculations for (2.4.6) the boundary conditions which exactly annihilate the wave train traveling to the left of the form (2.4.7) is given by

$$\left(\frac{dw}{dx} - \int \int e^{i \ (\eta \ y \ + \ \omega t)} \ i \ \sqrt{\omega^2-\eta^2} \ W(0,\eta,\omega) \ d\eta d\omega \right)_{|x=0} = 0 \tag{2.4.8}$$

which is analogous to

$$\left(\frac{d}{dx} - \sqrt{\frac{\partial^2}{\partial t^2} - \frac{\partial^2}{\partial y^2}} \right) \ w_{|x=0} = 0 \tag{2.4.9}$$

Next goal is to establish a local approximation to the perfectly absorbing boundary condition (2.4.9). We take the symbol of the boundary condition from (2.4.9) given by

$$\frac{d}{dx} - i \ \omega \ \sqrt{1 - \frac{\eta^2}{\omega^2}} \tag{2.4.10}$$

and approximate it at normal incidence $(\eta=0)$. Using the approximation $\sqrt{1 - \frac{\eta^2}{\omega^2}}_{|\eta=0} =$

$1 + O(\frac{\eta^2}{\omega^2})$ and realizing that $i \ \omega$ corresponds to $\frac{\partial}{\partial t}$ we obtain

1st approximation

$$\left(\frac{\partial}{\partial x} - \frac{\partial}{\partial t} \right) w_{|x=0} = 0 \tag{2.4.11}$$

Using the next approximation (the first Taylor or Pade) to the square root

$$\sqrt{1 - \frac{\eta^2}{\omega^2}}_{|\eta=0} = 1 - \frac{\eta^2}{2\omega^2} + O(\frac{\eta^4}{\omega^4})$$ in (2.4.10) and multiplying by $i\omega$ we obtain the symbol

$$i\omega \frac{\partial}{\partial x} + \omega^2 - \frac{\eta^2}{2}$$

and this yields boundary conditions of

2nd approximation

$$\left(\frac{\partial^2}{\partial x\, \partial t} - \frac{\partial^2}{\partial t^2} + \frac{\partial^2}{2\, \partial y^2} \right) w_{|x=0} = 0 \tag{2.4.12}$$

We can deliver higher order Taylor series approximations to the square root in (2.4.10), but it turns out that they all yield unstable boundary values (see Kreiss [1970]). The sequence of these approximations represent the *paraxial boundary*. The first approximation boundary, which corresponds to a viscous dash-pot, is devised earlier from engineering considerations by Lysmer&Kuhlemeyer [1969]. Since the boundary is frequency independent, it is directly applicable to the time domain analysis. Zienkiewicz et al. [1986] have discussed generalization of the viscous boundary for the cylindrical shape of the far-field boundary in 3D applications. Recent parametric studies (see Cohen&Jennings [1983] or Wolf [1986]) have shown that, once the transmitting boundaries are placed 1.5 wave lengths away from the source, all different enhancements of the viscous boundary are really unnecessary, since they all yield almost identical results.

To demonstrate that the same concept discussed for the wave equation (2.4.1) directly applies to elasticity problems, we further specialize the constitutive equations (2.1.3) to linear elasticity, and limit our discussion to plane strain problems. The equations (2.1.1) to (2.1.3) can be recast in the form

$$u_{,tt} - E_{11} u_{,xx} - E_{12} u_{,xy} - E_{22} u_{,yy} = 0 \qquad (2.4.13)$$

where

$$\mathbf{u} = \begin{pmatrix} u \\ v \end{pmatrix} \qquad\qquad E_{11} = \begin{bmatrix} c_d^2 & 0 \\ 0 & c_s^2 \end{bmatrix}$$

$$E_{12} = (c_d^2 - c_s^2) \begin{bmatrix} 0 & 1 \\ 1 & 0 \end{bmatrix} \qquad E_{22} = \begin{bmatrix} c_s^2 & 0 \\ 0 & c_d^2 \end{bmatrix}$$

and c_d is the dilatational wave velocity $(c_d = \sqrt{\dfrac{\lambda\ (1-v)}{\rho\ v}})$; c_s is the shear wave velocity

$(c_s = \sqrt{\dfrac{\mu}{\rho}})$; with λ and μ as Lame parameters, v as Poisson ratio and ρ as the mass density.

If we assume the solution to the elasticity equations (2.4.13), for both displacement components u and v, in the form (2.4.2), we obtain the characteristic equation

$$(I \omega^2 - E_{11} \xi^2 - E_{12} \xi \eta - E_{22} \eta^2) \begin{pmatrix} U \\ V \end{pmatrix} = 0 \qquad (2.4.14)$$

Guided by the procedure for the paraxial boundary for the scalar wave equations (2.4.1), we perform factorization of the characteristic equation (2.4.14) above and use Taylor series expansion on both terms

$$(I (\frac{\xi}{\omega}) - B_1 - B_2 (\frac{\eta}{\omega}) - B_3 (\frac{\eta}{\omega})^2)$$

$$(I (\frac{\xi}{\omega}) - B_4 - B_5 (\frac{\eta}{\omega}) - B_6 (\frac{\eta}{\omega})^2) \begin{pmatrix} U \\ V \end{pmatrix} = 0 \qquad (2.4.15)$$

To obtain the matrices $B_i, i=1,...,6$, we first substitute the first root of (2.4.15) into the (2.4.14) and get

$$(I - E_{11} B_1) (\frac{\eta}{\omega})^0 + (-E_{12} B_1 - E_{11} B_1 B_2 - E_{11} B_2 B_1) (\frac{\eta}{\omega})^1 +$$

$$(-E_{22} + E_{11} B_2 - E_{11} B_1 B_3 - E_{11} B_3 B_1 - E_{11} B_2^2) \, (\frac{\eta}{\omega})^2 + O((\frac{\eta}{\omega})^3) = 0 \quad (2.4.16)$$

Setting the coefficients of $(\frac{\eta}{\omega})^i, i = 0,1,2$ equal to 0, we get

$$B_1 = \begin{bmatrix} \dfrac{1}{c_d} & 0 \\ 0 & \dfrac{1}{c_s} \end{bmatrix} \qquad B_2 = -(c_d - c_s) \begin{bmatrix} 0 & \dfrac{1}{c_d} \\ \dfrac{1}{c_s} & 0 \end{bmatrix} \qquad B_3 = - \begin{bmatrix} c_s - \dfrac{1}{2} c_d & 0 \\ 0 & c_d - \dfrac{1}{2} c_s \end{bmatrix}$$

The same procedure for the second root of (2.4.15) gives $B_4 = -B_1$, $B_5 = B_2$ and $B_6 = -B_3$.

The first root of the characteristic equation represents a body wave propagating in the positive x direction. If we want to recover the differential equation governing that wave we would have:

1st approximation

$$I \, (\frac{\xi}{\omega}) - B_1 = 0 \quad \rightarrow \quad \begin{bmatrix} 1 & 0 \\ 0 & 1 \end{bmatrix} \omega - \begin{bmatrix} c_d & 0 \\ 0 & c_s \end{bmatrix} \xi = 0$$

which corresponds to the differential equation

$$\begin{bmatrix} 1 & 0 \\ 0 & 1 \end{bmatrix} \begin{pmatrix} u_{,t} \\ v_{,t} \end{pmatrix} - \begin{bmatrix} c_d & 0 \\ 0 & c_s \end{bmatrix} \begin{pmatrix} u_{,x} \\ v_{,x} \end{pmatrix} = 0 \qquad (2.4.18)$$

which is exactly in the form of the Lysmer&Kuhlemeyer [1969] standard viscous boundary.

2nd approximation

$$\begin{bmatrix} 1 & 0 \\ 0 & 1 \end{bmatrix} \omega^2 - \begin{bmatrix} c_d & 0 \\ 0 & c_s \end{bmatrix} \xi \omega - (c_d - c_s) \begin{bmatrix} 0 & 1 \\ 1 & 0 \end{bmatrix} \eta \omega = 0$$

which corresponds to the differential equation

$$\begin{bmatrix} 1 & 0 \\ 0 & 1 \end{bmatrix} \begin{pmatrix} u_{,tt} \\ v_{,tt} \end{pmatrix} - \begin{bmatrix} c_d & 0 \\ 0 & c_s \end{bmatrix} \begin{pmatrix} u_{,tx} \\ v_{,tx} \end{pmatrix} - (c_d - c_s) \begin{bmatrix} 0 & 1 \\ 1 & 0 \end{bmatrix} \begin{pmatrix} u_{,ty} \\ v_{,ty} \end{pmatrix} = 0 \qquad (2.4.19)$$

Third order approximation is also supplied in Cohen&Jennings [1983], but, just like for the wave equation (see Enquist&Majda [1977]), it proves to be unstable. Some ways in which the instability of the third approximation can be eliminated are discussed in Cohen&Jennings [1983].

Finite Element Implementation

The paraxial approximation to the transmitting boundary conditions within the discretized model (discussed in section 2.3), is utilized as a part of the domain Ω where the governing "equilibrium" equations are given by the first (2.4.18) or the second paraxial approximation (2.4.19). For the first paraxial approximation, or the standard viscous boundary, the simple lumping procedures can be successfully utilized for the 4-noded element (see Lysmer&Kuhlemeyer [1969]). For the higher order element a consistent discretized form of the viscous boundary yields a 3-diagonal form of the damping matrix C. Some lumping techniques that provide a diagonal form of C are discussed in Chew [1985], analogous to the mass matrix lumping. However, the consistent lumping procedure, which we use in this study, is provided by the nodal point quadrature rule (e.g. Simpson rule for 9-node element)

For the finite element discretization of the second paraxial approximation (2.4.19), a special transition 4-node element is devised by Cohen&Jennings [1983], in which one pair of nodes is assembled with the standard elasticity equilibrium equation, while for another pair of nodes, the field equations corresponds to the second paraxial approximation (2.4.19). Beside the nonstandard assembly procedure, the additional inconvenience arising from the second paraxial approximation is the nonsymmetry of the damping matrix C, which corresponds to a discretization of the second term in (2.4.19).

For either case of the paraxial boundary, the discretized damping mat has a *non-proportional form* (i.e. it is not related to neither stiffness nor mass matrix). _.ence, special techniques for the dynamic analysis have to be considered. This is done in Chapter 4.

Remark 2.4.1 In the discretized method, one should also mention the infinite element idea, (see Zienkiewicz et al. [1986]) as a possibility of enforcing the radiation condition. The idea is based on the use of an approximation to Green's function (e.g. exponential decay) as the shape function in the infinite finite element (i.e. the element that extends to infinity in at least one direction). The main advantage of the infinite element is its easy implementation within the standard finite element computer program.

Foundation

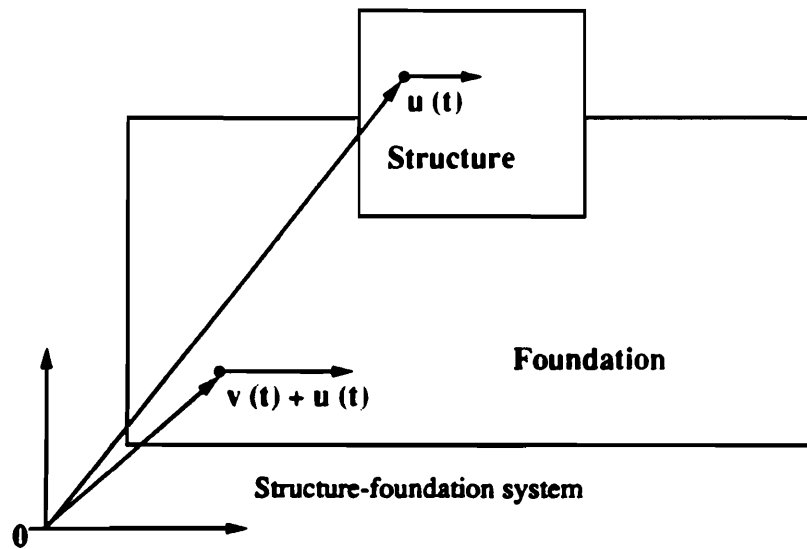v (t)

Free - field

0

v (t) = free-field motion
u (t) = added motion

u (t)

Structure

Foundation
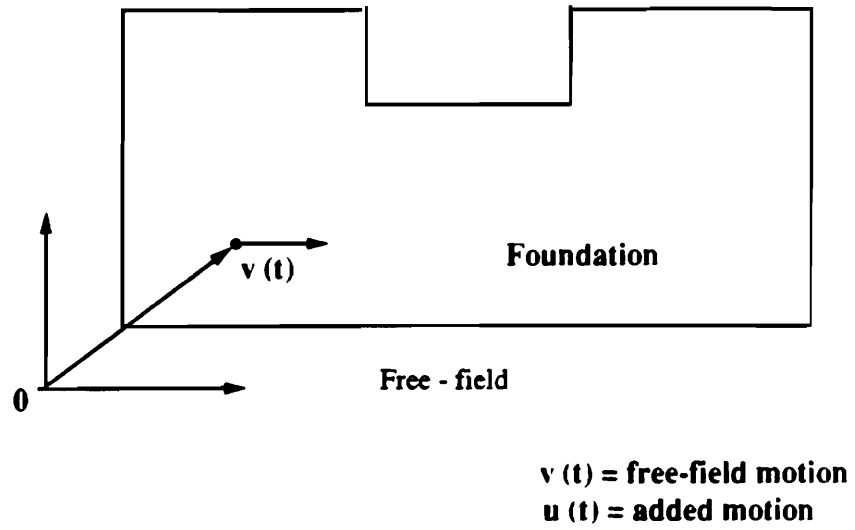
v (t) + u (t)

Structure-foundation system

0

Figure 2.3.1 - Structure-foundation system and free-field
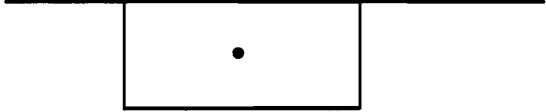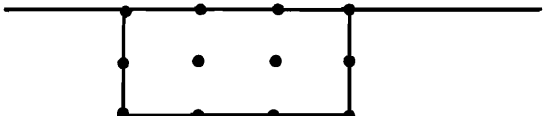
Method	Structure-foundation interface
Rigid Boundary	
Flexible Boundary	
Flexible Volume	

Figure 2.3.2 - Structure-foundation interface possibilities

Chapter 3
Parametric Study :
Structure-Foundation Interaction Effect

The main intention of this chapter is to indicate the class of problems where the interaction effect in dynamic analysis of the structure-foundation system is important. Since only qualitative results are sought, the analysis is performed utilizing some simplifying assumptions as discussed further. Two different types of structures have been considered : a typical high rise building (representative of flexible structures) and a concrete gravity dam (representative of stiff structures). The analysis is performed on reduced systems generated by Ritz vectors (as will be elaborated in the next chapter) with the SAP80 computer program (Wilson [1980]). In current practice, it is common to use time-history analysis with an artificially generated, spectrum-compatible, single ground motion. This approach neglects the fact that a smooth design response spectrum represents ensemble average of responses to different ground motions (see Clough&Penzien [1975]) and is a probabilistic description of an earthquake as a stochastic process (Lin [1967]). In addition, the time-history approach has been favored to accommodate the non-proportional damping that characterizes the problems under considerations. We employ the response spectrum approach (see Wilson et al. [1981]), since only the qualitative results are sought. This requires that consistent non-proportional damping be approximated by equivalent proportional damping. One possibility (Warburton&Sony [1977]), to simply neglect the off-diagonal terms in modal damping matrix, is easily adopted in our computations.

Remark 3.0.1 The response spectrum approach can be retained even for the non-proportional form of damping as demonstrated by Igusa&DerKiureghian [1983]. However, this requires generation of a complex Ritz vector basis which can be rather inefficient in applications to the problem on hand, as demonstrated in the next chapter.

3.1. Buildings

The primary interest of this parametric study is to establish the importance of the interaction effect for typical high rise buildings. To favor possible interaction effect, the study is performed with a foundation material that corresponds to soft soil deposits in Mexico City. A typical 2D frame is selected from a ten story office building damaged in 1985 Mexico City earthquake. The finite element models of the frame-foundation systems are presented on Figure 3.1.1. The models **frb1** and **frb2** are fixed base and simply supported frame models without the foundation, and **ff1** and **ff2** are frame foundation systems with different extent of the foundation domain, such that 80% and 90% of the total mass of the complete system is the mass of the foundation.

The free-field motion response spectra are calculated from the acceleration history of the 1985 Mexico City earthquake (SCT component S00E) and presented in Figure 3.1.2. The basic response quantities, fundamental period, frame base shear and top displacement, are used for the comparisons in dynamic analysis of the models in Figure 3.1.1.

Table 3.1.1.		Parametric Study of Frame-Foundation Interaction				
Model	Period (sec)	Ratio	Base Shear (kN)	Ratio	Top Displ. (m)	Ratio
frb1	1.674	0.976	6132	0.873	0.477	0.852
frb2	1.716	1.000	7026	1.000	0.560	1.000
ff1	1.750	1.020	7649	1.089	0.604	1.079
ff2	1.752	1.021	7696	1.095	0.609	1.088

It is obvious that the interaction effects for the soft structure such as the high rise building (fundamental period 1.674 - 1.752 sec.) are overall insignificant. There is almost no difference between the models with different foundation extent (**ff1** and **ff2**), once we have included the foundation extent that yields the dominant mass of the foundation in the complete system. We also note that the structure-foundation interaction effect may actually

increase response quantities, depending upon the particular earthquake record that analysis is performed for (although one should state this with caution, since the radiation damping is not modeled properly). This is even more pronounced for the parametric study presented in the Table 3.1.2. The analysis is performed on the finite element model ff1 with different mechanical properties for the foundation material.

Table 3.1.2.	Parametric Study of Foundation Flexibility				
Model	Shear Mod. (kN/m^2)	Mass Dens. (kg/m^3)	Period (sec)	Base Shear (kN)	Top Displ. (m)
frb2	-	-	1.716	7026	0.560
ff1	600000	1600	1.750	7649	0.604
ff1a	130000	1500	1.922	10716	0.856
ff1b	39000	1300	2.316	9245	0.609

To demonstrate the influence of a choice of a particular earthquake spectrum, a further parametric study compares the result for 1952 Taft earthquake (component S96E) with the equivalent ones for design earthquake presented on Figure 3.1.3. The equivalent design earthquake is constructed under the recommendations of Tentative Lateral Force Require-ments of Seismology Committee of California [1985] for the same peak ground acceleration of 0.1794 g (at 3.74 sec) as for the Taft earthquake. The analysis is performed for the models frb1 and ff1. The results, presented in Table 3.1.3., indicate a reduction in response due to the interaction effect (inverse to results in Table 3.1.1.), with approximately the same

ratio for both the Taft and the equivalent design earthquake.

Table 3.1.3.	Parametric Study of Sensitivity to Choice of Response Spectrum				
Model	Period (sec)	Base Shear (kN)		Top Displacement (m)	
-	-	Taft earth.	Design earth.	Taft earth.	Design earth.
frb2	1.716	1950	1737	0.148	0.121
ff1	1.750	1872	1730	0.138	0.117
Ratio	1.020	0.960	0.996	0.938	0.967

3.2. Gravity Dams

To demonstrate the interaction effect for the stiff structures, further parametric study is performed on the gravity dams. The model of the dam used in this analysis is similar to the Pine Flat Dam analyzed for hydrodynamic effects on dams by Chakrabarti&Chopra [1973]. In this analysis, hydrodynamic effects are completely disregarded (only hydrostatic pressure is considered). The finite element models **drb**, **df1 - df4** are presented on Figure 3.2.1. The largest model of the dam includes a total of 1154 degrees of freedom. The material properties for the dam and the foundation are given the same values : Young's modulus 22150 MN/m^2, mass density 2.5 kN sec^2/m^4 and Poisson ratio 0.25.

The first parametric study is performed on models of the dam-foundation system shown in Figure 3.2.1, which include different portions of foundation. The results of this

analysis are presented in Table 3.2.1.

Table 3.2.1.		Parametric Study of Dam-Foundation Interaction					
Model	Found. Ext.	Period (sec)	Ratio	Base Shear (kN)	Ratio	Top Displacement (m)	Ratio
drb	0	0.335	1.000	25078	1.000	0.030	1.000
df1	1.0	0.398	1.188	32889	1.311	0.043	1.428
df2	1.6	0.411	1.227	32160	1.282	0.043	1.418
df3	2.5	0.426	1.272	32705	1.304	0.042	1.392
df4	3.0	0.437	1.304	32210	1.284	0.042	1.384

In this case, the interaction effect is much higher than in the case of the high rise buildings. It appears that even the model with the foundation extent of the order of the dam base width yields almost converged values of the response quantities. This corroborates similar conclusions in Clough et al. [1984].

The sensitivity to the choice of a particular earthquake record (Taft earthquake) versus adequate smoothed design response spectrum is presented in Table 3.2.2.

Table 3.2.2.		Parametric Study of Sensitivity to Choice of Response Spectrum				
Model	Period (sec)	Base Shear (kN)		Top Displacement (m)	
-	-	Taft earth.	Design earth.	Taft earth.	Design earth.
drb	(. . .	22639	25078	0.031	0.030
df1	0.398	29051	32889	0.038	0.043
Ratio	1.188	1.283	1.311	1.226	1.417

The results presented by Clough et al. [1984] are obtained by utilizing the approximation of a *massless foundation*. This approximation was introduced so that the standard computer program they used could account for the structure-foundation interaction effect, adequate to formulation (3.3.10). To clarify the effect introduced by this approximation, we performed adequate analysis consistent with formulation (2.3.10). This comparison for model **ff1** is presented in Table 3.2.3.

Table 3.2.3.   Comparison of Consistent and Approximate Added Motion Formulations

Quantity		Massless Foundation	Consistent Model	Ratio
	T_1	0.396	0.398	1.005
p	T_2	0.195	0.204	1.046
e	T_3	0.160	0.178	1.113
r	T_4	0.111	0.138	1.243
i	T_5	0.070	0.103	1.471
o	T_6	0.067	0.093	1.388
d	T_7	0.051	0.086	1.686
	T_8	0.048	0.082	1.708
(sec)	T_9	0.040	0.078	1.950
	T_{10}	0.036	0.071	1.972
Base Shear	Taft earth.	29627	29051	0.981
(kN)	Design ear.	34211	32889	0.961
Top Displ.	Taft earth.	0.038	0.038	1.008
(m)	Design ear.	0.044	0.043	0.995

The response quantities in Table 3.2.3. obtained by two procedures, consistent and approximate, are in a very good agreement. However, this is mainly the consequence of the good approximation properties of the load dependent Ritz vectors utilized.

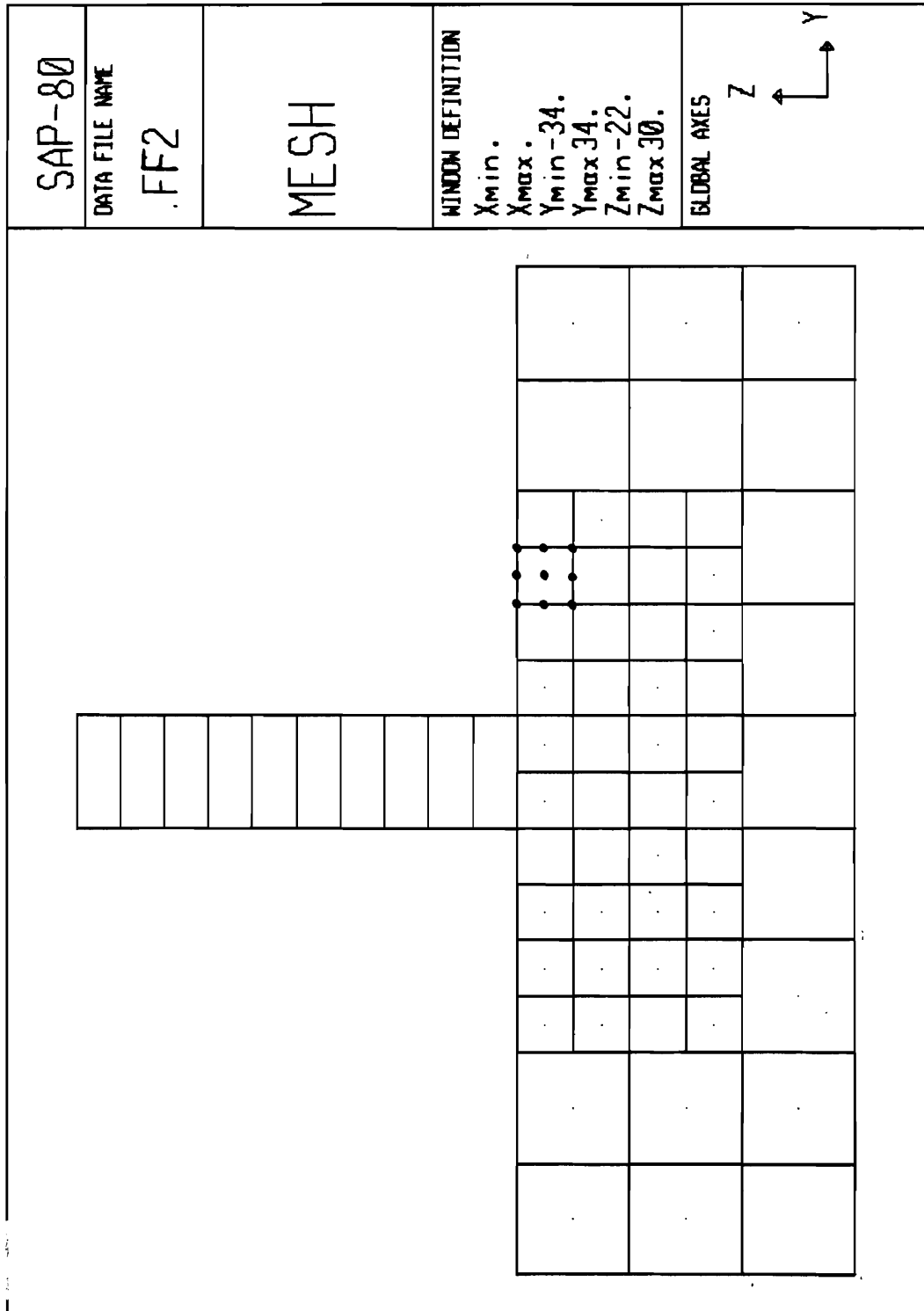**Figure 3.1.1 - Finite element models for frame-foundation systems**
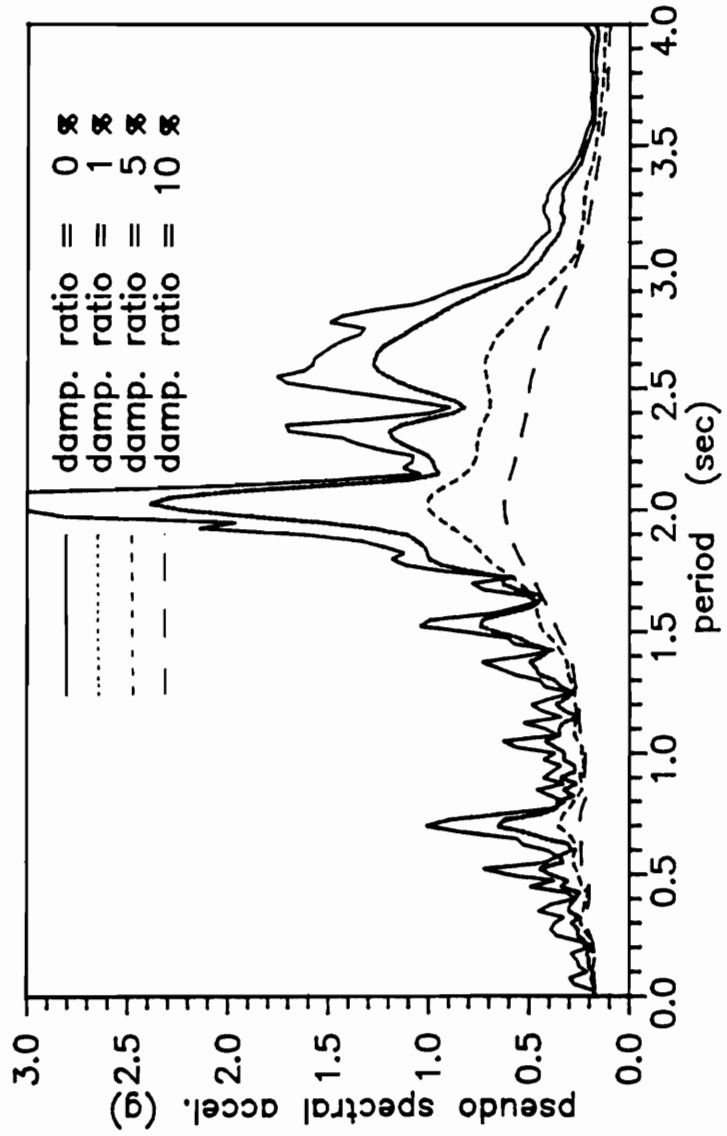
Figure 3.1.2 - 1985 Mexico City earthquake response spectra

**Figure 3.1.3 - 1952 Taft earthquake and design earthquake response spectra
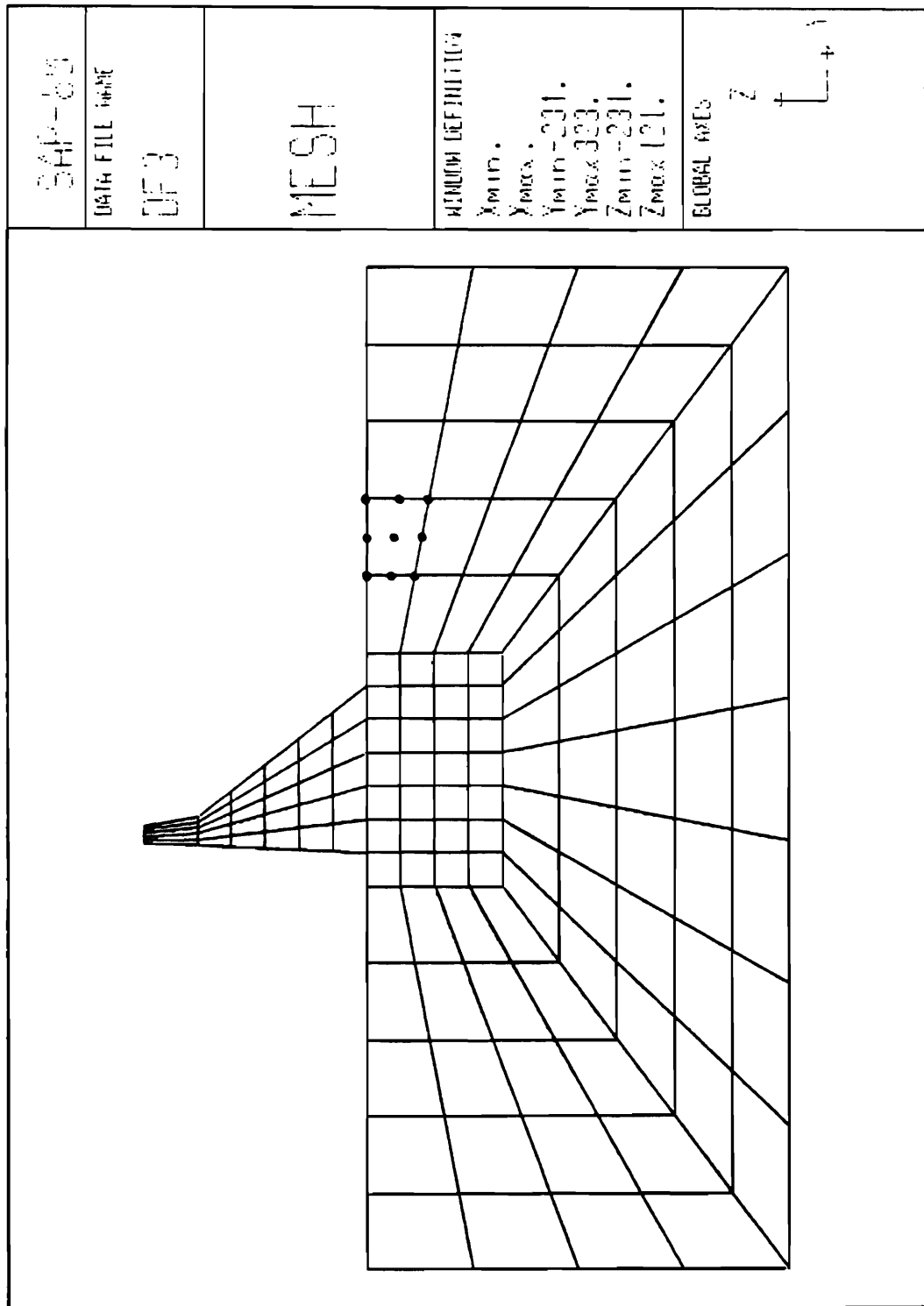(damping 5% of critical)**

Figure 3.2.1 - Finite element models for dam-foundation systems

Chapter 4
Numerical Procedures :
Linear Dynamic Analysis

The discretized models for dynamic analysis of structure-foundation systems commonly encountered in engineering practice have many dofs. To reduce the computational effort for the loading of long duration (such as earthquake loading) the modal analysis is usually used (see Wilson [1977]). In the process of selection of proper coordinate reduction scheme for the class of problems on hand, one has to consider two non-standard problems. First, the flexibility of the foundation (especially for 3D problems) requires a large subspace for modal analysis if eigenvectors are used. This problem can be successfully handled by the load dependent Ritz vector basis. Second, one has to account for the non-proportional damping form. Two methods based on complex and real Ritz vector basis are presented and compared. The techniques discussed in the first part of this chapter are then fitted within the context of dynamic substructuring, as a prelude to dynamic analysis of large linear system with local nonlinearities.

4.1. Coordinate Reduction Scheme - Modal Truncation

For the dynamic analysis of the linear systems, transformation to modal coordinates is usually performed, enhancing the computational efficiency by the modal truncation (Wilson [1977]). In other words, an approximate solution of the complete set of equations is sought by projecting them onto a subspace spanned by the chosen basis vectors. Rayleigh-Ritz approximations based on the static deflected shape (see Clough&Penzien [1975] or Agnosto-poulos [1982]), eigenvectors of the complete system (Bathe&Wilson [1976], Wilson&Itoh [1983]) and Krylov subspace (Nour&Clough [1984]) are three possibilities for generation of such a subspace. The quality of results obtained by this approximation depends on how

well the spatial distribution and the frequency content of loading are represented in the chosen subspace. It was observed (Nour&Clough [1984], Leger&Wilson [1987]) that the good representation of the loading spatial distribution within the generated Krylov subspace, improved results significantly with respect to adequate computation done by eigenvectors. Some truncation criteria for the loading representation within the generated Krylov subspace are developed, but no proper reference to possibly different frequency (spectral) content of excitation is given. Hence, we discuss the spectral content truncation criteria, which rely on concepts of the static correction (see Madox [1975] or Hansten&Bell [1979]). In passing, we also demonstrate the analogy of the static correction and mode acceleration (Cornwell et al. [1983]) methods.

Modal Dynamic Analysis of Linear System

The semidiscrete equations of motion for the linear system as given by (2.2.16) are

$$\mathbf{M} \ddot{\mathbf{u}}(t) + \mathbf{C} \dot{\mathbf{u}}(t) + \mathbf{K} \mathbf{u}(t) = \mathbf{f}(t) = \mathbf{f}_0 \, g(t) \tag{4.1.1}$$

Usual coordinate transformation (or projection onto subspace) is

$$\mathbf{u}_m(t) = \mathbf{\Phi}_m \, \mathbf{y}(t) \tag{4.1.2}$$

where $\mathbf{\Phi}_m = \left[\phi_1 \, \phi_2 \, ... \, \phi_m \right]$ is a set of projection vectors in Rayleigh-Ritz approximation (Clough&Penzien [1975]) and $\mathbf{y}(t) = (\, y_1, y_2, ... y_m \,)^T$ is a set of truncated modal coordinates.

If $\mathbf{\Phi}_m$, as the eigenvectors of the associated undamped system to (4.1.1) (that neglects $\mathbf{C}$), are to be employed in transformation (4.1.2), then the general linear eigenvalue problem given below has to be solved first.

$$\mathbf{K} \, \mathbf{\Phi}_m - \mathbf{\Omega}_m^2 \, \mathbf{M} \, \mathbf{\Phi}_m = \mathbf{0} \tag{4.1.3}$$

Introducing the transformation (4.1.2) into the equations (4.1.1) new set of differential equations is defined on the subspace

$$\ddot{\mathbf{y}}(t) + \mathbf{C}_m \, \dot{\mathbf{y}}(t) + \mathbf{\Omega}_m^2 \, \mathbf{y}(t) = \mathbf{f}_m(t) \tag{4.1.4}$$

where

$$\Phi_m^T M \Phi_m = I$$

$$\Phi_m^T C \Phi_m = C_m \qquad (4.1.5)$$

$$\Phi_m^T K \Phi_m = \Omega_m^2 = diag \ (\omega_i^2)$$

$$\Phi_m^T f(t) = f_m(t)$$

If, for the moment, we consider only a proportional damping matrix (e.g. Rayleigh damping), the equation set (4.1.4) can be restated in the uncoupled form, since : $C_m = diag$ (2 $\xi_i \ \omega_i$). However, this is not a crucial restriction for the present considerations. In the next section we consider the efficient ways to solve the coupled set of modal equations for a non-proportional damping by both mode summation and mode acceleration methods.

Remark 4.1.1. More generally, the uncoupled form of the equations of motion (4.1.4) can be obtained if the damping matrix C shares the same eigenvectors of (4.1.3). Caughey [1960] gives the power series for $C = M \sum_{j \le n} a_j \ (M^{-1} \ K)^j$ that yields the uncoupled modal equations of motion. By the spectral decomposition theorem (see Parlett [1980]), j - th powers of mass M and stiffness matrix K can be computed as :

$$M^j = \sum_{i=1}^{n} \phi_i \ \phi_i^T, K^j = \sum_{i=1}^{n} \omega_i^{2 \ j} \ \phi_i \ \phi_i^T$$

As generally n-dimensional, the loading vector can be represented in the complete set of modal coordinates as

$$f(t) = K \ \Phi \ y(t) = \sum_{i=1}^{m} K \ \phi_i \ y_i(t) + \sum_{i=m+1}^{n} K \ \phi_i \ y_i(t) = f_m(t) + f_l(t) \qquad (4.1.6)$$

where $f_m(t)$ is the loading representation in m-dimensional subspace spanned by Φ_m vector basis, while $f_l(t)$ (with $l = n-m$) is the loading component orthogonal to that subspace, due to the orthogonality property of the eigenvectors. Therefore, the response obtained in the selected subspace will not contain contribution of the loading component $f_l(t)$. The

methods we discuss differ in the way by which an approximation for the loading component $f_i(t)$ is provided.

(a) Static Correction and Mode Acceleration

The static correction concept (see Madox [1975] and Hansten&Bell [1979]) is one way to account for the normal component of the loading $f_i(t)$ in an approximate static fashion. Successful application of the static correction concept requires the proper account of the frequency content of the loading. This we address in the next section.

One modal equation in the completely uncoupled set (4.1.4) can be written

$$\ddot{y}_i(t) + 2\,\xi_i\,\omega_i\,\dot{y}_i(t) + \omega_i^2\,y_i(t) = f_i(t)\,, \quad i = 1,2,\ldots n \tag{4.1.7}$$

For usual modal truncation dynamic response is computed by the solution of the equation (4.1.7) for a number of equations m smaller than the complete set n. For the rest of the modal equations $(m>n)$ the solution is obtained as the static response that follows from the equation (4.1.7) disregarding inertial and damping forces. Hence the complete response by the static correction method is readily obtained as:

$$\mathbf{u}(t) = \sum_{i=1}^{m} \boldsymbol{\phi}_i\,y_i(t) + \sum_{i=m+1}^{n} \frac{1}{\omega_i^2}\,\boldsymbol{\phi}_i\,f_i(t) = \sum_{i=1}^{m} \boldsymbol{\phi}_i\,y_i(t) + \sum_{i=m+1}^{n} \frac{1}{\omega_i^2}\,\boldsymbol{\phi}_i\,\boldsymbol{\phi}_i^T\,\mathbf{f}(t) \tag{4.1.8}$$

or rearranging the summation

$$\mathbf{u}(t) = \sum_{i=1}^{n} \frac{1}{\omega_i^2}\,\boldsymbol{\phi}_i\,\boldsymbol{\phi}_i^T\,\mathbf{f}(t) + \sum_{i=1}^{m} \boldsymbol{\phi}_i\left(y_i(t) - \frac{1}{\omega_i^2}\,f_i(t)\right) \tag{4.1.9}$$

The first part of the equation (4.1.9) represents the spectral decomposition of the inverse of stiffness matrix, since by the spectral theorem (Parlett [1980]) it holds :

$$\mathbf{K}^{-1} = \sum_{i=1}^{n} \omega_i^{-2}\,\boldsymbol{\phi}_i\,\boldsymbol{\phi}_i^T \tag{4.1.10}$$

where $\boldsymbol{\phi}_i,\omega_i$ are the solutions for eigenpairs of the complete set of equations (4.1.3) i.e. for $m=n$. For the sake of compact notation we introduce

$$- \sum_{i=1}^{m} \phi_i \, \frac{1}{\omega_i^2} \, f_i(t) = - \sum_{i=1}^{m} \frac{1}{\omega_i^2} \, \phi_i \, \phi_i^T \, \mathbf{f}(t) = - \, \Phi_m \, \Omega_m^{-2} \, \Phi_m^T \, \mathbf{f} = - \, \mathbf{K}_m^{-1} \, \mathbf{f}(t) \quad (4.1.11)$$

Hence, we arrive to computational form of the equation (4.1.9)

$$\mathbf{u}(t) = \sum_{i=1}^{m} \phi_i \, y_i(t) + \left(\mathbf{K}^{-1} - \mathbf{K}_m^{-1} \right) \mathbf{f}(t) \quad (4.1.12)$$

Analogy of the static correction method (Hansten&Bell [1979]) to the mode acceleration (Cornwell et al. [1983]) can be easily demonstrated by rewriting the modal equation (4.1.7) in the form :

$$- \frac{1}{\omega_i^2} \, \ddot{y}_i(t) - \frac{2 \, \xi_i}{\omega_i} \, \dot{y}_i(t) = y_i(t) - \frac{f_i(t)}{\omega_i^2} \quad (4.1.13)$$

and further employing the relation (4.1.13) in the equation (4.1.9) we arrive at mode acceleration method (Cornwell et al. [1983]) given by :

$$\mathbf{u}(t) = \mathbf{K}^{-1} \, \mathbf{f}(t) - \sum_{i=1}^{m} \phi_i \left(\frac{\ddot{y}_i(t)}{\omega_i^2} + \frac{2 \, \xi \, \dot{y}_i(t)}{\omega_i} \right) \quad (4.1.14)$$

(b) Combination of Exact Particular and Approximate Homogeneous Solution

Another possibility for improving the approximation properties of a subspace formed by the exact eigenvectors is stated by Borino&Muscolino [1986] in application to the system of first order differential equations. The transformation of equations (4.1.1) to first order system (size $2n \times 2n$) is introduced as a standard way to deal with the non-proportional damping. Here we derive the equations in direct application to second order system (size $n \times n$) and leave the discussion of an efficient way to handle non-proportional damping within so formed subspace for the next section.

Solution of the set of linear ordinary differential equations, which, from mathematics standpoint, the semidiscrete equations of motion are, can always be obtained as a direct summation of the solution of an appropriate set of homogeneous equations and a particular

solution. In the computational sense, this approach could be considered if a particular solution is easily obtained. One case like that is for the piece-wise linear excitation with the fixed spatial loading distribution which has direct application to the dynamic analysis of structural system under earthquake excitation (specified as discrete acceleration record).

Namely, if the loading variation in the equation (4.1.1) within one step is

$$\mathbf{f}(t) = \mathbf{f}_0 \left(a_0 + a_1 t \right) \quad , \quad \dot{\mathbf{f}}(t) = \mathbf{f}_0 \, a_1 \tag{4.1.15}$$

The particular solution of the equations (4.1.1) for the loading variation in (4.1.15) is then

$$\mathbf{u}_p(t) = \mathbf{K}^{-1} \, \mathbf{f}(t) - \mathbf{K}^{-1} \, \mathbf{C} \, \mathbf{K}^{-1} \, \dot{\mathbf{f}}(t) \tag{4.1.16}$$

which could be checked by the direct substitution of (4.1.16) into the equations (4.1.1).

Solution of the homogeneous equations set can be approximated from the subspace as the difference between the complete solution and a particular solution for reduced set (4.1.4):

-first the solution in modal coordinates

$$\mathbf{y}_{mh}(t) = \mathbf{y}_m(t) - \mathbf{y}_{mp}(t) = \mathbf{y}_m(t) - \mathbf{\Omega}_m^{-2} \, \mathbf{f}_m(t) + \mathbf{\Omega}_m^{-2} \, \mathbf{C}_m \, \mathbf{\Omega}_m^{-2} \, \dot{\mathbf{f}}_m(t) \tag{4.1.17}$$

-transformation to global coordinates

$$\mathbf{u}_h(t) = \mathbf{\Phi}_m \, \mathbf{y}_{mh}(t) = \mathbf{\Phi}_m \, \mathbf{y}_m(t) - \mathbf{\Phi}_m \, \mathbf{\Omega}_m^{-2} \, \mathbf{\Phi}_m^T \, \mathbf{f}(t) +$$

$$\mathbf{\Phi}_m \, \mathbf{\Omega}_m^{-2} \, \mathbf{\Phi}_m^T \, \mathbf{C} \, \mathbf{\Phi}_m \, \mathbf{\Omega}_m^{-2} \, \mathbf{\Phi}_m^T \, \dot{\mathbf{f}}(t) \tag{4.1.18}$$

By utilizing the compact notation introduced by (4.1.11) again and combing the equations (4.1.16) and (4.1.18) we can get the final form for the computational purposes

$$\mathbf{u}(t) = \sum_{i=1}^{m} \phi_i \, y_i(t) + \left(\mathbf{K}^{-1} - \mathbf{K}_m^{-1} \right) \mathbf{f}(t) - \left(\mathbf{K}^{-1} \, \mathbf{C} \, \mathbf{K}^{-1} - \mathbf{K}_m^{-1} \, \mathbf{C} \, \mathbf{K}_m^{-1} \right) \dot{\mathbf{f}}(t) \tag{4.1.19}$$

The equation (4.1.19) differs from the static correction equation (4.1.12) only by the additional third term on the right hand side. It was observed in Borino&Muscolino [1986]

that in the case of a small time step employed usually in dynamic response computation due to earthquake excitation, the contribution of this term was very small and additional computational expense arising due to the inclusion of this term may not be justified.

(c) Load Dependent Vector Algorithm

In the first version of the load dependent algorithm (Wilson et al [1982]), the complete analogy existed in the computational process to Lanczos algorithm with full orthogonalization (Lanczos [1950]). However, the idea has initiated from the static correction concept, not from the intent of eigenvalues computation. Further modification of the algorithm in Leger&Wilson [1987] put higher emphasis on the role of the initial static deflected shape which has been updated and added to the basis optionally, but without the adequate reference to excitation spectral content. In this modification of load dependent vector algorithm we refer to the spectral content of excitation to properly account for the static correction concept. The analogy that exists between the Lanczos algorithm with the selective orthogonalization and the load dependent vector algorithm used herein is utilized in defining orthogonalization strategy.

The load dependent vector algorithm we use, is the same as the original proposed by Wilson et al. [1982], except that the reorthogonalization procedure is performed with respect to previous two vectors only :

-set starting vector

$$r_0 = K^{-1} f$$

$$q_0 = 0 \qquad\qquad\qquad\qquad\qquad\qquad\qquad (4.1.20)$$

$$\beta_1 = \sqrt{r_0^T M r_0}$$

$$q_1 = r_0 / \beta_1$$

-for j=1,2,...m

$$f_j = K^{-1} M q_j - q_{j-1} \beta_j$$

$$\alpha_j = \mathbf{q}_j^T \mathbf{M} \, \hat{\mathbf{f}}_j$$

$$\mathbf{r}_j = \hat{\mathbf{f}}_j - \mathbf{q}_j \, \alpha_j \qquad\qquad (4.1.21)$$

$$\beta_{j+1} = \sqrt{\mathbf{r}_j^T \mathbf{M} \, \mathbf{r}_j}$$

$$\mathbf{q}_{j+1} = \mathbf{r}_j \, / \, \beta_{j+1}$$

The algorithm given above will produce a set of Lanczos vectors $\mathbf{Q}_m = [\mathbf{q}_1, \mathbf{K}^{-1} \mathbf{M} \, \mathbf{q}_1, \dots , (\mathbf{K}^{-1} \mathbf{M})^{m-1} \, \mathbf{q}_1]$ which spans Krylov subspace. Alternative possibility to span Krylov subspace is by Ritz vectors $\mathbf{\Psi}_m$ (approximation for eigenvectors of the large system) that can be determined after the solution to standard eigenvalue problem for $\mathbf{T}_m = \mathbf{Q}_m^T \mathbf{M} \mathbf{K}^{-1} \mathbf{M} \mathbf{Q}_m$ is obtained.

$$\mathbf{T}_m \mathbf{Z} = \mathbf{\Lambda}_m \mathbf{Z} \, , \qquad \mathbf{Z}^T \mathbf{Z} = \mathbf{I} \, , \qquad \mathbf{\Lambda}_m \approx \mathbf{\Omega}_m^{-2}$$

$$\mathbf{\Psi}_m = \mathbf{Q}_m \mathbf{Z} \, , \qquad \mathbf{\Psi}_m \approx \mathbf{\Phi}_m \qquad\qquad (4.1.22)$$

The load dependent vector algorithm, as defined by the equations (4.1.20) and (4.1.21), can be carried out only in the exact arithmetics. In numerical computations the accumulation of roundoff errors has similar effect like in inverse iteration Stodola method used for computing several fundamental eigenvalues (Clough&Penzien [1975]). Error analysis, first performed by Paige [1971] and later elaborated by Parlett [1980], hinges upon following two statements :

- measure of approximation for eigenpair (ϕ_i, ω_i^2) by Ritz pair (ψ_i, λ_i)

$$\| \mathbf{K}^{-1} \mathbf{M} \, \psi_j - \psi_j \, \lambda_j \|_M = \| \beta_{j+1} \, \mathbf{q}_{j+1} \, \mathbf{e}_j^T \mathbf{z} \|_M = \left| \beta_{j+1} \, \mathbf{e}_j^T \mathbf{z} \right|$$

-measure of orthogonality of Ritz vector and Lanczos vector

$$\left| \psi_i^T \mathbf{M} \, \mathbf{q}_{j+1} \right| = \frac{const. \ \varepsilon \ \| \mathbf{K}^{-1} \mathbf{M} \|_M}{\left| \beta_{j+1} \, \mathbf{e}_j^T \mathbf{z} \right|} \qquad\qquad (4.1.23)$$

where :

$$\mathbf{e}_j^T = \begin{pmatrix} 0 & 0 & .. & 0 & 1 \end{pmatrix} \quad \text{and} \quad \|\mathbf{q}_j\|_M = \mathbf{q}_j^T \mathbf{M} \mathbf{q}_j = 1$$

Namely, convergence of Ritz value (occurring when the right hand side of (4.1.23[1]) becomes very small) will cause the loss of orthogonality between Lanczos vectors and Ritz vector, (note that the inner product (4.1.23[2]) becomes equal to the quotient of roundoff error ε and a very small value). In that case, we have to perform selective orthogonalization (see Parlett [1982]). As soon as eigenvalue $\lambda_i = \omega_i^{-2}$ converges (at step j, say), we compute the corresponding Ritz vector $\psi_i = \phi_i$, and orthogonalize against it the new Lanczos vector $\mathbf{q}_{j+1}$ (and also $\mathbf{q}_{j+2}$ at the next step). Orthogonalization also has to be performed with respect to previously converged Ritz vectors (The reason for that is given by the second part of Paige theorem). This task requires monitoring stabilization of eigenvalues of tridiagonal matrix $\mathbf{T}_j$ at each step j. For this we use the scheme developed previously by Parlett&Nour [1985].

Spectral Content Truncation Criteria

Spectral content truncation criterion is easily obtained for the loading of the special form separable in space and time :

$$\mathbf{f}(t) = \mathbf{f}_0 \, g(t) \tag{4.1.24}$$

The special form of loading given in (4.1.24) is required for successful application of load dependent vector algorithm. It also enhances the computational efficiency for the static correction method, since the first term in the equation (4.1.9) has to be obtained only once and can be used throughout if scaled appropriately by the value $g(t_i)$.

(a) Static Correction and Mode Acceleration

The easiest loading case that enables proper account of the static correction is harmonic excitation (e.g. $g(t) = \sin \bar{\omega} \, t$). For that loading we consider one modal equation :

$$\ddot{y}_i(t) + 2 \, \xi_i \, \omega_i \, \dot{y}_i(t) + \omega_i^2 \, y_i(t) = f_{0i} \, \sin\bar{\omega} \, t \qquad (4.1.26)$$

with a particular solution given :

$$y_i(t) = \frac{f_{0i} \, / \omega_i^2}{\sqrt{\left(1-\beta_i^2\right)^2 + \left(2 \, \xi_i \, \beta_i\right)^2}} \, \sin\left(\bar{\omega}t - \theta_i\right) \qquad (4.1.27)$$

$$\theta_i = \tan^{-1} \frac{2 \, \xi_i \, \beta_i}{1-\beta_i^2} \, , \quad \beta_i = \frac{\bar{\omega}}{\omega_i}$$

For different values of ratio $\beta = \dfrac{\bar{\omega}}{\omega}$ maximum dynamic response is plotted on Figure 4.1.1 versus maximum static response ($\dfrac{f}{\omega^2}$)

From Figure 4.1.1, the spectral truncation criteria for the harmonic excitation and usual values of damping in engineering structures follow as :

(i)   For $\dfrac{\bar{\omega}}{\omega} < 0.25$ static correction will give excellent results

(ii)   For $0.25 < \dfrac{\bar{\omega}}{\omega} < 1.25$ static correction will always improve results but not always considerably

(iii)   For $\dfrac{\bar{\omega}}{\omega} > 1.6$ static correction, if applied, will yield incorrect results that overestimate the response

It should be stated that for the harmonic excitation the static correction method need not be used. The exact steady-state response can be obtained directly by

$$y = b_1 \sin\bar{\omega}t + b_2 \cos\bar{\omega}t \qquad (4.1.28)$$

where

$$b_1 = \left(K_{\bar{\omega}} + \bar{\omega}^2 \, C \, K_{\bar{\omega}}^{-1} \, C \right)^{-1} f_0$$

$$b_2 = -\bar{\omega} \, K_{\bar{\omega}}^{-1} \, C \, b_1 \qquad\qquad (4.1.29)$$

$$K_{\bar{\omega}} = K - \bar{\omega}^2 \, M$$

For the general excitation form $g(t)$ some measure of spectral content has to be obtained to provide similar truncation criteria as in the case of the harmonic excitation. Fourier amplitude spectrum is one possibility to provide the measure of total vibrational energy at the end of the specified time period (see Hudson [1979]). Fast Fourier transform (Clough&Penzien [1975]) should be used for efficient computation.

Another measure of the spectral content of excitation common in earthquake engineering is the response spectrum. Pseudo-velocity response spectrum (Hudson [1979]) provides the maximum strain energy measure over the excitation spectrum. Adequate measure for strain energy arises in random excitation theory in terms of power spectra density (see Lin [1967]).

The spectral content truncation criteria for the general excitation form are discussed further within presentation of some numerical results.

(b) Load Dependent Vector Algorithm

The choice of starting vector as static deflected shape to fixed loading spatial distribution is what separates load dependent vector algorithm we use from Lanczos algorithm with selective orthogonalization (Parlett [1980]). For the dynamic response computation, the static vector will prevent generation of eigenvectors orthogonal to loading and will also utilize the static correction concept. To provide the analogy to the static correction concept the convergence of Ritz values within the dominant frequency range should be obtained, while the static correction (chosen as starting Lanczos vector) will be retained in the subspace spanned by nonconverged remaining Ritz vectors.

Hence, in the load dependent vector algorithm we use one termination criterion is the convergence of all eigenvalues within specified interval. Another truncation criterion is ensurance of good representation of loading spatial distribution within truncated subspace.

Numerical Results

Example 4.1.1 - Two degrees of freedom system

The first numerical example that we present here aims to clarify the role of frequency content of the loading excitation in the context of static correction method. The simple two degrees of freedom model presented on Figure 4.1.2 is used with the loading variation specified first as the harmonic sinusoidal function.

The error in the approximate maximum response for the displacement at node 2, (computed by one mode only and one mode supplemented with the static correction for the second mode), is presented in Table 4.1.1, for the different values of exciting frequency $\bar{\omega}$.

The exact response is computed by utilizing the equation (4.1.28).

Table 4.1.1	Ratio of $\dfrac{x_{2exact} - x_{2approx.}}{x_{2approx.}}$	
Freq. (rad/sec)	One Mode Only	Stat. Cor.
5	0.0526	0.0005
10	0.0439	0.0018
15	0.0248	0.0023
20	0.0035	0.0005
25	0.0426	0.0084
30	0.1318	0.0487
35	0.2298	0.0952
40	0.4142	0.2024
45	1.4707	0.9844
50	11.9550	9.4474
100	0.4972	4.7082

It is obvious that the results obtained for practical system analysis completely reinforce the spectral content truncation criteria (i), (ii) and (iii). For this example with $\omega_2 =$ 51.17 rad/sec for all harmonic excitation with the frequency $\bar{\omega} \leq 25$ rad/sec the static correction yields the results that are within 1% from the exact. For the harmonic excitation with $\bar{\omega} = 100$ rad/sec the static correction actually introduces larger errors than if completely omitted. However, this case of high exciting frequency is of rare occurrence in practical engineering problems and benefits of the static correction are almost always ensured (when the proper account to the spectral content of excitation is taken in modal transformation).

To provide the spectral content truncation criteria for general excitation form (adequate to (i),(ii) and (iii) for harmonic excitation) a series of simulated earthquake motions is

generated from filtered white noise given by Kanai-Tajimi filter with one-sided power spectra density as :

$$G(\omega) = G_0 \frac{\omega_g^4 + 4\,\xi_g^2\,\omega_g^2\,\omega^2}{\left(\omega_g^2 - \omega^2\right)^2 + 4\,\xi_g^2\,\omega_g^2\omega^2}$$

(4.1.30)

The values of dominant frequency ω_g and damping ratio ξ_g for the filter are varied over the range of frequencies specified on Figure 4.1.3.

The time variation of the loading is computed from decomposition of normal stationary process by

$$\ddot{u}_g = \sum_{i=0}^{N} \sqrt{2\,\Delta\omega\,\,G(\omega_i)}\,\cos\left(\omega_i\,t + \phi_i\right)$$

(4.1.31)

where ϕ_i is uniformly distributed random phase in the interval $(0, 2\pi)$.

To demonstrate the analogy between these simulated earthquake motions and the real earthquake records in application to our problem, the computation is repeated for ground acceleration records of 1952 Taft earthquake and 1985 Mexico City earthquake. Fourier amplitude spectra (as the measures of energy) for these earthquake records are presented on Figures 4.1.4 and 4.1.5.

The displacement at node 2 and the force in element 2 are both computed by one mode contribution only and by one mode supplemented with the static correction for second mode and divided by the appropriate exact response quantity (for 2 modes included). The

results of this analysis are given in Table 4.1.2.

Table 4.1.2	Ratio of Approximate and Exact Maximum Response				
Simulated	earthquake	Node 2	Displacement	Elem. 2	Force
ω_g (rad/sec)	ξ_g	1 Mode/Exact	St.Cor./Exact	1 Mode/Exact	St.Cor./Exact
2 π	0.3	0.972	0.995	0.837	0.989
4 π	0.5	0.971	1.009	0.799	0.994
5 π	0.6	0.963	0.976	0.758	0.840
Mexico	earthquake	0.987	0.999	0.917	0.991
Taft	earthquake	1.038	1.033	0.748	0.919

Obviously, from the Table 4.1.2 above, for earthquake record that can be characterized as narrow band random process (such as Mexico City earthquake or simulated earthquake by filter with $\omega_g = 2\pi$, $\xi_g = 0.3$) the static correction concept applied adequately with respect to excitation frequency content yields excellent approximate results all within 1% from the exact solution. However, in the case of broad band random process (such as Taft earthquake or simulated earthquake by filter with $\omega_g = 5\pi$, $\xi_g = 0.6$) the static correction concept certainly improves results but does not make them accurate.

From the analysis to simulated earthquake motions we can state that for the general loading form spectral content truncation criterion (i) can be even further relaxed to :

(i[1]) for all the modes with $\omega \geq$ two times the maximum frequency of interest in general excitation spectrum the static correction will provide excellent approximation to the exact response.

Example 4.1.2 - Truss structure

The second example is a truss structure presented on Figure 4.1.6. It is similar to the one analyzed previously by Lanczos vectors (Nour&Clough [1984]), which are just a different basis for the same Krylov subspace we use spanned by Ritz vectors. The structure has 100 degrees of freedom with 170 two dimensional truss elements. The fundamental period is chosen as $T_1 \approx 1$. sec.

The excitation used in computation is simulated earthquake motion with power spectra densities presented on Figure 4.1.3 for filter characteristics $\omega_g = 4\pi$, $\xi_g = 0.5$. The analysis of this example should indicate the relation of the frequency content and the loading participation as two different cut-off criteria in generating the Krylov subspace in the case of earthquake excitation.

The spatial representation of the loading within generated Krylov subspace is defined in Leger&Wilson [1987] for general loading form and earthquake excitation. For earthquake excitation participating mass is currently used method (specified by the API recommended practise for planning designing and constructing fixed offshore platforms [1980] as 90%). It is defined by Leger&Wilson [1987] :

$$e_{j,m} = \left[1 - \left(M_{j,m} / M_j \right) \right] \times 100 \quad (\%) \tag{4.1.32}$$

where

$$M_j = r_j^T \, M \, r_j \tag{4.1.33}$$

$$M_{j,m} = r_j^T \, M \, \Psi_m \, \Psi_m^T \, M \, r_j$$

and r_j is influence vector (Clough&Penzien [1975]) that accounts for direction of earthquake excitation.

For general loading form it is recommended in Leger&Wilson [1987] that error in representation of loading spatial distribution be computed as :

$$e_{j,m} = \left[\frac{\|\mathbf{f}_j - \mathbf{f}_{j,m}\|_2}{\|\mathbf{f}_j\|_2} \right] \times 100 \quad (\%) \tag{4.1.34}$$

where

$$\mathbf{f}_{j,m} = \mathbf{M} \, \mathbf{\Psi}_m \, \mathbf{\Psi}_m^T \, \mathbf{f}_j \tag{4.1.35}$$

and

$$\mathbf{f}_j = \mathbf{r}_j \, \mathbf{f}$$

The error norm for general loading spatial representation (4.1.34) indicates that exact eigenvectors subspace will not ensure convergence if the loading is applied at massless degree of freedom.

Two fixed loading distributions were used : one that corresponds to "directional" mass for horizontal earthquake ground motion and another, that corresponds to wave loading on offshore platform, specified as horizontal concentrated force at second story level. All damping ratios are given the constant value that equals 2%. The results of the analysis are presented in Tables 4.1.3,4,5 and 6.

The maximum response for top story displacement and axial force in bottom story diagonal element were computed within the Krylov subspace generated by different number of Ritz vectors and compared with the exact solution (computed with all 100 vectors used). Computation is performed by employing the exact solution for piece-wise linear excitation of simulated earthquake specified at $\Delta t = 0.01$ sec. The results of the analysis are given

next.

Table 4.1.3	Ratio of Approximate and Exact Maximum Response			
Loading	Earthquake		Concentrated Force	
No. of Vectors	Top Disp.	Ax. Force	Top Disp.	Ax. Force
4	0.988	1.049	0.780	1.984
5	0.998	0.959	0.990	0.924
10	1.000	1.001	0.993	0.961
15	1.000	1.001	0.998	0.986
20	1.000	1.001	0.998	0.987

Frequency spectrum of matrix pencil (K,M) for the first 19 eigenvectors as well as the highest frequency are given in Table 4.1.4.

Table 4.1.4	Frequency Spectrum of Matrix Pencil (K,M)						
No.	ω_i (rad/sec)	No.	ω_i (rad/sec)	No.	ω_i (rad/sec)	No.	ω_i (rad/sec)
1	5.323	6	35.416	11	49.165	16	59.641
2	11.749	7	35.514	12	54.183	17	60.807
3	15.625	8	43.775	13	54.945	18	63.086
4	29.115	9	47.143	14	55.515	19	63.485
5	⠂⠆⠄	10	48.568	15	57.974	100	180.83

The number of converged frequencies (and exact eigenvectors) as well as the highest Ritz value (frequency approximation referred yet as spectrum end $\hat{\omega}_m$) within the Krylov subspace generated in computations we performed are given in Table 4.1.5 bellow for

different numbers of vectors.

Table 4.1.5	Number of Converged Frequencies and Spectrum End $\hat{\omega}_m$			
Loading	Earthquake		Concentrated Force	
No. of Vectors	No. Conv. Freq.	$\hat{\omega}_m$ (rad/sec)	No. Conv. Freq.	$\hat{\omega}_m$ (rad/sec)
4	0	46.743	0	41.957
5	1	63.686	0	68.812
10	2	119.188	3	111.122
15	4	146.335	3	133.300
20	5	163.435	4	142.156

For different numbers of vectors retained in generated Krylov subspace we summarize errors in representation of the loading spatial distribution in Table 4.1.6. For the concentrated force, the error in spatial distribution of loading is given by the equation (4.1.34), while for horizontal earthquake excitation the error in representation of "directional" partici-

pating mass is stated as defined by equation (4.1.32).

Table 4.1.6	Errors in Spatial Loading Representation	
Loading	Earthquake	Concentrated Force
No. of Vectors	$e_{j,m}$ (%)	$e_{j,m}$ (%)
4	0.96	73.00
5	0.94	49.36
10	0.62	4.91
15	0.40	0.29
20	0.36	0.01
100	0.00	0.00

For loading distribution in the form of directional mass for horizontal earthquake almost exact displacements (within 1% from the exact solution) are obtained with only 4 Ritz vectors. However, for the same accuracy of the axial force recovery as many as 10 vectors are needed. On the other hand, the participating mass as an spatial distribution truncation criterion indicate that errors sholud be less then 1% for all vector sets. Hence, the participating mass can be overly optimistic criterion for accuracy of stress recovery.

For the concentrated force where the different measure for loading spatial distribution, as defined in (4.1.34), is used, the accuracy of force recovery is better related to error norm. Accurate approximate solution for this case requires the set of 15 Ritz vectors. It is impor-t⋅ note the large overestimate of axial force value which occurs for the set of 4 Ritz v⋅, rs in modal transformation (Table 4.1.3). This reinforces the truncation criterion (iii), since in this case the static correction (used as a starting vector) is applied to the modes below the frequency range of interest. The similar phenomenon is previously noted in Agnostopoulos [1982].

In both loading cases, the convergence of eigenvalues within a range of interest (for this case of excitation ≈ 15 rad/sec) is encountered coincidentally with the satisfaction of truncation criterion for spatial representation. This result is very important since it indicates that for the excitation characterized by narrow band spectrum only the spatial representation needs to be monitored in the progress of algorithm. Hence, the original load dependent vector algorithm (Wilson et al. [1982]), with full orthogonalization and spatial truncation criterion only, is quite sufficient in the case of narrow band earthquake and wave loading.

Remark 4.1.2. The primary objective of this section was to generate a subspace for dynamic analysis to loading of special form separable in space and time which has direct application to earthquake excitation. To accommodate a general loading form, vector function $f(t)$ can be expressed in Fourier series form : $f(t) = \sum_{j=1}^{k} f_{j0} \ g_j(t)$ and each series component treated separately. Block Lanczos method (see Nour&Clough [1985]) is ideally suited for such a case. To provide good quality of results engineering judgment has to be exercised in constructing the loading series form for a particular problem.

4.2. Method for Non-Proportional Damping

Several possibilities exist, as given by Clough&Mojtahedi [1976], to treat the non-proportionally damped dynamic linear system by mode superposition procedure within the framework of real eigenvector basis. Rigorous procedure to devise the coordinates that uncouple equations of motion utilizes complex vector basis for modal transformation given by Foss [1958] or Veletsos&Ventura [1986].

Recent research (see Wilson et al. [1982], Nour&Clough [1984] and Lagar&Wilson [1987]) indicated superiority of Lanczos algorithm for use in Rayleigh-Ritz procedure for generating vector basis for mode superposition in the case of proportional damping. It is to be expected that fast convergence properties of Krylov subspace for the dynamic analysis will be retained in the case of linear systems with the non-proportional damping.

Two procedures for generating real and complex vector basis by Lanczos algorithm are compared in this section. The real vector basis is generated by the Lanczos algorithm with selective orthogonalization (see Parlett [1980]), and numerical integration of modal equations coupled by velocity proportional forces is performed by an efficient iterative procedure described further. The complex vector basis is generated by the Lanczos algorithm described in Chen&Taylor [1988].

Modal Summation for Non-Proportional Damping

The set of vectors Φ_m generated either as the exact eigenvectors or Ritz vectors by using only stiffness and mass matrix will not uncouple equations of motion transformed in modal coordinates due to coupling of velocity proportional forces in the case of the non-proportional damping.

In this case, the modal equations (4.1.7) can be rewritten as

$$\ddot{y}_i(t) + \sum_{j=1}^{m} C_{m_{ij}} \dot{y}_j(t) + \omega_i^2 \, y_i(t) = f_i(t) \, , \quad i=1,2,...,m \tag{4.2.1}$$

To uncouple the set of modal equations, we introduce an additive split of coupled modal damping matrix

$$\mathbf{C}_m = \mathbf{C}_d + \hat{\mathbf{C}} = diag\left(2 \, \xi_i \, \omega_i\right) + \hat{\mathbf{C}} \tag{4.2.2}$$

and modal equation (4.1.7) can be restated

$$\ddot{y}_i(t) + 2 \, \xi_i \, \omega_i \, \dot{y}_i(t) + \omega_i^2 \, y_i(t) = f_i(t) - \sum_{j=1}^{m} \hat{C}_{ij} \, \dot{y}_j(t), \quad i=1,2,...,m \tag{4.2.3}$$

The equation set (4.2.3) is then solved by iterative procedure. Departure from a similar idea in Claret&Filho [1989] at this stage is that we employ the exact solution for piece-wise linear loading variation of uncoupled equations of motion in the form :

$$\ddot{y}_i^{(k)}(t) + 2 \, \xi_i \, \omega_i \, \dot{y}_i^{(k)}(t) + \omega^2 \, y_i^{(k)}(t) = f_i(t) - \sum_{j=1}^{m} \hat{C}_{ij} \, \dot{y}_j^{(k-1)}(t) \, , \quad i=1,2,...m \tag{4.2.4}$$

One application of this procedure is apparently to structural dynamic analysis for earthquake excitation, where ground acceleration is specified as discretized record. From the analogy between Jacobi and Gauss-Seidel iteration in the solution of system of linear equations, computational variant of equation (4.2.4) can be written as :

$$\ddot{y}_i^{(k)}(t) + 2\,\xi_i\,\omega_i\,\dot{y}_i^{(k)}(t) + \omega_i^2\,y_i^{(k)}(t) = f_i(t) - \sum_{j=1}^{i-1} \hat{C}_{ij}\,\dot{y}_j^{(k-1)}(t) - \sum_{j=i+1}^{m} \hat{C}_{ij}\,\dot{y}_j^{(k)}(t) \qquad (4.2.5)$$

where new values for velocities are substituted as soon as they are computed. Some numerical experiments for the system with dominant response in lower modes indicated that one iteration sweep is often enough. The complete summary of the numerical algorithm is given in Table 4.2.1.

Table 4.2.1.- Algorithm for the Integration of Modal Equations for Non-Proportionally Damped System

----

A. Initial Computations :

1.Precompute exponential and trigonometric expressions for constant time step $\Delta t = t_1 - t_0$

$$B_{i1} = e^{-\xi_i \omega_i\, \Delta t} \cos \omega_{Di}\, \Delta t$$

$$B_{i2} = e^{-\xi_i \omega_i \Delta t} \sin \omega_{Di}\, \Delta t$$

B. For each time step ($\Delta t = t_1 - t_0$) :

1. Set initial condition for iteration process

$$\dot{y}^{(0)}\,(t_1) = y\,(t_0)$$

2. Compute loading

$$f_i(t) = a + b\,t \,, \quad where : a = f_i(t_0) \qquad b = \frac{f_i(t_1) - f_i(t_0)}{\Delta t}$$

C. Iterate through the number of modes :

1. Compute off-diagonal damping forces

$$\left(\hat{C} \, y^{(k-1)}(t) \right)_i = c + d \, t$$

2. Update loading

$$a^* = a - c \, , \qquad b^* = b - d$$

3. Compute coefficients

$$A_0 = \frac{a^*}{\omega_i^2} - \frac{2 \, \xi_i \, b^*}{\omega_i^3} \, , \qquad A_1 = b^* / \omega_i^2$$

$$A_2 = y_i \, (t_0) - A_0$$

$$A_3 = \frac{1}{\omega_{Di}} \left(\dot{y}_i \, (t_0) + \xi_i \, \omega_i \, A_2 - A_1 \right)$$

4. Compute the new values for displacements and velocities

$$y_i^{(k)} \, (t_1) = A_0 + A_1 \, \Delta t + A_2 B_{i1} + A_3 \, B_{i2}$$

$$\dot{y}_i^{(k)} \, (t_1) = A_1 + \left(\omega_{Di} \, A_3 - \xi_i \, \omega_i \, A_2 \right) B_{i1} - \left(\omega_{Di} \, A_2 + \xi_i \, \omega_i A_3 \right) B_{i2}$$

5. Check convergence

$$\text{if} : \quad \left| \dot{y}^{(k)}(t_1) - \dot{y}^{(k-1)}(t_1) \right|_\infty \Big/ \left| \dot{y}^{(k)}(t_1) \right|_\infty \leq tol.$$

Further results on algorithm performance and its extension to periodic loading are given in Ibrahimbegovic&Wilson [1988].

Mode Acceleration Summation

Here presented algorithm can be fitted within the static correction framework. First, the equation (4.1.8) should be rewritten as

$$\mathbf{u}(t) = \sum_{i=1}^{m} \boldsymbol{\phi}_i \left[\frac{1}{\omega_i^2} f_{i0}\, g(t) - \frac{1}{\omega_i^2} \sum_{j=1}^{m} C_{m_{ij}}\, \dot{y}_j(t) - \frac{\ddot{y}_i(t)}{\omega_i^2} \right]$$

$$+ \sum_{i=m+1}^{n} \boldsymbol{\phi}_i \frac{f_{i0}\, g(t)}{\omega_i^2} \qquad\qquad (4.2.6)$$

or rearranging summation

$$\mathbf{u}(t) = \sum_{i=1}^{n} \frac{1}{\omega_i^2}\, \boldsymbol{\phi}_i\, f_{i0}\, g(t) - \sum_{i=1}^{m} \boldsymbol{\phi}_i \left[\frac{1}{\omega_i^2} \sum_{j=1}^{m} C_{m_{ij}}\, \dot{y}_j(t) - \frac{\ddot{y}_i(t)}{\omega_i^2} \right] \qquad (4.2.7)$$

By further using definition of $f_i(t)$ from equation (4.1.5[4]) and additive split of modal damping matrix $\mathbf{C}_m$ from equation (4.2.2), we can rewrite the equation (4.2.7) as

$$\mathbf{u}(t) = \sum_{i=1}^{n} \frac{1}{\omega_i^2}\, \boldsymbol{\phi}_i\, \boldsymbol{\phi}_i^T \mathbf{f}_0\, g(t) - \sum_{i=1}^{m} \boldsymbol{\phi}_i \left[\frac{2\, \xi_i\, \dot{y}_i(t)}{\omega_i} - \frac{\ddot{y}_i(t)}{\omega_i^2} \right] -$$

$$\sum_{i=1}^{m} \boldsymbol{\phi}_i \left[\frac{1}{\omega_i^2} \sum_{j=1}^{m} \hat{C}_{ij}\, \dot{y}_j(t) \right] \qquad\qquad (4.2.8)$$

By utilizing the spectral decomposition theorem (see Parlett [1980]), the first term on the right hand side of the last equation can be rewritten as the inverse of stiffness matrix multiplying loading vector. Hence, we arrive at the final form of the equations for the mode acceleration method applied in our case of non-proportionally damped system

$$\mathbf{u}(t) = \mathbf{K}^{-1} \mathbf{f}_0\, g(t) - \sum_{i=1}^{m} \boldsymbol{\phi}_i \left[\frac{2\, \xi_i\, \dot{y}_i(t)}{\omega_i} - \frac{\ddot{y}_i(t)}{\omega_i^2} \right] - \sum_{i=1}^{m} \boldsymbol{\phi}_i \left[\frac{1}{\omega_i^2} \sum_{j=1}^{m} \hat{C}_{ij}\, \dot{y}_j(t) \right] (4.2.9)$$

The first term on the right hand side of the equation (4.2.9) is the static response to fixed spatial variation of loading that needs to be obtained only once and directly scaled by an appropriate value of excitation at specified time $g(t_i)$. The second term is the standard mode acceleration form (see Cornwell et al. [1983]) for proportional damping case that can be computed with high accuracy by utilizing here proposed procedure, as opposed to

inaccuracies associated with computation of acceleration by Newmark family integration schemes. For the purpose of accommodating computation of this term, the proposed algorithm has to be expanded by one equation only :

-in predictor form :

$$\ddot{y}_i^{(k)}(t_1) = - \xi_i \, \omega_i \, \dot{y}_i^{(k)}(t_1) - \omega_{Di} \left(\omega_{Di} \, A_3 - \xi_i \, \omega_i \, A_2 \right) B_{i2}$$

$$- \omega_{Di} \left(\omega_{Di} \, A_2 + \xi_i \, \omega_i A_3 \right) B_{i1} \tag{4.2.10}$$

-in corrector form :

$$\ddot{y}_i^{(k)}(t_1) = f_{i0} \, g(t) - \omega_i^2 \, y_i^{(k)}(t_1) - 2 \, \xi_i \, \omega_i \, \dot{y}_i^{(k)}(t_1) \tag{4.2.11}$$

The third term in the equation (4.2.9) is computed as the intermediate value in the algorithm presented in Table 4.2.1 and can be accumulated in indexed variable for later use in summation process.

Complex Vector Basis

Theoretical basis for formation of the complex vector basis that will uncouple equations of motion (4.1.1) for the case of non-proportional damping is introduced three decades ago by Foss [1958]. Additional publications (e.g. Veletsos&Ventura [1986]) tried to provide some physical insight into the use of complex vector basis aiming to raise the popularity of the method in engineering community. However, beside the lack of physical understanding, an equally important reason for the rare use of complex vector basis is that the method tends to be computationally very expensive for practical large systems. Quite recently devised Lanczos algorithm in Chen [1987] for the solution of quadratic eigenvalue problem can ease the burden of large computational expense.

Only a short summary of the algorithm we use to generate complex vector basis is given here. For more thorough discussion the reader is referred to Chen&Taylor [1988].

To generate the complex vector basis, second-order differential equations are transformed into a first-order one (see Frazer et al. [1946]) as

$$A \, \hat{u}(t) - B \, \tilde{u}(t) = \tilde{f}(t) \tag{4.2.12}$$

where

$$A = \begin{bmatrix} C & M \\ M & 0 \end{bmatrix} \qquad B = \begin{bmatrix} -K & 0 \\ 0 & M \end{bmatrix} \tag{4.2.13}$$

and

$$\tilde{u}(t) = \begin{bmatrix} u(t) \\ \dot{u}(t) \end{bmatrix} \qquad \tilde{f}(t) = \begin{bmatrix} f(t) \\ 0 \end{bmatrix} \tag{4.2.14}$$

A variant of the standard Lanczos algorithm can be constructed (see Chen [1987]) to generate an A-orthogonal set of vectors by applying the Gram-Schmidt orthogonalization procedure on the Krylov subspace spanned by $[\tilde{q}_1, D\tilde{q}_1, D^2\tilde{q}_1, \ldots, D^{m-1}\tilde{q}_1]$, where $D = B^{-1} A$ and $\tilde{q}_1$ is a starting vector. The three-term recurrence formula now is

$$\gamma_{j+1} \, \tilde{q}_{j+1} = \tilde{r}_{j+1} = B^{-1} A \, \tilde{q}_j - \alpha_j \, \tilde{q}_j - \beta_{j-1} \, \tilde{q}_{j-1} \tag{4.2.15}$$

The dimension of the Lanczos vectors $\tilde{q}_j$ here is $2n$ instead of n. However, the cost of computing these Lanczos vectors is not doubled because the structure of the matrices A and B can be exploited.

After m steps, we have the Lanczos vectors $\tilde{Q}_m = [\, \tilde{q}_1, \ldots, \tilde{q}_m \,]$ satisfying the following relation

$$\tilde{Q}_m^T A \, \tilde{Q}_m = \Delta_m \tag{4.2.16}$$

and

$$\tilde{Q}_m^T A \, B^{-1} A \, \tilde{Q}_m = \Delta_m \, \tilde{}_{} \tag{4.2.17}$$

where Δ_m is an $m \times m$ diagonal matrix with the diagonal elements δ_i being 1 or -1, and $\tilde{T}_m$ is a tridiagonal matrix :

$$
\tilde{T}_m = \begin{bmatrix} \alpha_1 & \beta_1 & & & & \\ \gamma_2 & \alpha_2 & \beta_2 & & & \\ & \cdot & \cdot & \cdot & & \\ & & \cdot & \cdot & \cdot & \\ & & & \gamma_{m-1} & \alpha_{m-1} & \beta_{m-1} \\ & & & & \gamma_m & \alpha_m \end{bmatrix} \tag{4.2.18}
$$

The Ritz vectors are computed from $\tilde{\Psi}_m = \tilde{Q}_m \tilde{S}_m$, where $\tilde{S}_m$ is the solution for eigen-vectors of the following eigenproblem :

$$
\Delta_m \tilde{T}_m \tilde{S}_m = \Delta_m \tilde{S}_m \Theta_m^{-1} \tag{4.2.19}
$$

By using the transformation $\tilde{u}(t) = \tilde{\Psi}_m \tilde{y}(t)$, we can obtain the uncoupled form of the equations of motion

$$
\dot{\tilde{y}}_j(t) - \theta_j \tilde{y}_j(t) = \tilde{f}_j(t) \tag{4.2.20}
$$

where both the θ_j and the $\tilde{f}_j(t)$ are complex-valued for underdamped modes.

For the piece-wise linear variation of excitation, the exact solution of equation (4.2.20) can then be utilized in computational process.

Numerical Results

Two typical dynamic systems with the non-proportional damping are analyzed : the flexible mechanical system with concentrated dampers and the structure-foundation interaction problem for a model of gravity dam.

Example 4.2.1. Mechanical system with concentrated damper

The first example studied is a frame structure presented on Figure 4.2.1. The structure is modeled by a discrete model of 10 beam elements (each with length equals 1 m) with a total of 24 degrees of freedom. Young's modulus for the beam material is taken as 500 N/m^2, while the mass density, the section area and inertia are specified of unit value. The damping coefficient of the concentrated damper equals 10 N sec/m.

This structural model could be considered as a representative of a control system or a passively damped space structure. Due to the model flexibility its frequency spectrum spans from 7.64 rad/sec as the lowest frequency to 1097.49 as the highest.

To ensure that the non-proportional damping arising from the damper attached to node 3 is less than *critical* (underdamped system), the procedure described in Inman&Andry [1980] is used. Namely, positive definiteness of the matrix $(2 \ \tilde{K}^{1/2} - \tilde{C})$ is checked (where : $\tilde{K} = M^{-1/2} \ K \ M^{-1/2}$, $\tilde{C} = M^{-1/2} \ C \ M^{-1/2}$).

The structure is analyzed previously by Chen&Taylor [1988] within the framework of complex Ritz vectors and eigenvectors that are generated from the first order system (4.2.12). The analysis in Chen&Taylor [1988] is performed for the loading variation specified as step function. Equivalent computations were performed in Ibrahimbegovic&Wilson [1988] by utilizing real valued subspace generated either by the exact eigenvectors or Ritz vectors directly from the set of the second order differential equations. Two sets of 4 and 10 exact eigenvectors and 4 and 10 Ritz vectors generated from both the second and the first order system are used in the analysis and compared with exact solution (obtained with all 24 vectors included). The same computation is repeated for another loading variation specified as 1952 Taft earthquake described in section 3.1.

The plots for the horizontal displacement at node 8 computed by different number of real vectors and complex vector pairs are given on Figure 4.2.2 for the step function loading variation and on Figure 4.2.3 for Taft earthquake.

From the plots presented on Figure 4.2.3 we observe that the results computed within the subspace spanned by either 10 pairs of complex vectors or 10 real vectors are very similar, although in theory different vectors are generated. That applies both to the eigenvectors and Ritz vectors and to both kinds of loading we used. The reason for that is partly due to the low values of the equivalent damping ra*ios* (on average 2% for all the modes) that is computed from the non-proportional damping matrix neglecting off-diagonal terms (see Warburton&Sony [1977]). However, even for larger values of the non-proportional damping, it is reasonable to assume that the convergence rates for both vector bases, complex and real, will be in a very good agreement. This we demonstrate in the second example.

For the computation performed utilizing a set of 4 real Ritz vectors or 4 pairs of complex Ritz vectors, much better approximation to peak response is obtained than for the adequate computation done by eigenvectors. To illustrate that, we present the ratios of peak response computed by the different numbers of real vectors and complex vector pairs versus the exact solution. These results are given for both kinds of loading, step function and Taft earthquake, in Table 4.2.1.

Table 4.2.1	Ratios of Maximum Response for Different Vector Bases Versus Exact Solution	
Complex Vector Basis		
No. Vect.	Step Function	Taft Earthquake
4 eig. v.	0.754	0.830
4 Ritz v.	1.019	1.057
10 eig. v.	1.044	1.016
10 Ritz v.	0.992	0.994
Real Vector Basis		
No. Vect.	Step Function	Taft Earthquake
4 eig. v.	0.775	0.850
4 Ritz v.	0.928	1.057
10 eig. v.	1.046	1.017
10 Ritz v.	1.011	0.999

Example 4.2.2. Dam-foundation interaction

The structure-foundation model for concrete gravity dam described in section 3.2. is used in this example. The finite element model of the dam-foundation system is given on Figure 3.2.1. Rayleigh damping is used to account for energy dissipation due to material damping in dam and foundation material, constructed with the second (frequency equals 13.27 rad/sec) and the fifth mode (frequency equals 21.39 rad/sec) chosen as control modes with modal damping ratio value equals 5%. Consistent transmitting boundaries, constructed as discussed in section 2.4., give rise to non-proportional damping matrix.

The presence of overdamped modes which are property of wave propagation problems, as described by Wolf [1985], can be checked by the procedure described in Inman&Andry [1980], applied directly to the truncated set of equations in modal coordinates. In all the runs we performed both the complex and the real vector basis yielded the same number of overdamped modes, i.e. they both followed the same pattern. Hence this procedure to establish the number of overdamped modes can be used for modal analysis that utilizes complex vector basis to *a priori* indicate the problems that may occur in that case (see Chen&Taylor [1988]).

The computations are performed for two loading variations as in example 4.2.1. : step function and Taft earthquake. Two sets of 5 and 10 real vectors and complex vector pairs in vector basis generated by both eigenvectors and Ritz vectors are used in computations.

As a measure for computational efficiency CPU times spent in different phases of the

analysis performed on VAX II/GPX workstation are presented in Table 4.2.2

Table 4.2.2	CPU Times for Complex and Real Vector Basis (sec)		
Complex Vector Basis			
No. Vect.	Lanczos Vec.	Ritz Vec.	Modal Equations
5 eig. v.	1935.98	285.80	0.43
5 Ritz v.	570.23	27.70	0.43
10 eig. v.	2797.90	594.95	0.90
10 Ritz v.	1037.83	86.55	0.90
Real Vector Basis			
No. Vect.	Lanczos Vec.	Ritz Vec.	Modal Equations
5 eig. v.	255.33	26.50	1.93
5 Ritz v.	71.97	4.31	1.89
10 eig. v.	391.12	52.80	4.82
10 Ritz v.	138.80	9.55	4.73

The extraction of a number of complex Ritz vector pairs requires on the average 7.75 times more effort than for the adequate number of real vectors. On the other hand, for the solution of modal equations the average CPU time ratio is inverse to the value above, which reflects the advantage of uncoupled equations set in the case of complex vector basis. However, the effort involved in modal equations solution is overall insignificant.

For both programs FEAP (see Taylor [1977]) and SAP (see Wilson [198.)]) that we used to generate complex and real vector basis respectively, common computational expense of factorizing stiffness matrix required 220 CPU sec (without use of optimal equation numbering routine). Hence, from Table 4.2.2 it is obvious that generating Ritz vector basis

of 10 real vectors which yields excellent approximation to dynamic response, is merely half the effort adequate to static response computation.

To develop further appreciation for the efficiency resulting from the selection of load dependent real Ritz vector basis in modal transformation, a complete comparison of CPU time for the different phases of dynamic mode superposition analysis versus static analysis is performed. Discretization of dam model on Figure 3.2.1 resulted in 1154 equations with the average band-width of 104. The comparison is performed for two sets of 5 and 10 real

Ritz vectors, and presented in Table 4.2.3 below.

Table 4.2.3	CPU Times for Real Vector Basis and Static Solution (sec)		
Solution Phases	Static Solution	5 Ritz Vec.	10 Ritz Vec.
input	10.97	10.96	10.93
form element stiffness	45.88	45.67	45.52
form structural stiffness	11.87	11.88	11.92
factorize struct. stiffness	220.30	220.25	220.03
Lanczos vectors	-	71.97	138.80
Ritz vectors	-	4.31	9.55
modal equations (100 steps)	-	1.89	4.73
displacement history (10 nodes)	-	2.02	3.96
stress history (10 elements)	-	446.76	461.60
nodal displacement	5.87	-	-
nodal stress (10 elements)	4.78	-	-
total time	299.67	815.71	907.04

From Table 4.2.3 above, we can note that the total solution process for the case of dynamic analysis triples the effort of the static solution process. This seemingly unfavorable ratio results from the solution strategy of nodal stress recovery by time history of stress, which essentially requires repetition of the same computation as in the static loading case for each time step. However, for design purposes only maxi ·· u values of stress and displacement are of interest. To obtain design values for earthquake input one can use response spectrum approach for the case of non-proportional damping as introduced by Igusa and DerKiureghian [1983]. Since the time for recovery of maximum values for stress and displacement by CQC method is only slightly larger than the adequate computation for

the static loading case, the ratio of dynamic and static analysis reduces to 1.5.

The horizontal displacement at the dam tip computed for the set of 5 real vectors and 5 complex vector pairs is plotted on Figure 4.2.4 and for 10 vectors and vector pairs on Figure 4.2.5, together with the "exact" response obtained by the set of 100 real vectors.

For both vector basis, real and complex, remarkable approximation properties are encountered for use of Ritz vectors. This is illustrated in Figures 4.2.4 and 4.2.5 and Table 4.2.4.

Table 4.2.4	Ratios of Maximum Response for Different Vector Bases Versus Exact Solution	
Complex Vector Basis		
No. Vect.	Step Function	Taft Earthquake
5 eig. v.	1.121	1.029
5 Ritz v.	1.061	1.033
10 eig. v.	1.054	1.025
10 Ritz v.	1.007	1.017
Real Vector Basis		
No. Vect.	Step Function	Taft Earthquake
5 eig. v.	1.030	0.951
5 Ritz v.	0.965	0.987
10 eig. v.	0.969	0.978
10 Ritz v.	0.996	1.007

Both the eigenvector and Ritz vector bases possess equivalent fast convergence properties for nodal displacement computation.

Error norm for loading spatial representation can be computed as given in Leger&Wilson [1987] by :

$$\| e_f \|_2 = \frac{\| (I - M \, \Psi \, \Psi^T) \, f \|_2}{\| f \|} \times 100 \quad (\%)$$
(4.2.21)

Error norm defined by the equation (4.2.21) is presented in Table 4.2.5 for different numbers of real eigenvectors and real Ritz vectors used in modal transformation.

Table 4.2.5.-	Error Norm for Spatial Loading Representation
No. Vect.	**Error Norm (%)**
10 eig. v.	52.677
10 Ritz v.	24.396
100 Ritz v.	15.873

Spatial representation of the loading with truncated vector basis is much better for the case of Ritz vector basis. Consequently, stresses and forces recovery is much more accurate within vector basis spanned by Ritz vectors constructed by load dependent algorithm. To illustrate that, dam structure base shear force computed by the appropriate numbers of Ritz vectors and eigenvectors is presented on Figure 4.2.6.

Remark 4.2.2 Krylov subspace keeps its advantageous approximation properties versus the exact eigenvector subspace in the case of the non-proportionally damped system. This is enhanced in the case of broad band excitation.

Remark 4.2.3 The selection of proper real load dependent Ritz vector basis for the modal transformation, combined with an efficient m   ~d for maximum stress recovery, reduces the total effort required for the dynam\   ~~a~ysis to only 1.5 times of an adequate static analysis of the same problem.

Remark 4.2.4 For the cases studied, the real vector basis yields comparable accuracy and convergence properties as adequate complex vector basis, but requires much smaller

CPU time for total solution. Possible room for use of complex vector basis is still left in analysis of structural systems under the loading with time variation given as large piece-wise linear steps, where high accuracy can be ensured by employing the exact solution.

4.3. Dynamic Substructuring

In this section, techniques for coordinate reduction and non-proportional damping, discussed in sections 4.1. and 4.2., are fitted within the framework of dynamic substructuring. Dynamic substructuring is yet called component mode synthesis, which reflects the basic idea that originated from the need to simplify dynamic analysis of a complex structure by relating independent analysis of its components. An extensive review of dynamic substructuring methods can be found in Craig [1981]. Most of the work on dynamic substructuring was motivated by eigenvalue problem solution; however, Wilson&Bayo [1986] on the analysis of small examples have demonstrated that the concept can be applied with success in dynamic response computation as well.

Two basic versions of dynamic substructuring are recognized (see Craig [1981]) with respect to the selection of vector basis for component (substructure) representation : fixed interface modes and free interface modes. Naturally, combinations of these two are also possible. Dynamic substructuring can be thought of as an extension of the Galerkin method to discretized system. Namely, the semidiscrete equations of motion (3.2.16) are projected onto the subspace spanned by the interface modes and the component modes of the substructures. If only the interface modes are retained in the subspace basis, Guyan reduction (see Guyan [1965]) is recovered.

The basic transformation which uses the fixed interface modes and no component modes for one dynamic substructure is

$$\begin{pmatrix} u_i(t) \\ u_r(t) \end{pmatrix} = \begin{bmatrix} R \\ I \end{bmatrix} u_r(t)$$

and if component modes Ψ are included

$$\begin{pmatrix} \mathbf{u}_i(t) \\ \mathbf{u}_r(t) \end{pmatrix} = \begin{bmatrix} \Psi & \mathbf{R} \\ \mathbf{0} & \mathbf{I} \end{bmatrix} \begin{pmatrix} \mathbf{y}_i(t) \\ \mathbf{u}_r(t) \end{pmatrix} = \mathbf{T}\, \mathbf{u}_r^*(t) \qquad (4.3.1)$$

where $\mathbf{u}_i$ and $\mathbf{y}_i$ are substructure finite element internal dofs and their generalized Ritz coordinates representation, while $\mathbf{u}_r$ are finite element dofs retained for the analysis of total system. Transformation matrix $\mathbf{R} = -\mathbf{K}_{ii}^{-1}\, \mathbf{K}_{ir}$ is again influence coefficient matrix of pseudo-static transformation (2.3.8). For the high accuracy of dynamic response computation, the set of component modes Ψ has to be constructed following the considerations of section 4.1. The efficiency of computation in dynamic analysis of the complete system is again enhanced by modal truncation, ie, capitalizing on the fact that dynamic response of each component is represented by a small number of generalized Ritz coordinates $(dim(\mathbf{y}_i) \ll dim(\mathbf{u}_i))$.

By utilizing the transformation (4.3.1) on the semidiscrete equations of motion of a single component (in the form (2.2.16)), we can restate the equations of motion as

$$\mathbf{M}^* \, \ddot{\mathbf{u}}_r^*(t) + \mathbf{C}^* \, \dot{\mathbf{u}}_r^*(t) + \mathbf{K}^* \, \mathbf{u}_r^*(t) = \mathbf{f}^*(t) \qquad (4.3.2)$$

where

$$\mathbf{u}_r^*(t) = \begin{pmatrix} \mathbf{y}_i(t) \\ \mathbf{u}_r(t) \end{pmatrix}$$

and

$$\mathbf{M}^* = \begin{bmatrix} \mathbf{I} & \Psi^T \mathbf{M}_{ii} \mathbf{R} + \Psi^T \mathbf{M}_{ir} \\ \mathbf{R}^T \mathbf{M}_{ii} \Psi + \mathbf{M}_{ri} \Psi & \mathbf{R}^T \mathbf{M}_{ii} \mathbf{R} + \mathbf{M}_{ri} \mathbf{R} + \mathbf{R}^T \mathbf{M}_{ir} + \mathbf{M}_{rr} \end{bmatrix} \qquad (4.3.3)$$

$$\mathbf{C}^* = \begin{bmatrix} \Psi^T \mathbf{C}_{ii} \Psi & \Psi^T \mathbf{C}_{ii} + \Psi^T \mathbf{C}_{ir} \\ \mathbf{R}^T \mathbf{C}_{ii} \Psi + \mathbf{C}_{ri} \Psi & \mathbf{R}^T \mathbf{C}_{ii} \mathbf{R} + \mathbf{C}_{ri} \mathbf{R} + \mathbf{R}^T \mathbf{C}_{ir} + \mathbf{C}_{rr} \end{bmatrix}$$

$$\mathbf{K}^* = \begin{bmatrix} \mathbf{\Omega}^2 & 0 \\ 0 & \mathbf{R}^T\mathbf{K}_{ii}\mathbf{R} + \mathbf{K}_{ri}\mathbf{R} + \mathbf{R}^T\mathbf{K}_{ir} + \mathbf{K}_{rr} \end{bmatrix}$$

$$\mathbf{f}^*(t) = \begin{pmatrix} \mathbf{\Psi}^T\mathbf{f}(t) \\ \mathbf{R}^T\mathbf{f}_i(t) + \mathbf{f}_r(t) \end{pmatrix}$$

where component modes $\mathbf{\Psi}$ are mass orthonormalized. The submatrix $\mathbf{\Omega}^2$ in matrix $\mathbf{K}^*$ is a diagonal matrix with some of the elements equal to squares of natural frequencies of the substructure with fixed interface, while another non-zero submatrix of $\mathbf{K}^*$ is computed by static condensation of internal finite element dofs.

For an arbitrary non-proportional form of damping matrix $\mathbf{C}$, this choice of component modes $\mathbf{\Psi}$ will not yield diagonal form of the upper left submatrix in $\mathbf{C}^*$. However, a straightforward extension of the algorithm described in section 4.2. can be introduced to correct this deficiency. Additive split of upper left submatrix of $\mathbf{C}^*$ to diagonal and off-diagonal part introduces pseudo-force term that ought to be handled iteratively, but also yields diagonal form of that submatrix of $\mathbf{C}^*$. Hence, all the matrices in (4.3.3) have an arrow, fill-in free structure. For the nonlinear analysis, the iterative procedure introduced with the additive split of submatrix in $\mathbf{C}^*$, is just a part of the iterative solution of nonlinear set of equations that arises in implicit step-by-step scheme we utilize.

Retained dofs for any substructure are related to global dofs by assembly matrix $\mathbf{A}$ such that

$$\mathbf{u}_r(t) = \mathbf{A}\,\mathbf{u}_g(t) \tag{4.3.4}$$

$\mathbf{A}$ is usually Boolean matrix, or in particular identity. However, some other forms of $\mathbf{A}$ are possibly useful in some applications (e.g. rigid body transformation matrix in large interface sliding as discussed in the next chapter), Hence, the complete form of transformation for a single substructure is

$$\begin{pmatrix} \mathbf{u}_i(t) \\ \mathbf{u}_r(t) \end{pmatrix} = \mathbf{T} \begin{bmatrix} \mathbf{I} & 0 \\ 0 & \mathbf{A} \end{bmatrix} \begin{pmatrix} \mathbf{y}_i(t) \\ \mathbf{u}_g(t) \end{pmatrix} = \mathbf{T}_A\,\mathbf{u}_g^*(t) \tag{4.3.5}$$

Remark 4.3.1. Dynamic substructuring method (as Galerkin procedure for discretized system) provides a *consistent* way of reducing the number of dofs of the semidiscretized model for the dynamic analysis of the complete system. One can think of it as two-step Galerkin procedure. For some problems (usually with simple domains and mechanical properties of material), it may be possible to select the global shape functions over large parts of the domain (or the whole domain), thus reducing the number of dofs with a one-step Galerkin method (Ritz method). For some applications along these lines we refer to Mote [1971].

Remark 4.3.2. Usual application of the dynamic substructuring method is an extension of static condensation algorithm as given by Clough&Wilson [1979] or Bathe&Gracewski [1981]. Namely, the transformation (4.3.1) is used within step-by-step algorithm to reduce the linear part of the effective stiffness matrix (see Table 2.1.1). For here proposed dynamic substructuring, linear part of effective stiffness matrix is represented by a diagonal submatrix with a significantly smaller dimension due to modal truncation. Even for the step-by-step integration of the linear system, the reduced cost of forming effective load vector at each step (see Table 2.1.1) will compensate for the cost of extracting a number of component mode shapes, especially for the loading of long duration (e.g. earthquake loading). For the nonlinear analysis, if step-size control implicit integration scheme is utilized (desirable for the dynamic contact problem we consider in Chapter 6), and Newton method solves a set of nonlinear equations at each time step, than the performance of the dynamic substructuring method that we employ will be even more enhanced compared to the standard dynamic substructure method, since the reforming and refactorizing of effective stiffness matrix will dominate the computational expense.

Figure 4.1.1 - Response amplitude and phase for harmonic excitation
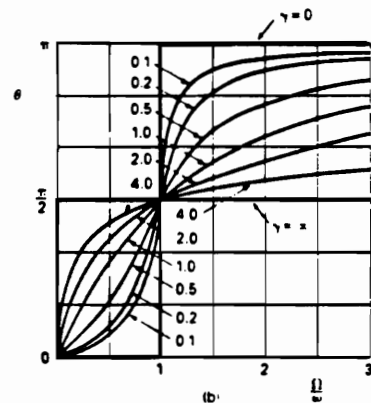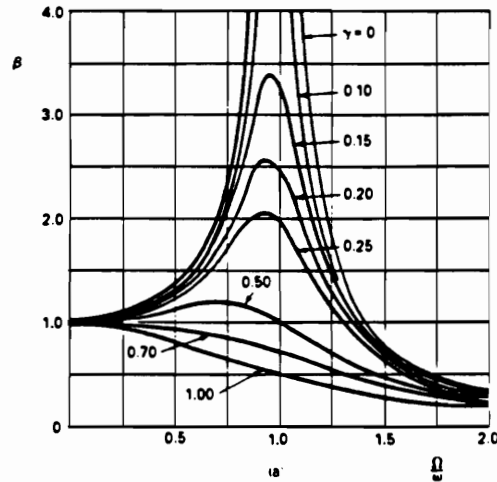
(a) Magnification factors;
(b) phase angles.

$k_1 = k_2 = 1000 \ N/m$

$m_1 = m_2 = 1 \ kg$

$c = 1 \ Ns/m$

$\omega_1 = 19.54 \ rad/sec$

$\omega_2 = 51.17 \ rad/sec$

$f(t) = 1 \ N$ (*Heaviside function*)
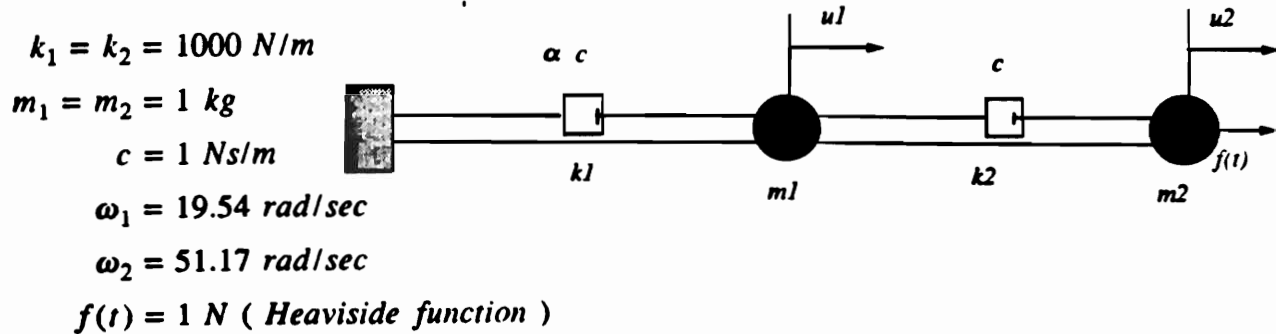
Figure 4.1.2 - Two degrees of freedom system characteristics
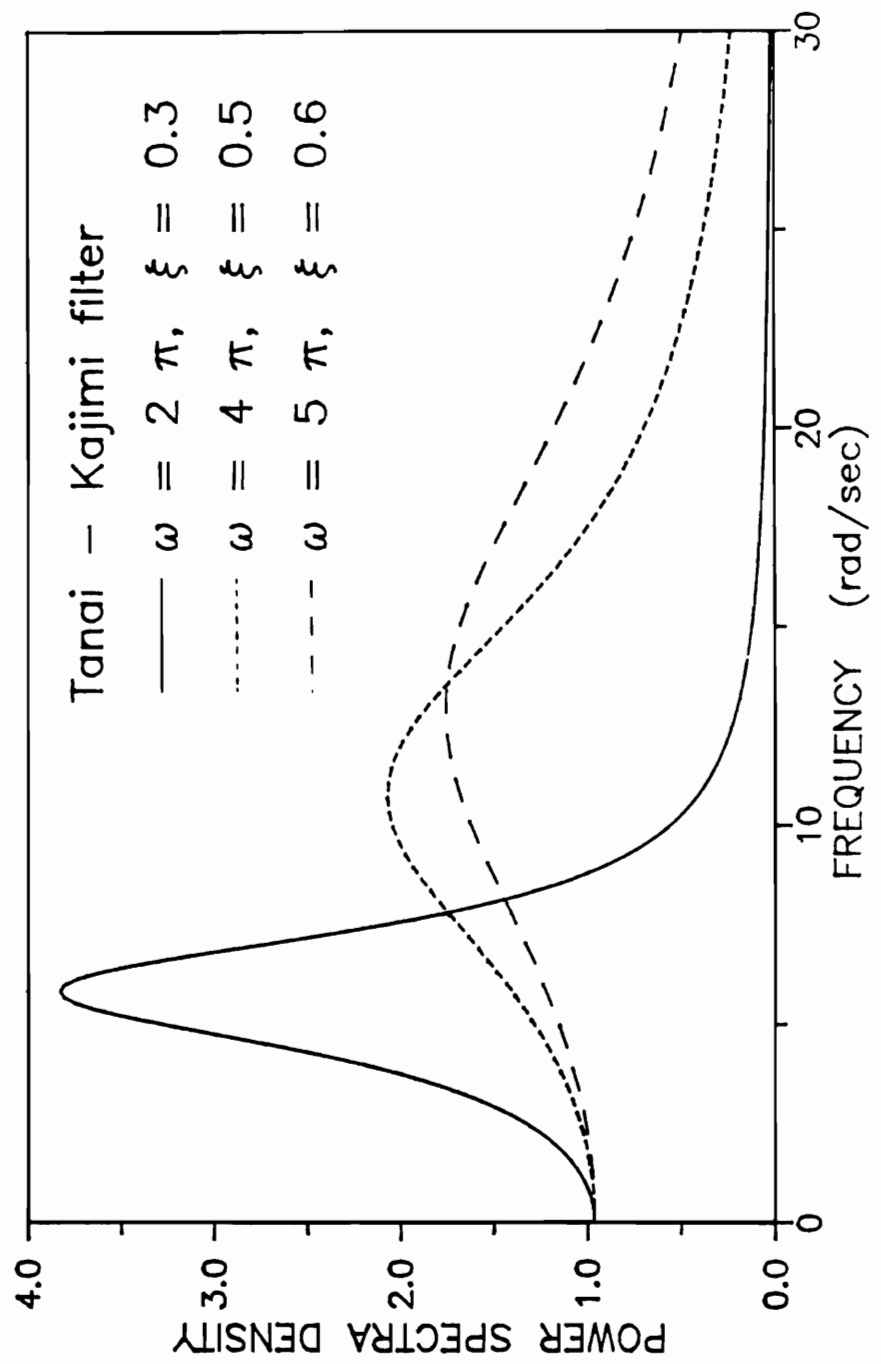
Figure 4.1.3 - One sided PSDs for simulated earthquake motions
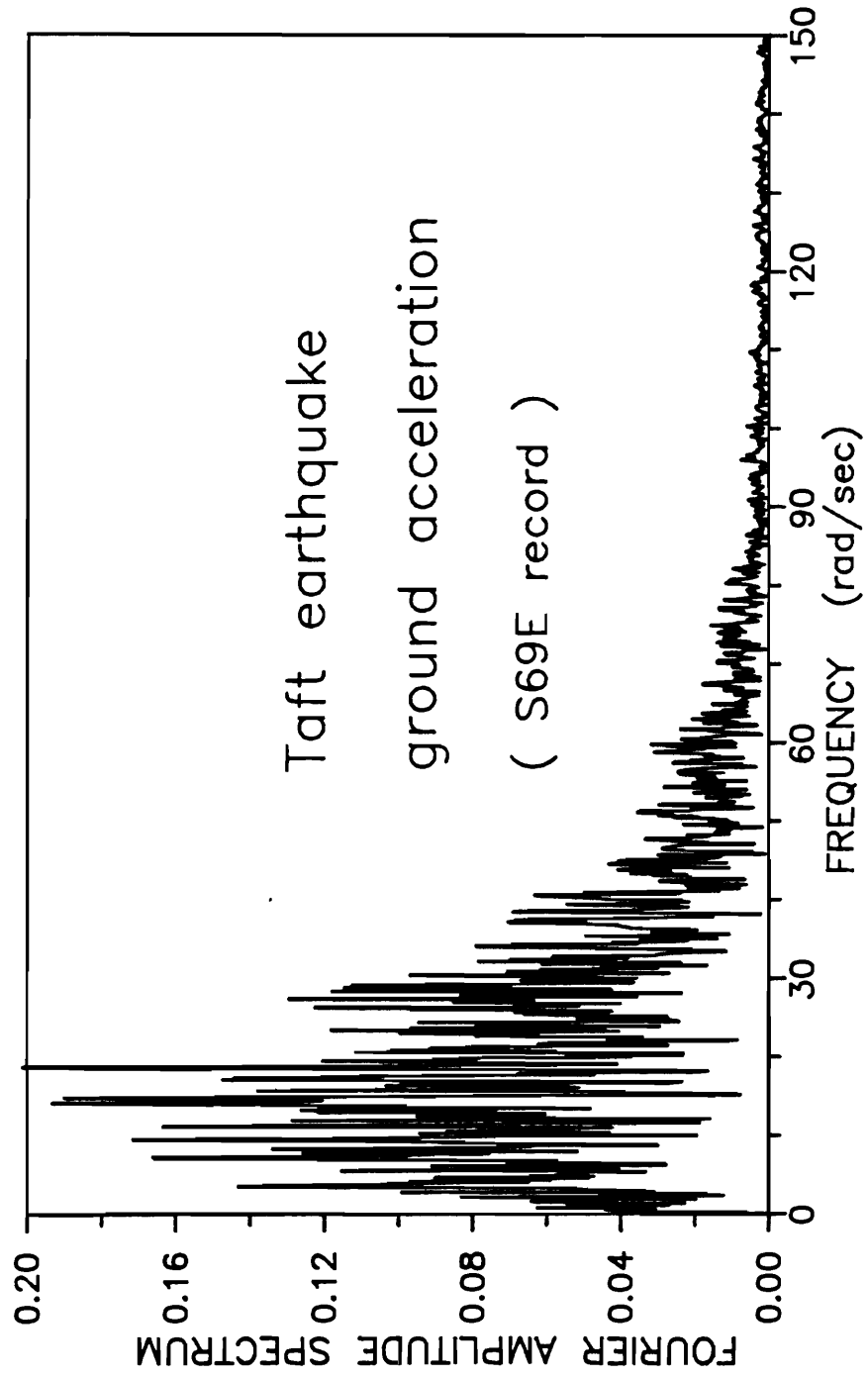
Figure 4.1.4 - Fourier amplitude spectrum for 1952 Taft earthquake
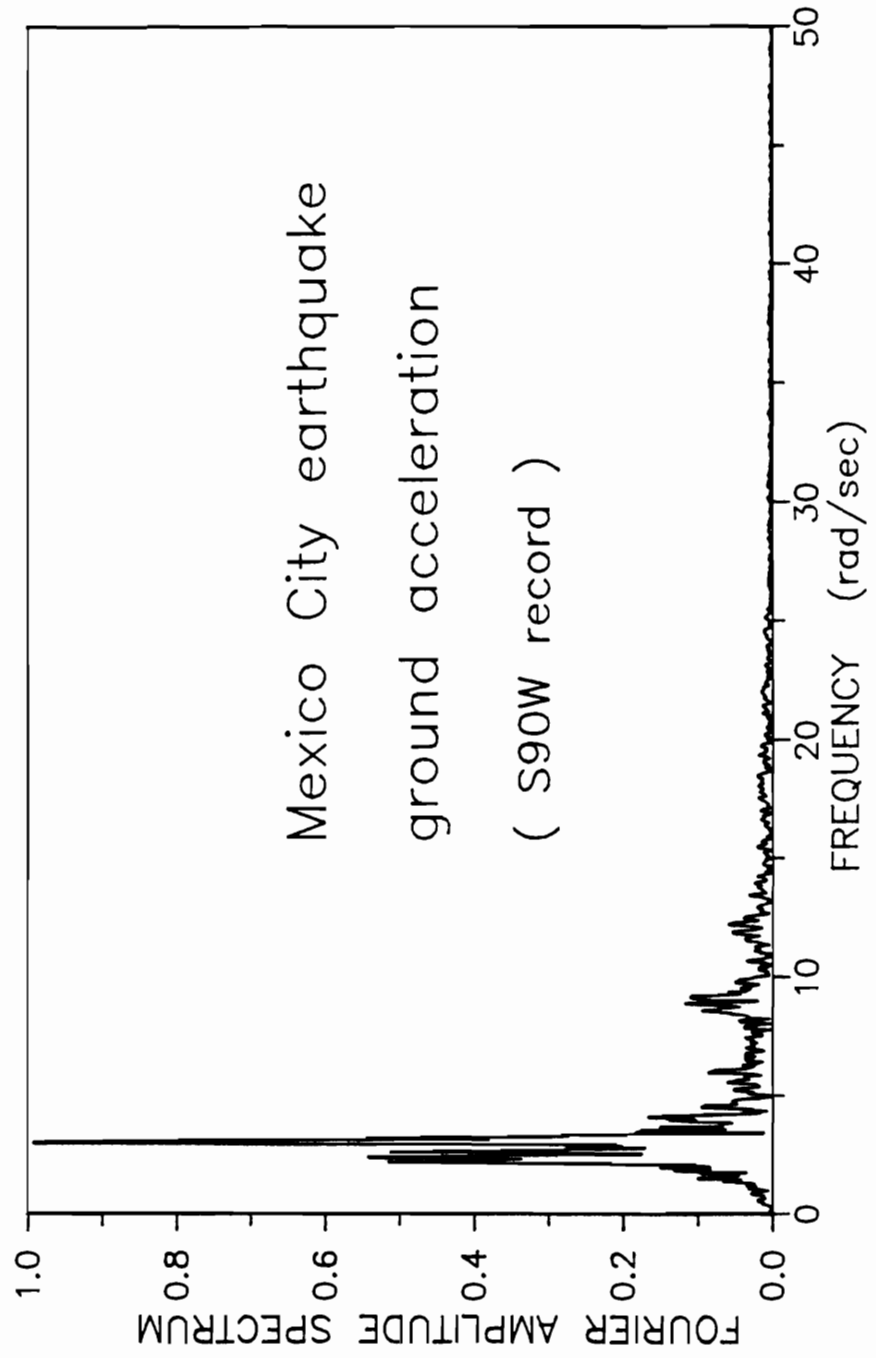
Figure 4.1.5 - Fourier amplitude spectrum for 1985 Mexico City earthquake
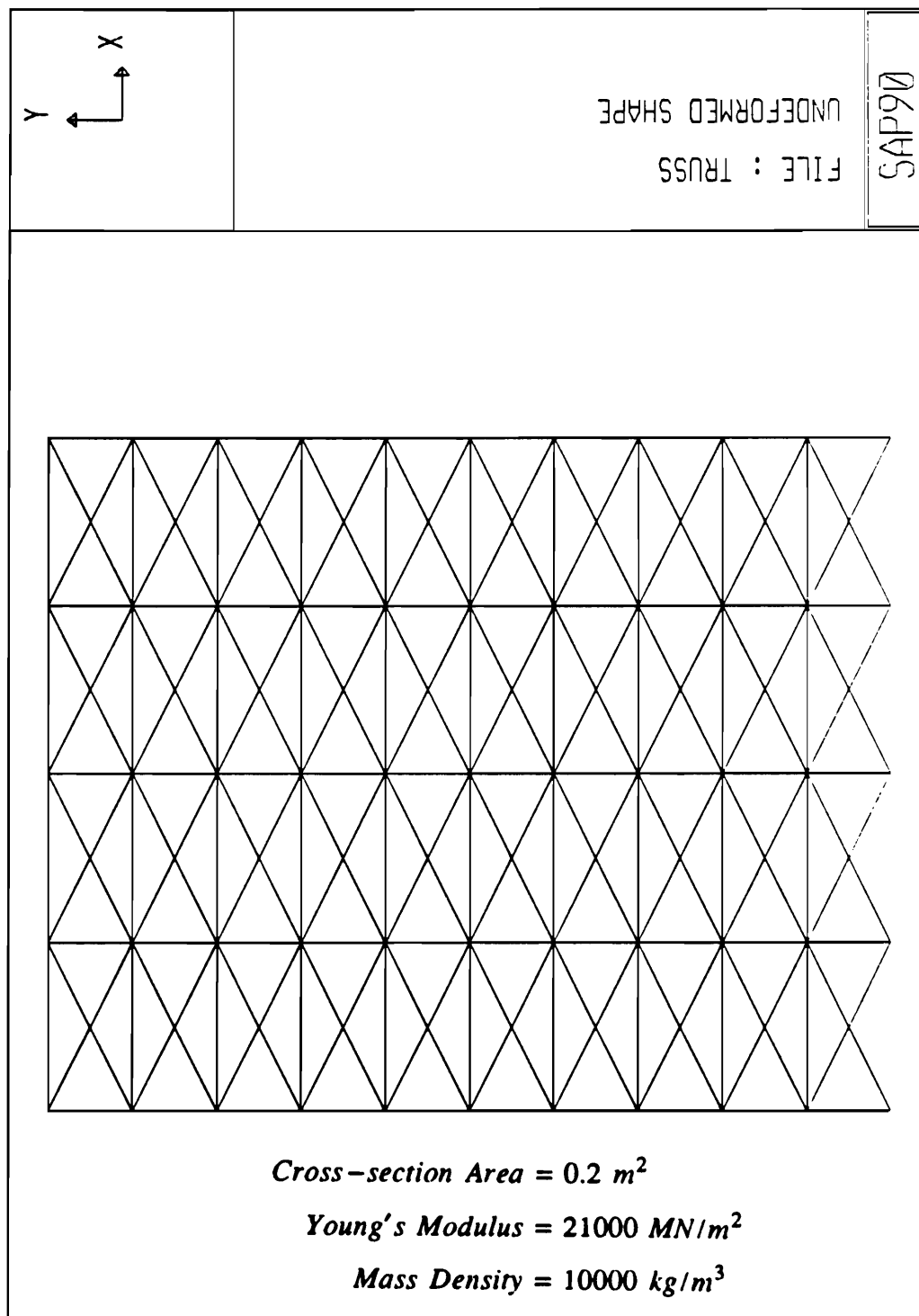
Figure 4.1.6 - Truss model characteristics
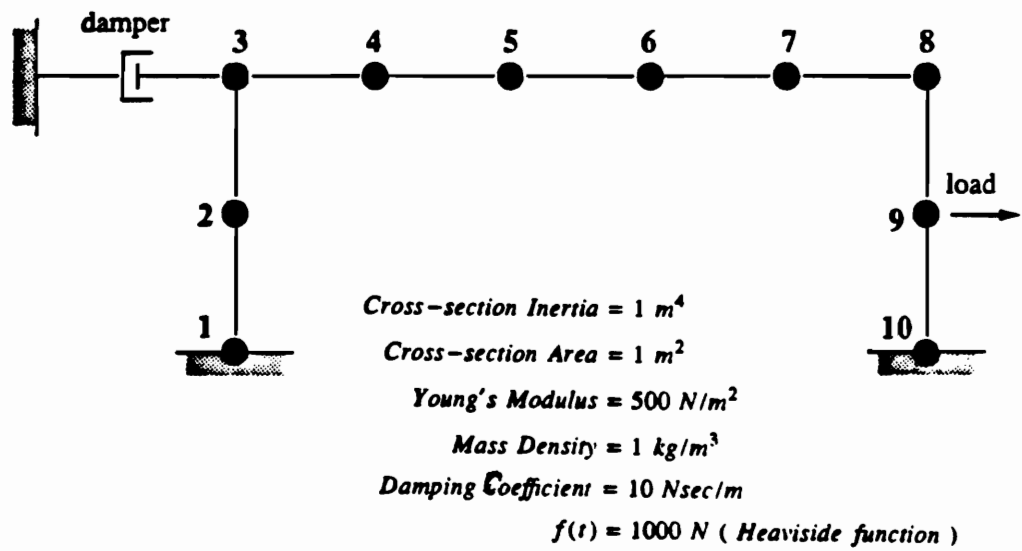
Figure 4.2.1 - A damped dynamic system

4 real eigenvectors and 4 complex eigenvector pairs
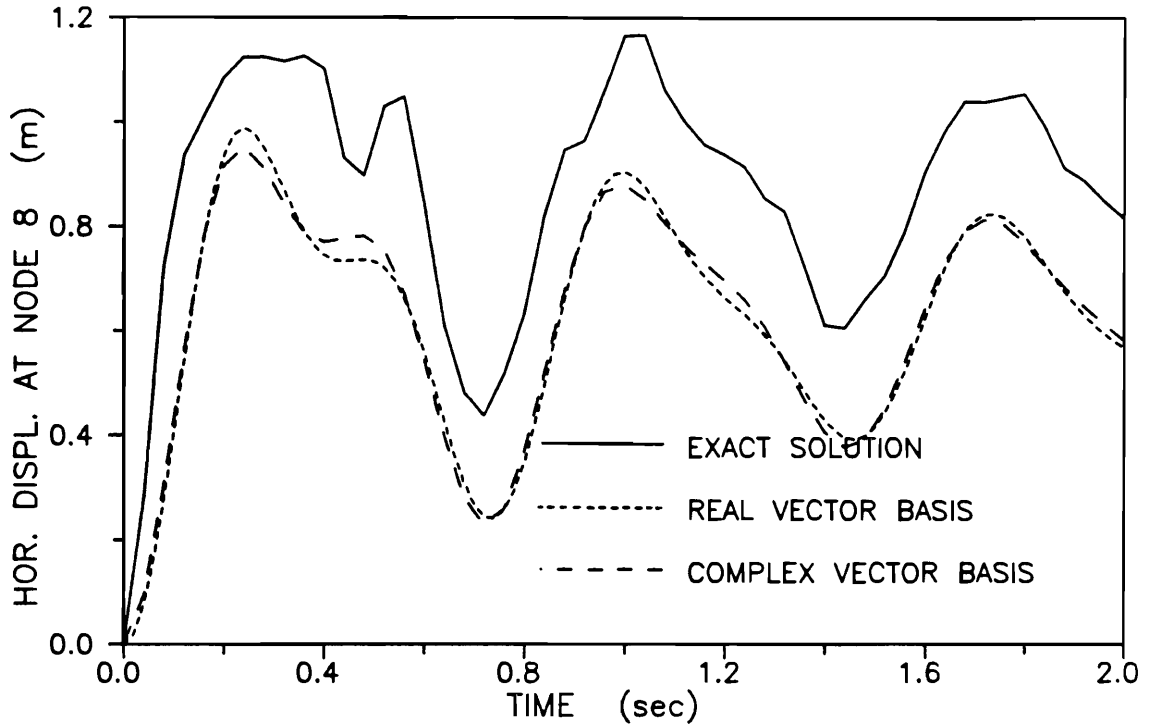
4 real Ritz vectors and 4 complex Ritz vector pairs
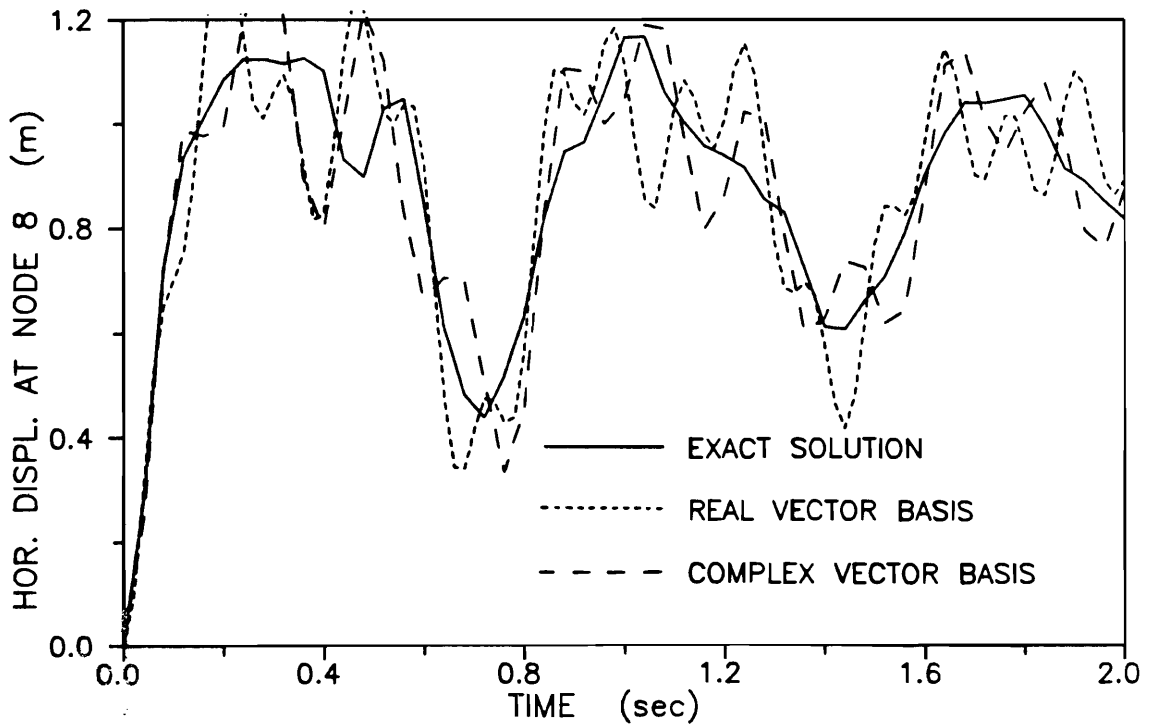
Figure 4.2.2.a - Horizontal displacement at node 8 for step function

10 real eigenvectors and 10 complex eigenvector pairs

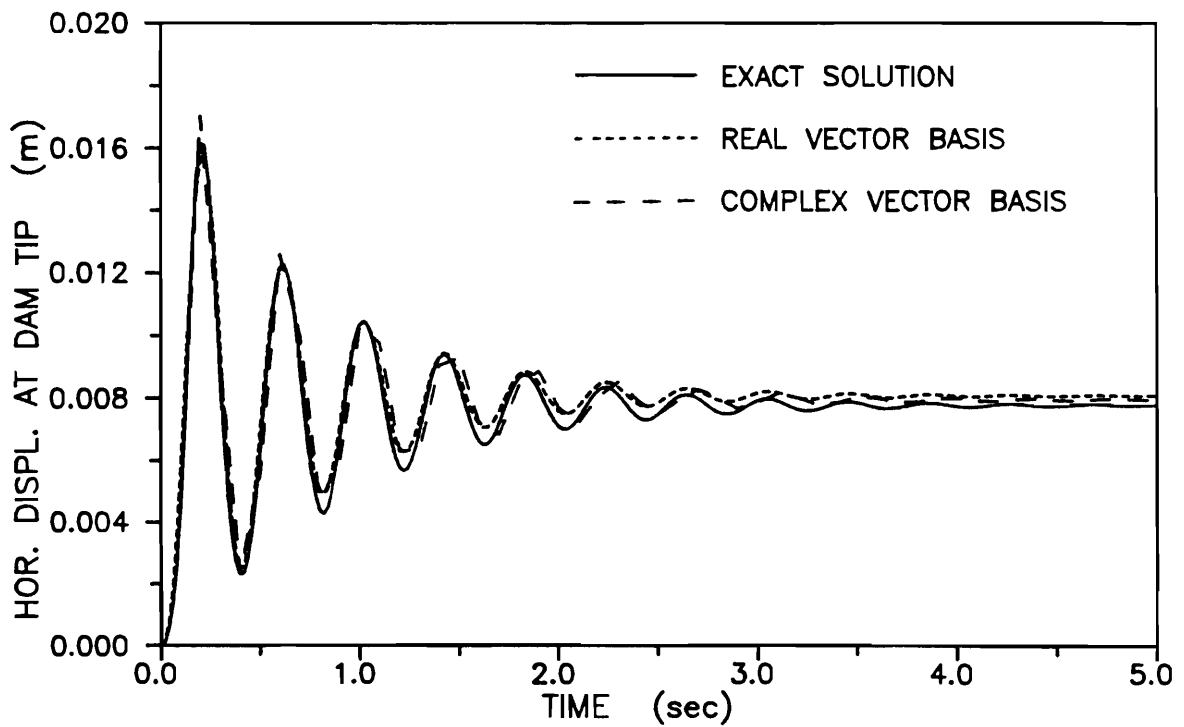

10 real Ritz vectors and 10 complex Ritz vector pairs
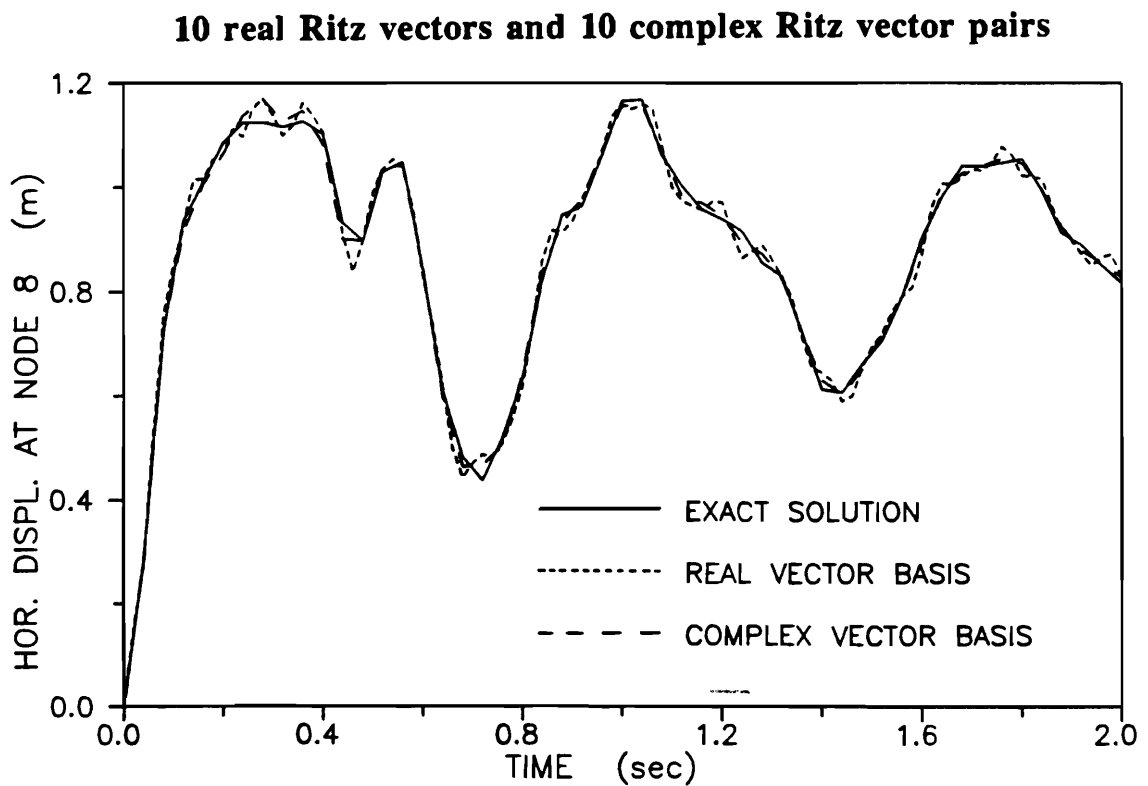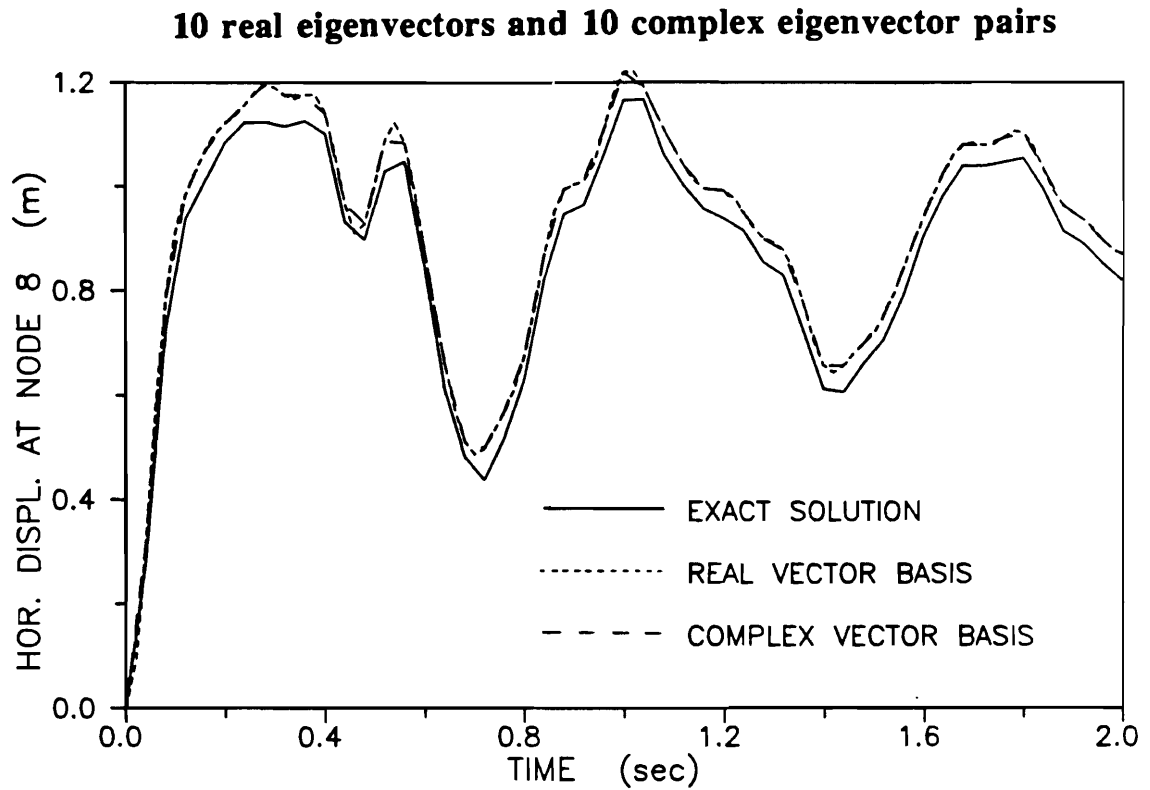
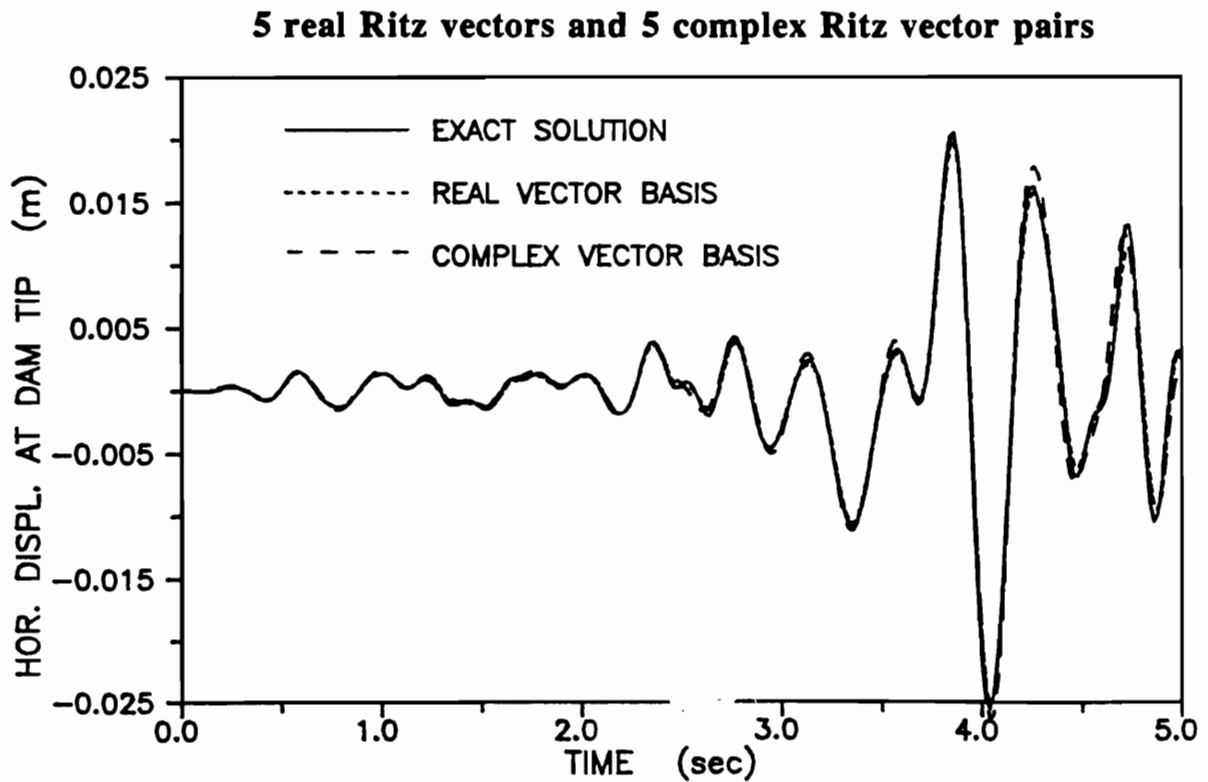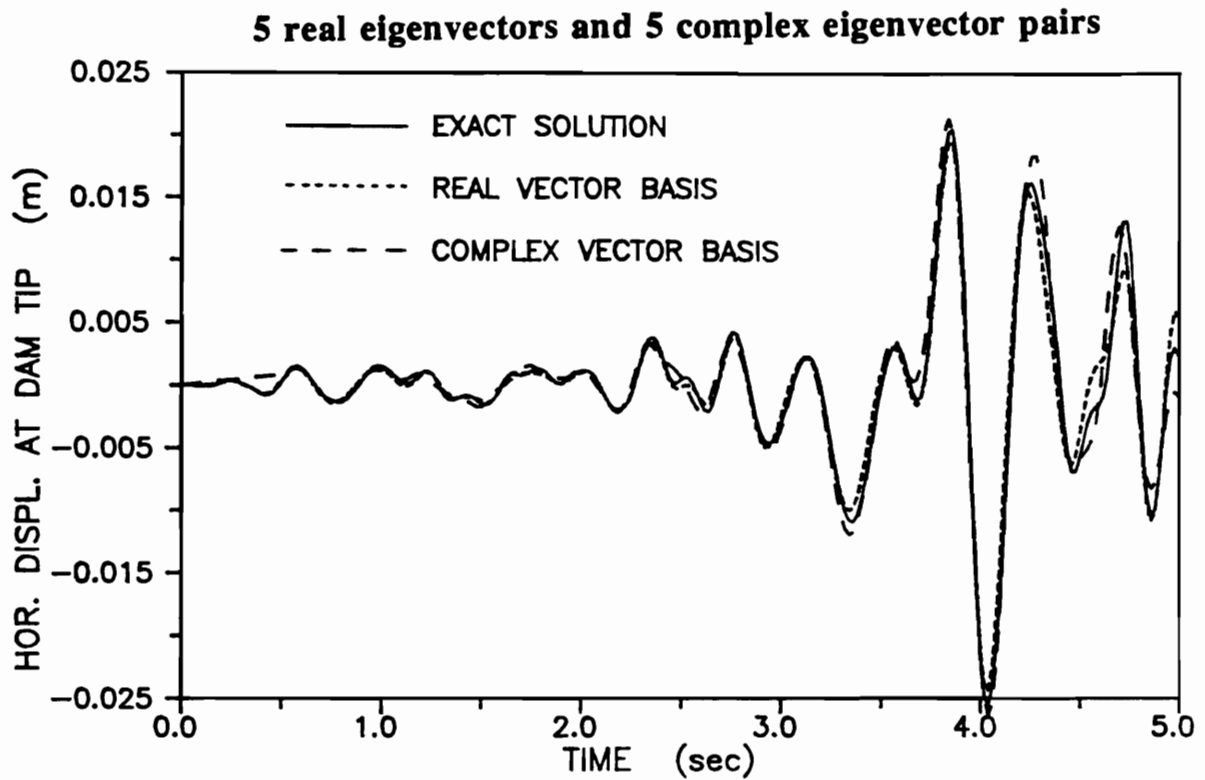Figure 4.2.2.b - Horizontal displacement at node 8 for step function

4 real eigenvectors and 4 complex eigenvector pairs
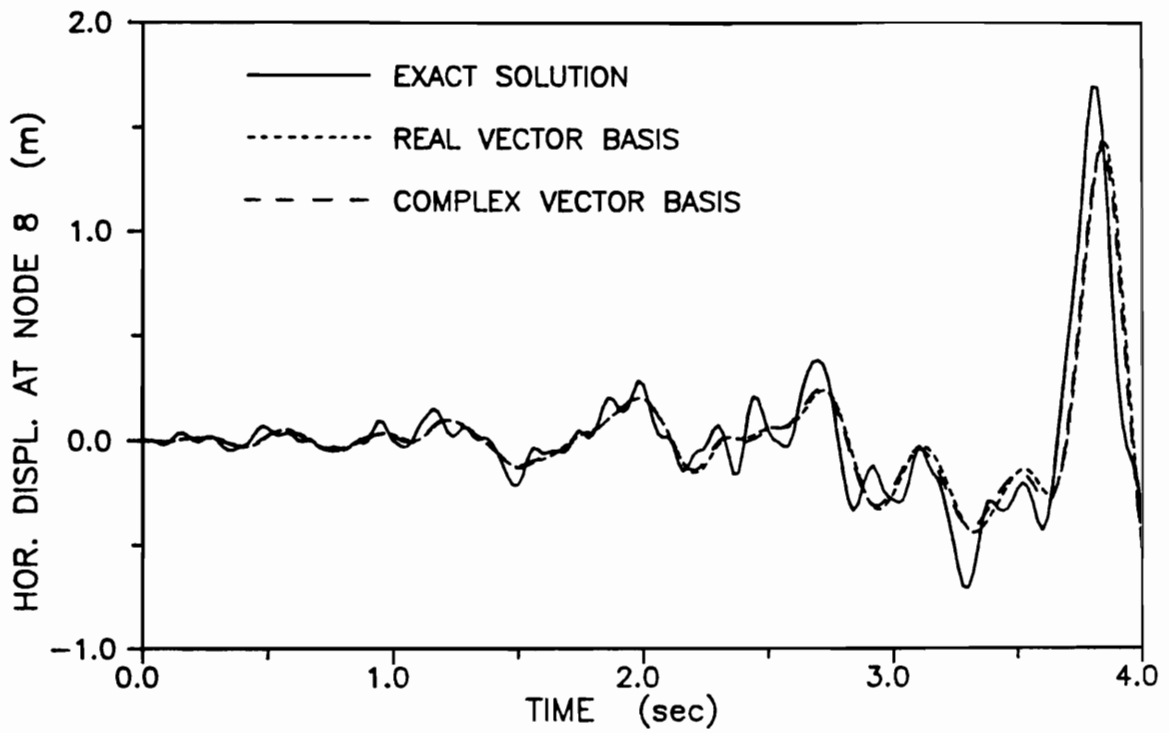
4 real Ritz vectors and 4 complex Ritz vector pairs
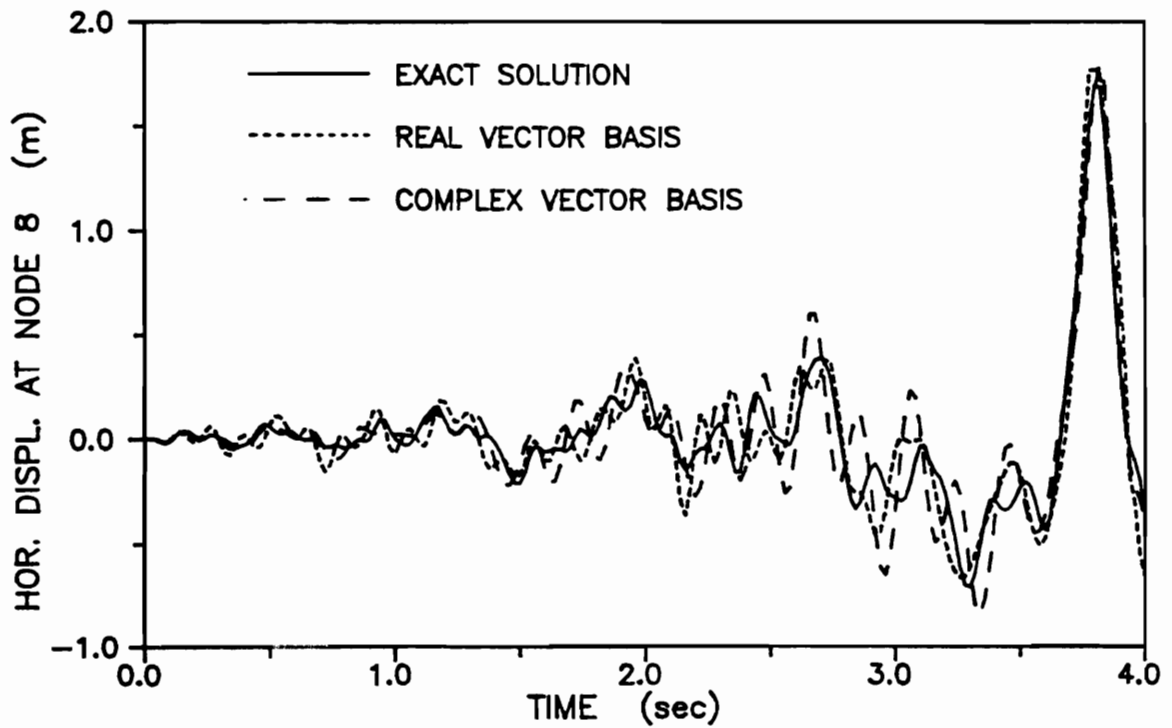
Figure 4.2.3.a - Horizontal displacement at node 8 for Taft earthquake

10 real eigenvectors and 10 complex eigenvector pairs

10 real Ritz vectors and 10 complex Ritz vector pairs
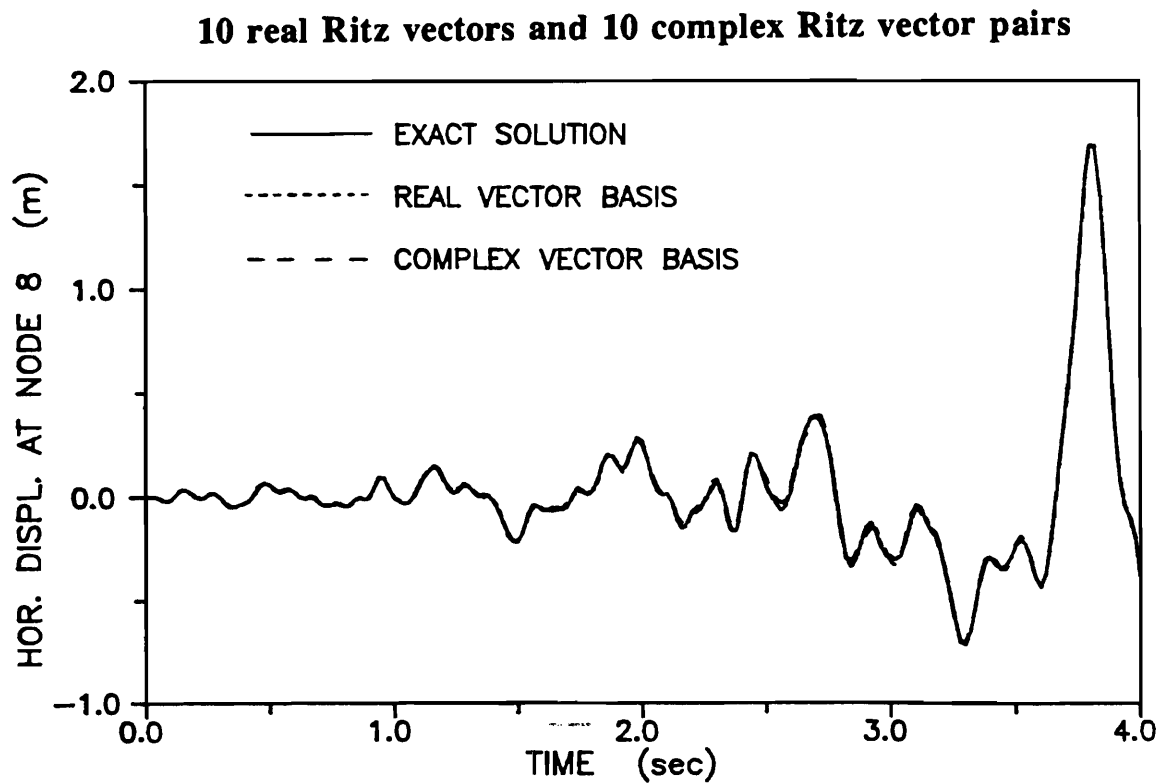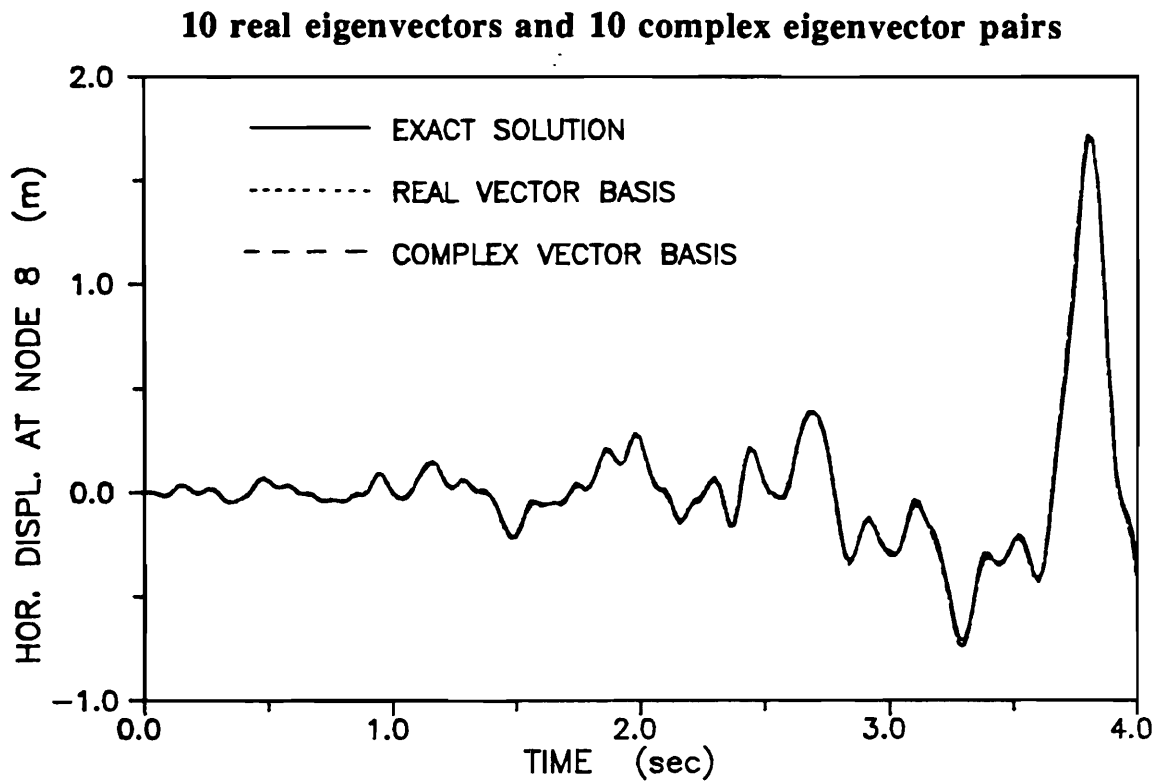
Figure 4.2.3.b - Horizontal displacement at node 8 for Taft earthquake

5 real eigenvectors and 5 complex eigenvector pairs
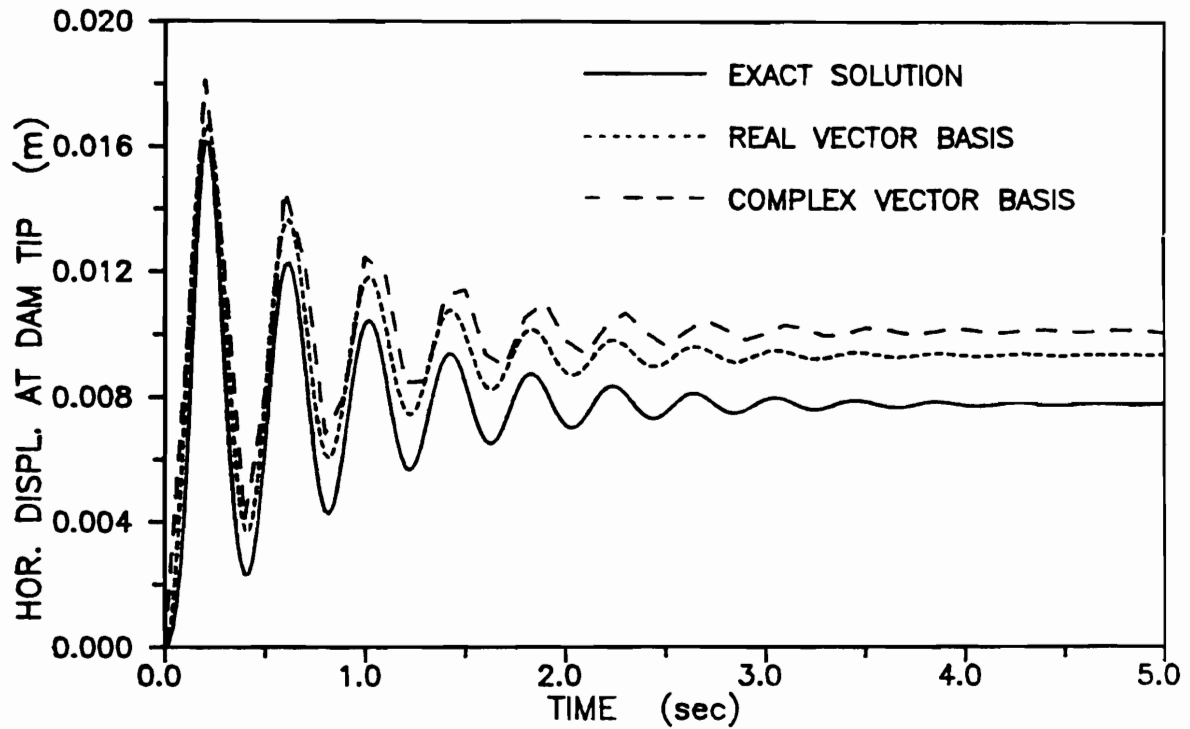
5 real Ritz vectors and 5 complex Ritz vector pairs
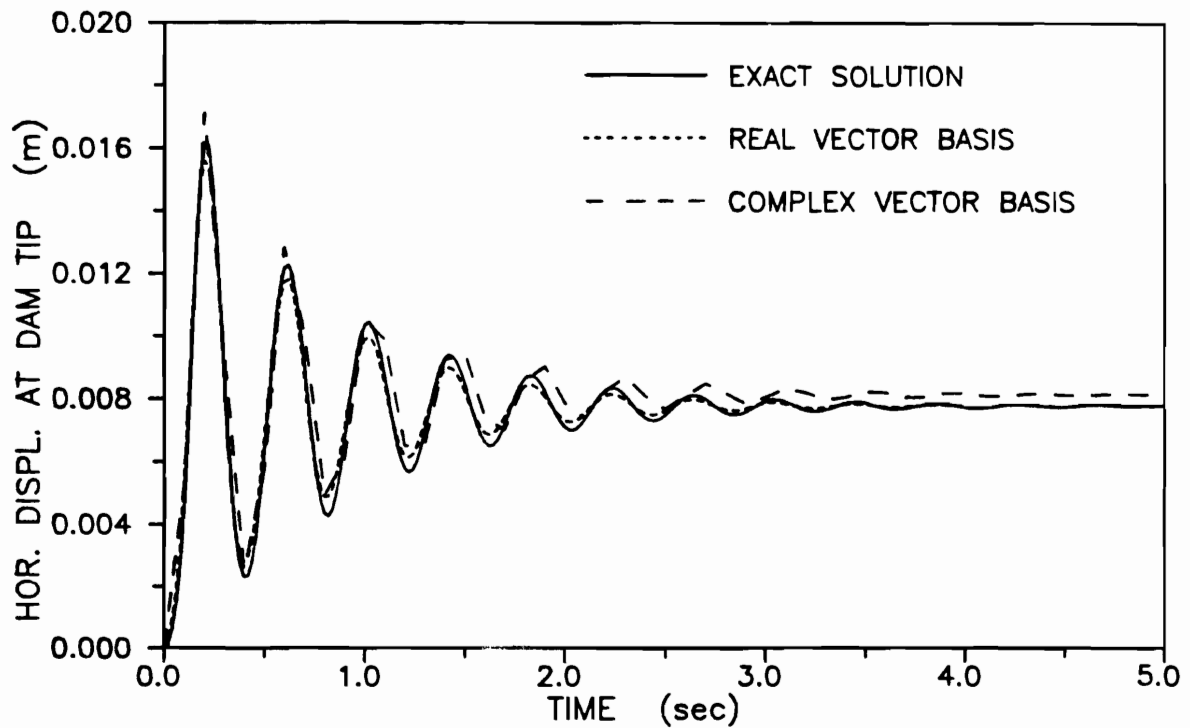
Figure 4.2.4.a - Horizontal displacement at dam tip for step function

10 real eigenvectors and 10 complex eigenvector pairs
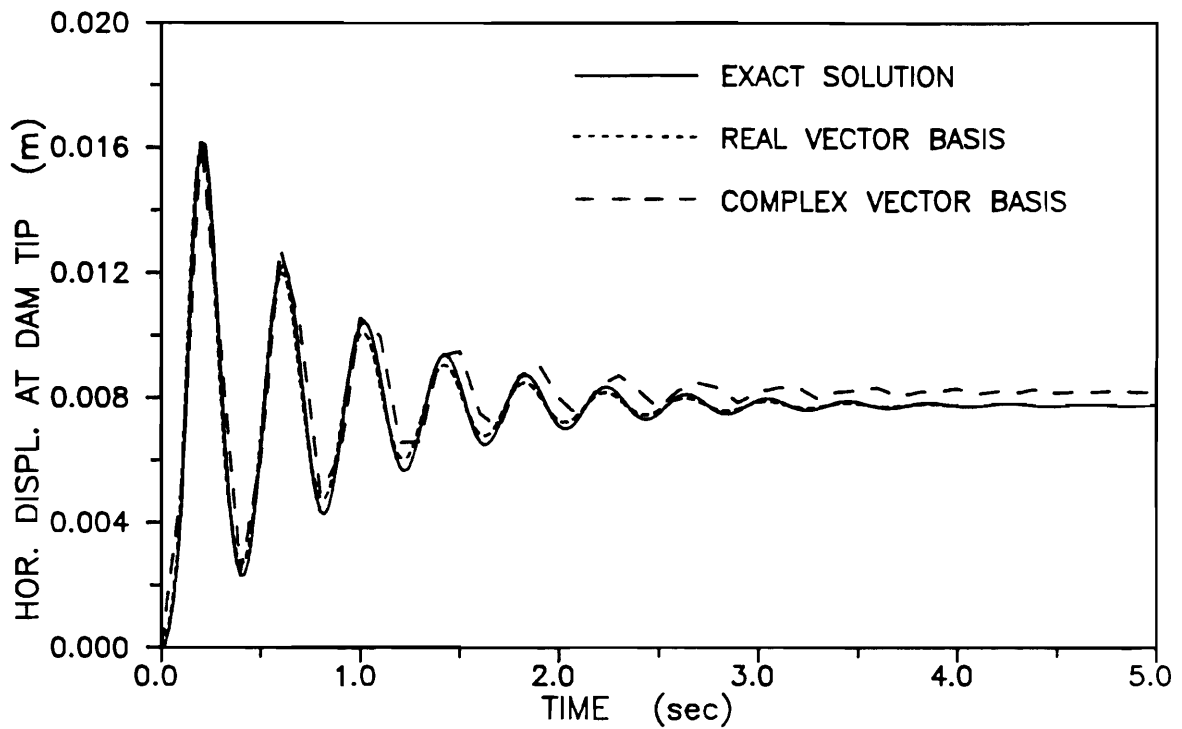
10 real Ritz vectors and 10 complex Ritz vector pairs

Figure 4.2.4.b - Horizontal displacement at dam tip for step function

5 real eigenvectors and 5 complex eigenvector pairs

5 real Ritz vectors and 5 complex Ritz vector pairs

Figure 4.2.5.a - Horizontal displacement at dam tip for Taft earthquake

10 real eigenvectors and 10 complex eigenvector pairs

10 real Ritz vectors and 10 complex Ritz vector pairs
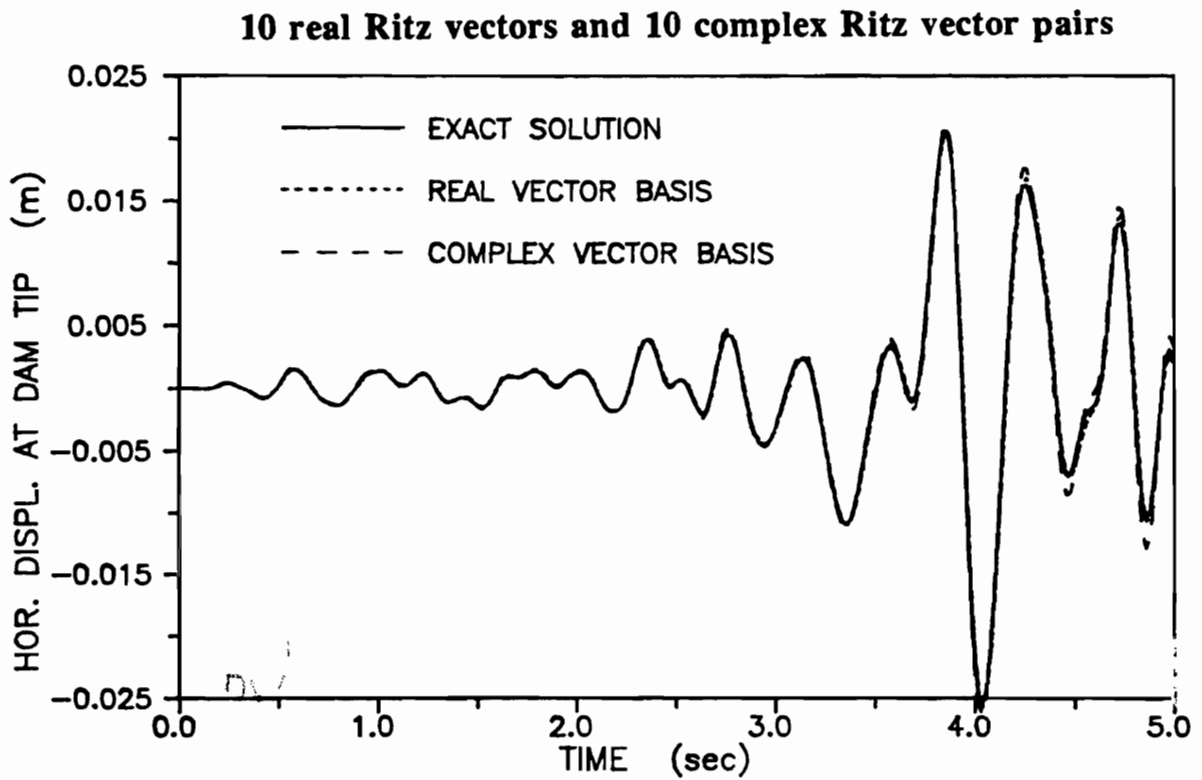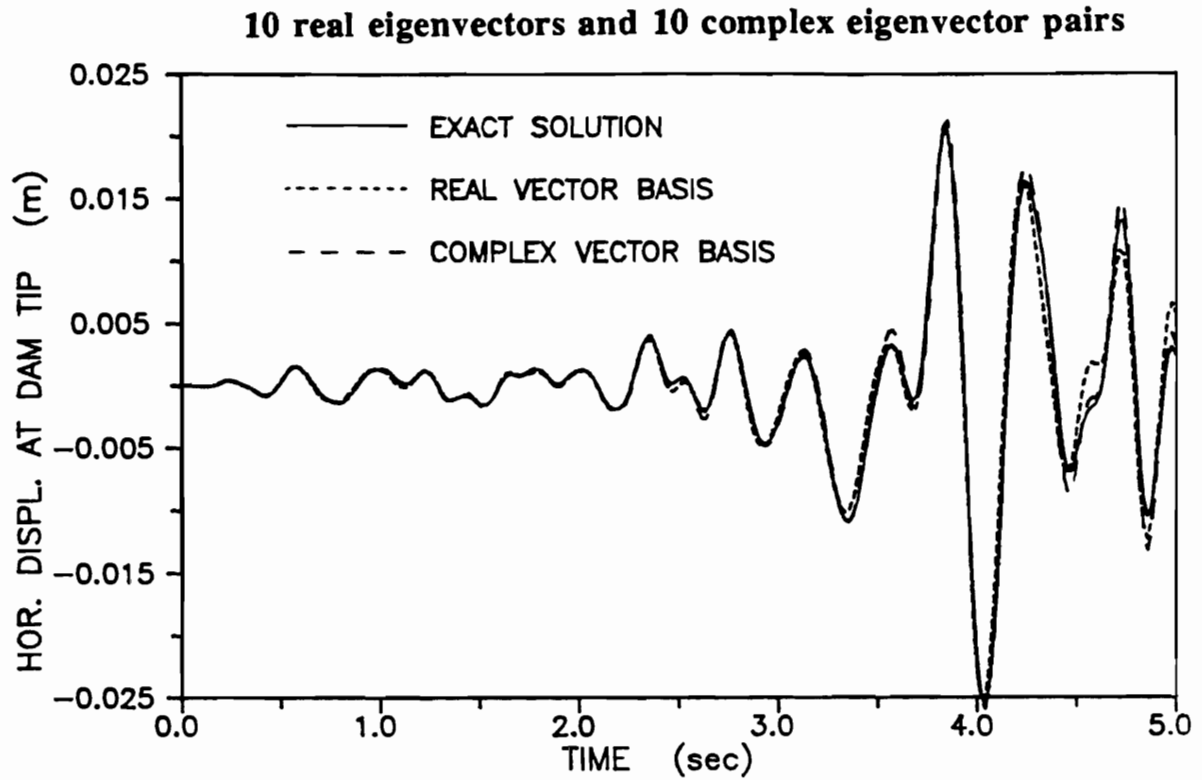
Figure 4.2.5.b - Horizontal displacement at dam tip for Taft earthquake
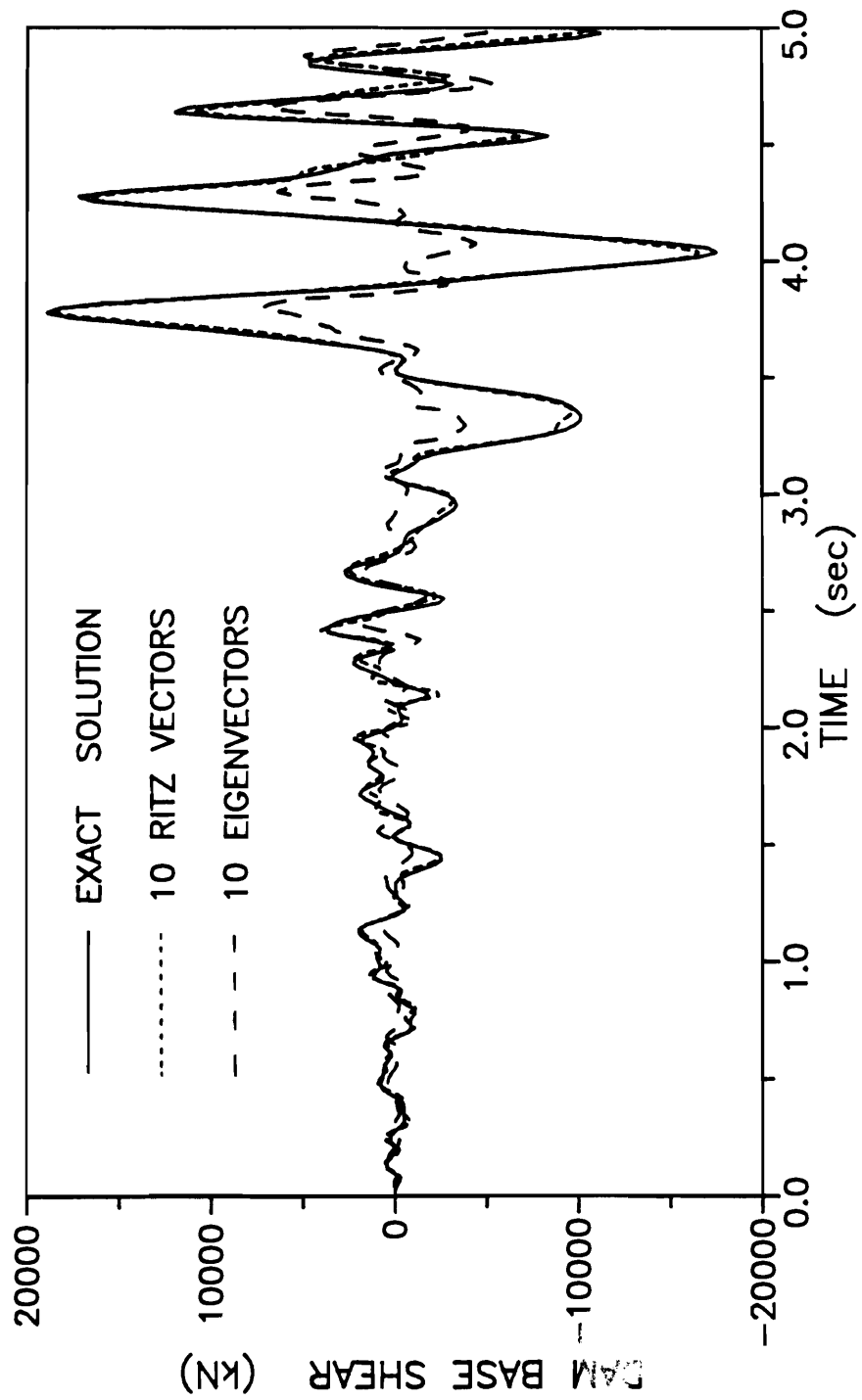
**Figure 4.2.6 - Dam base shear force for eigenvector and Ritz vector basis
(Taft earthquake loading)**

Chapter 5
Nonlinear Dynamic Analysis : Structure-Foundation
Systems with Inelastic Constitutive Equations

5.1. General Formulation

Dynamic analysis of a structure-foundation system can be formulated as a standard problem, if the complete system includes the source of earthquake excitation. However, for seismic excitation, many uncertainties in the source mechanism and in the geological parameters along the transmission path and, most of all, the sheer size of this model, require a different approach. Namely, the earthquake motion is usually recorded at a single point, commonly referred to as *control point*. The control point has to be selected at the boundary of the model, either the foundation surface or bedrock boundary (see Roesset&Yim [1987]). Some measurements of spatial variation of the earthquake ground motion (control motion) are also provided (SMART array of measuring instruments at Taiwan). Hence, starting with the known motion at the control point, the free-field motion is recovered by the deconvolution process of kinematic interaction. The kinematic interaction problem is governed by the following initial-boundary value problem: the equations (2.1.1), (2.1.2) and (2.1.3) stand for kinematics, equilibrium and constitutive equations. However, as opposed to boundary conditions (2.1.5) a new set of boundary conditions is specified as

$$u_i = \bar{u}_i = u_i^{cp} \qquad t_i = \sigma_{ij}\, n_j = 0 \qquad \text{for } x \in \Gamma_{fs}\,, \quad \Gamma_{fs} \subset \Gamma \qquad (5.1.1)$$

where u_i^{cp} is the free-field motion at the free surface boundary Γ_{fs}, which is only a part of the complete boundary Γ.

The question we want to address further is whether the boundary value problem specified above has a unique solution. First, we give the uniqueness argument for the

standard boundary value problem in elastodynamics (Chapter 2.1) specialized for linear elasticity : suppose there are two solutions to standard boundary value problem i.e. two displacement and stress fields $(u^{(1)}, \sigma^{(1)})$ and $(u^{(2)}, \sigma^{(2)})$ that satisfy all the field equations (2.1.1) to (2.1.3) as well as the boundary conditions (2.1.5) and the initial conditions (2.1.6). Uniqueness follows if we make the difference between these two solutions (for any quantity ϕ difference is $\bar{\phi} = \phi^{(2)} - \phi^{(1)}$) equal to zero. This difference is governed by the following initial-boundary value problem:

-linearized kinematics

$$\bar{\varepsilon}_{ij} = \frac{1}{2} \ (\ \bar{u}_{i,j} + \bar{u}_{j,i} \ ) \ \ ..... \quad \text{for } \mathbf{x} \in \Omega, \ t \in (0,T] \qquad (5.1.2)$$

-equilibrium equations

$$\bar{\sigma}_{ij,j} - \rho \ddot{\bar{u}}_i = 0 \ \ ..... \quad \text{for } \mathbf{x} \in \Omega, \ t \in (0,T] \qquad (5.1.3)$$

-constitutive equations

$$\bar{\sigma}_{ij} = D_{ijkl} \ \bar{\varepsilon}_{kl} \ \ ..... \quad \text{for } \mathbf{x} \in \Omega, \ t \in (0,T] \qquad (5.1.4)$$

-boundary conditions

$$\bar{u}_i = 0 \ \ ..... \quad \text{for } \mathbf{x} \in \Gamma_u, \ t \in (0,T] \qquad (5.1.5)$$

$$\bar{t}_i = \bar{\sigma}_{ij} \ n_j = 0 \ \ ..... \quad \text{for } \mathbf{x} \in \Gamma_\sigma, \ t \in (0,T]$$

with $\Gamma = \Gamma_u \cup \Gamma_\sigma$.

-initial conditions

$$\bar{u}_i = 0 \ \ ..... \quad \text{for } \mathbf{x} \in \Omega, \ t = 0 \qquad (5.1.6)$$

$$\dot{\bar{u}}_i = 0 \ \ ..... \quad \text{for } \mathbf{x} \in \Omega, \ t = 0$$

Or, the boundary conditions (5.1.5) can be rewritten as

$$\bar{u}_i \ \bar{\sigma}_{ij} \ n_j = 0 \ \ ..... \quad \text{for } \mathbf{x} \in \Gamma, \ t \in (0,T] \qquad (5.1.7)$$

The virtual work equation (weak form of equilibrium equations) is now

$$\int_{\Gamma} \bar{u}_i \, \bar{\sigma}_{ij} \, n_j \, d\Gamma - \int_{\Omega} \rho \, \ddot{\bar{u}}_i \, \bar{u}_i \, d\Omega = 0 \qquad (5.1.8)$$

and by Gauss divergence theorem applied to the first term of (5.1.8) we can rewrite it as

$$\int_{\Omega} \left(\bar{u}_i \, \bar{\sigma}_{ij} \right)_{,j} d\Omega - \int_{\Omega} \rho \, \ddot{\bar{u}}_i \, \bar{u}_i \, d\Omega = 0 \qquad (5.1.9)$$

or, using Leibnitz rule for the differentiation of a product and utilizing the constitutive equations (5.1.4) it is further

$$\int_{\Omega} \left(\bar{\sigma}_{ij,j} - \rho \, \ddot{\bar{u}}_i \right) \bar{u}_i \, d\Omega + \int_{\Omega} D_{ijkl} \, \bar{\varepsilon}_{ij} \, \bar{\varepsilon}_{kl} \, d\Omega = 0 \qquad (5.1.10)$$

The first term in (5.1.10) equals zero by the equilibrium equation (5.1.4). Hence, it follows that the second term of (5.1.10) also has to be equal to zero. By the ellipticity (positive definiteness) of elasticity tensor D_{ijkl}, it follows that the strain field is uniquely defined. From the constitutive equations (5.1.3) it follows that the stress field is also unique, while from the governing kinematics (5.1.1) it follows that the displacement field is unique apart from arbitrary rigid body displacements.

If we now want to extend the uniqueness result of the standard boundary value problem to boundary value problem that describes kinematic interaction, the key difficulty to be faced is the lack of boundary conditions in the form (5.1.7). Namely, it holds

$$\bar{u}_i \, \bar{\sigma}_{ij} \, n_j = 0 \quad \ldots \quad \text{for } x \in \Gamma_{fs} \subset \Gamma, \, t \in (0,T] \qquad (5.1.11)$$

while on the rest of the boundary Γ no condition of the form (5.1.11) can be stated; consequently, the boundary value problem that governs kinematic interaction has more than one solution. Stakgold [1979] refers to the problems with non-unique solution as ill-posed (as opposed to well-posed). The ill-posedness of the kinematic interaction problem is usually eliminated by placing restrictions upon the wave pattern (motion properties). In particular, vertically propagating seismic shear waves are often assumed. Some parametric studies of different choices for assumed wave pattern are performed by Wolf [1985].

Instead, we present a more consistent way to solve the kinematic interaction by impos-
ing an appropriate assumption on non-prescribed boundary conditions. The discussion is
left for the next section, where the elastic constitutive equations for the foundation material
are assumed. For the inelastic constitutive equations of the foundation material, the decon-
volution analysis of kinematic interaction is not possible. In this case, the free-field motion
of the system in general represents an irreversible process. Hence, the prospective of a suc-
cessful deconvolution process of the kinematic interaction is limited to a linear elastic part
of constitutive relations. Otherwise, an arbitrary assumption on bedrock boundary motion
has to be introduced.

After the kinematic interaction problem is solved (or bedrock motion assumed), the
dynamic analysis of the structure-foundation model is transformed into the standard prob-
lem. Suppose that the inelastic constitutive equations for both the structure and the founda-
tion are given the general form

$$\sigma_{ij} = \hat{\sigma}_{ij}(\varepsilon_{kl}, \dot{\varepsilon}_{kl}) \tag{5.1.12}$$

where $\hat{\sigma}_{ij}$ is tensor function that relates the stress tensor components to strain and strain
rates.

For linearized kinematics, the rest of the equations for the standard boundary value
problem (2.1.1) to (2.1.6) are the same.

Remark 5.1.1 For the inelastic constitutive equations, it may not be possible to relate the
total stress directly to total strain and strain rates. Usually, the relation between the
rates (or the increments) of strain and stress components is specified instead. In that
case, the same considerations given further would apply, but in incremental fashion.
One model that complies with the constitutive equations (5.1.12) is the deformational
theory of plasticity (see e.g. Hill [1950]). It is well established that the deformational
theory of plasticity is not suitable for constitutive equations of metals. However, some
modification of the deformational theory of plasticity give good results for soil, con-
crete and other brittle materials (see Lubliner [1989]).

Thus, the equivalent variational problem, following the procedure described by (2.1.7) to (2.1.11) is

$$\int_\Omega \rho \; \ddot{u}_i \; w_i \; d\Omega + \int_\Omega \hat{\sigma}_{ij}(\varepsilon_{kl},\dot{\varepsilon}_{kl}) \; \varepsilon_{ij}^w \; d\Omega = \int_{\Gamma_\sigma} \bar{t}_i \; w_i \; d\Gamma + \int_\Omega \rho \; b_i \; w_i \; d\Omega \qquad (5.1.13)$$

By further utilizing the matrix notation introduced in section 2.2, we can write the equivalent matrix form of (5.1.13) above

$$\mathbf{w}_I^T(t) \left\{ \mathbf{M}_{IJ} \; \ddot{\mathbf{u}}_J(t) + \mathbf{r}_I(\mathbf{u}_J(t),\dot{\mathbf{u}}_J(t)) = \mathbf{f}_I(t) \right\} \qquad I,J = 1,2,...,N_{np} \qquad (5.1.14)$$

where the only new notation is introduced for the internal force vector

$$\mathbf{r}_I(\mathbf{u}_J(t),\dot{\mathbf{u}}_J(t)) = \int_\Omega \mathbf{B}_I^T \; \boldsymbol{\sigma}(\mathbf{u}_J(t),\dot{\mathbf{u}}_J(t)) \; d\Omega \qquad (5.1.15)$$

Again, for the independent components of $\mathbf{w}(t)$, the complete set of semidiscrete equations of motion is given as

$$\mathbf{M} \; \ddot{\mathbf{u}}^t(t) + \mathbf{r}(\mathbf{u}^t(t),\mathbf{u}^t(t)) = \mathbf{f}_{ff}(t) \qquad (5.1.16)$$

In the equations (5.1.16), the motion field $\mathbf{u}^t(t)$ carries superscript t to denote a total motion of the complete structure-foundation system. The total motion field $\mathbf{u}^t(t)$ can not be separated to simplify a computational procedure, as we did in section 2.3, because of the nonlinear form of the dependence of the internal force upon the total motion, i.e. $\mathbf{r}(\mathbf{u}^t(t),\dot{\mathbf{u}}^t(t))$.

For the solution of the set of semidiscrete equations (5.1.16) either explicit or implicit step-by-step integration schemes can be utilized (see Belytschko&Hughes [1983]). For the explicit integration scheme only conditional st:⋅⋅ is achieved, however, the reward is linear set of equations at each time step. In a case of a diagonal form of the mass matrix $\mathbf{M}$, the explicit scheme becomes very efficient. The implicit integration schemes grant unconditional stability, but require the solution of a set of nonlinear equations at each time step. For the large structure-foundation system, the implicit schemes are prohibitively expensive.

However, if the nonlinearities are limited to a small part of the complete system, the implicit schemes become competitive again.

5.2. Formulation for Linear Viscoelastic Foundation

If the constitutive equations for the foundation material are specialized to linear viscoelastic, then the set of semidiscrete equations of motion (5.1.16) can be restated as

$$\left[\, M_s + M_f \,\right] \left(\ddot{v}(t) + \ddot{u}(t)\right) + \left[\, C_f \,\right] \left(\dot{v}(t) + \dot{u}(t)\right) +$$

$$\left[\, K_f \,\right] \left(v(t) + u(t)\right) + r_s(u(t),\dot{u}(t)) = f_{ff}(t) \tag{5.2.1}$$

where we used again the notation defined in section 2.3.

Note that we introduced the additive split of the total motion $u'(t)$ into the free-field motion $v(t)$ and the added motion $u(t)$. This is consistent with both the linear foundation (superposition allowed for linear constitutive equations) and the nonlinear structure (added motion is equal to total motion). We also recall that the free-field motion is governed by equations (2.3.1). Hence, by combining the equations (2.3.1) and (5.2.1) above, an expanded form of the semidiscrete equations of motion of the complete system is given

$$\begin{bmatrix} M_{ss} & M_{si} & 0 \\ M_{is} & M_{ii}^s + M_{ii}^f & M_{if} \\ 0 & M_{fi} & M_{ff} \end{bmatrix} \begin{pmatrix} \ddot{u}_s(t) \\ \ddot{u}_i(t) \\ \ddot{u}_f(t) \end{pmatrix} + \begin{bmatrix} 0 & 0 & 0 \\ 0 & C_{ii}^f & C_{if} \\ 0 & C_{fi} & C_{ff} \end{bmatrix} \begin{pmatrix} \dot{u}_s(t) \\ \dot{u}_i(t) \\ \dot{u}_f(t) \end{pmatrix} + \begin{bmatrix} 0 & 0 & 0 \\ 0 & K_{ii}^f & K_{if} \\ 0 & K_{fi} & K_{ff} \end{bmatrix} \begin{pmatrix} u_s(t) \\ u_i(t) \\ u_f(t) \end{pmatrix} +$$

$$\begin{pmatrix} r_s(u(t),\dot{u}(t)) \\ r_i^s(u(t),\dot{u}(t)) \\ 0 \end{pmatrix} = - \begin{bmatrix} M_{si} \\ M_{ii}^s \\ 0 \end{bmatrix} \ddot{v}_i(t) - \begin{bmatrix} C_{si} \\ C_{ii}^s \\ 0 \end{bmatrix} \dot{v}_i(t) - \begin{bmatrix} K_{si} \\ K_{ii}^s \\ 0 \end{bmatrix} v_i(t) \tag{5.2.2}$$

where the free field motion $v_i(t)$ is defined for the traction free interface of the foundation and the structure (as presented on Figure 2.3.1).

The form of the equations of motion (5.2.2) is also obtained by Bielak&Cristiano [1984], from somewhat different considerations of the standard dynamic substructure concept, i.e. looking at the structure and the foundation as different substructures. For that

reason, the traction free interface for the free field motion is not correctly recognized and a somewhat loose definition of the interface force in the free-field appears in the formulation analogous to (5.2.2).

Remark 5.2.1 The computational efficiency in the dynamic analysis of the structure-foundation system (whose motion is governed by equations (5.2.2)) can be enhanced by application of dynamic substructuring concept, as discussed in section 4.3. Namely, the foundation substructure can be represented by reduced number of generalized Ritz coordinates. This is elaborated in the next section, where both the foundation and the structure have linear constitutive equations and only the interface is inelastic.

If the constitutive equations for the structure are given in linear viscoelastic form, then from (5.2.2) we recover the semidiscrete equations of motion (2.3.6). Note again that, by the solution of equation (5.2.2), only the added motion field for the complete system is obtained. For the structure this represents the total motion, hence, the stress recovery is directly available even for the structure with the nonlinear constitutive equations. However, if the stress in the foundation is of interest, then first the total motion field of the foundation component has to be recovered. For that reason, it is important that the model of the foundation for the kinematic interaction is adequate to the model of the foundation for the inertial interaction. One way to perform kinematic interaction on the same model used later for inertial interaction is presented next.

Kinematic Interaction

For the structure-foundation system with the inelastic constitutive equations for the structure and the linear viscoelastic constitutive model for the foundation, we describe further one way to perform the kinematic interaction deconvolution, *without imposing a priori assumption on wave patter* ich is the approach usually taken (see e.g. Wolf [1985]). Instead, we make an assumption on the distribution of prescribed displacement $\bar{u}(t)$ along the boundary Γ_u. Namely, for boundary value problem governing kinematic interaction, along the free surface boundary Γ_{fs}, traction is known (prescribed) to be zero, i.e. $\Gamma_{fs} = \Gamma_\sigma$. To transform the boundary value problem which governs the kinematic interaction

into the form of well-posed standard boundary value problem in elastodynamics (section 2.1), the rest of the boundary (aside from Γ_{fs}) is turned into Γ_u boundary, where displacements are prescribed

$$\mathbf{u}(\mathbf{x},t) = \bar{\mathbf{u}}(t) \qquad \text{for } \mathbf{x} \in \Gamma_u$$

or, to be consistent with the free-field notation

$$\bar{\mathbf{u}}(t) = \mathbf{v}_g(t)$$

where $\mathbf{v}_g(t)$ is the free-field motion along the remainder of the boundary Γ apart from the free surface. From the specified motion at the control point $\mathbf{v}_{cp}(t)$, we can determine the variation of motion $\mathbf{v}_g(t)$ at the boundary Γ_u, by the deconvolution process. In order to make the deconvolution possible, the number of components of $\mathbf{v}_g(t)$ (in the semidiscretized model of the foundation used for that purpose), has to match the number of components of *measured* motion at the control point.

Let us assume that the time history of only one component of acceleration at the control point is specified as $\ddot{v}_{cp}(t)$. That will give us only one condition to solve for unknown input motion at the base. For that reason, we assume that the model of the foundation in the free-field is excited by imposing *rigid base* motion $v_g(t)$.

The semidiscrete equations of the motion in the free-field are then

$$\mathbf{M}_f \, \ddot{\mathbf{v}}(t) + \mathbf{C}_f \, \dot{\mathbf{v}}(t) + \mathbf{K}_f \, \mathbf{v}(t) = \mathbf{f}_{ff}(t) = \mathbf{M}_f \, \mathbf{r} \, \ddot{v}_g(t) \qquad (5.2.3)$$

where the equation (5.2.3) has the same meaning as the previously used form (2.3.1). In this case, however, we make an assumption on the specific form of the far-field forcing function as given in (5.2.3), as a rigid base motion $\ddot{v}_g(t)$ multiplied by the "directional" mass of the foundation, $\mathbf{M}_f \, \mathbf{r}$.

The set of the semidiscrete equations of motion (5.2.3), can be further projected onto the Ritz vector subspace of the foundation by utilizing modal transformation, and again, enhancing the computational efficiency by modal truncation. Hence, one modal equation (assuming proportional damping) is

$$\ddot{y}_i(t) + 2\xi_i\omega_i \; \dot{y}_i(t) + \omega_i^2 \; y(t) = \boldsymbol{\psi}_i^T \mathbf{M}_f \; \mathbf{r} \; \ddot{v}_g(t) \qquad i = 1,2,...,m < n \qquad (5.2.4)$$

Or, if we transform the equation (5.2.4) into the frequency domain, by the application of the Fourier transform

$$H_i(\bar{\omega}) \; Y_i(\bar{\omega}) = \boldsymbol{\psi}_i^T \; \mathbf{M}_f \; \mathbf{r} \; \ddot{V}_g(\bar{\omega}) \qquad (5.2.5)$$

where $Y_i(\bar{\omega})$ and $\ddot{V}_g(\bar{\omega})$ are Fourier transform pairs to $y_i(t)$ and $v_g(t)$ ($\bar{\omega}$ and t being dual variables), while

$$H_i(\bar{\omega}) = \omega_i^2 - \bar{\omega}^2 + 2i\xi_i\omega_i\bar{\omega} \qquad (5.2.6)$$

is impedance (complex stiffness); and adequately, compliance (complex flexibility) can be determined as

$$G_i(\bar{\omega}) = \frac{\omega_i^2 - \bar{\omega}^2 - 2i\xi_i\omega_i\bar{\omega}}{\sqrt{(\omega_i^2 - \bar{\omega}^2)^2 + 4\xi_i^2\omega_i^2\bar{\omega}^2}} \qquad (5.2.7)$$

Using the equations (5.2.6) and (5.2.7), (5.2.5) can be rewritten as

$$Y_i(\bar{\omega}) = G_i(\bar{\omega}) \; \boldsymbol{\psi}_i^T \mathbf{M}_f \; \mathbf{r} \; \ddot{V}_g(\bar{\omega}) \qquad (5.2.8)$$

Further, by differentiation (corresponds to multiplication by $i\bar{\omega}$) of (5.2.8) we get

$$\ddot{Y}_i(\bar{\omega}) = -\bar{\omega}^2 \; G_i(\bar{\omega}) \; \boldsymbol{\psi}_i^T \mathbf{M}_f \; \mathbf{r} \; \ddot{V}_g(\bar{\omega}) \qquad (5.2.9)$$

By mode superposition analysis, the component of the acceleration vector at the control point in finite element coordinates ($\ddot{V}_{cp}$ - subscript cp denotes measured component) can be recovered from the specified accelerations at each of the generalized Ritz coordinates

$$\ddot{V}_{cp}(\bar{\omega}) = \sum_{i=1}^{m} \boldsymbol{\psi}_{i_{cp}} \; \ddot{Y}_i(\bar{\omega}) \qquad (5.2.10)$$

By utilizing the equation (5.2.9), we can restate the new form for relative acceleration component at the control point

$$\ddot{V}_{cp}(\bar{\omega}) = -\sum_{i=1}^{m} \psi_{i_{cp}} \, \bar{\omega}^2 \, G_i(\bar{\omega}) \, \psi_i^T \, M_f \, r \, \ddot{V}_g(\bar{\omega}) = T_g \, \ddot{V}_g(\bar{\omega}) \tag{5.2.11}$$

The total acceleration at the control point (usually measured), will be the direct summation of its dynamic component, defined by the equation (5.2.11) above, and its pseudo-static component

$$\ddot{V}_{cp}(\bar{\omega}) = T_g \, \ddot{V}_g(\bar{\omega}) + r_{cp} \, \ddot{V}_g(\bar{\omega}) = T_{g-ps} \, \ddot{V}_g(\bar{\omega}) \tag{5.2.12}$$

Hence, for the measured total acceleration at the control point, the base acceleration directly follows from (5.2.12)

$$\ddot{V}_g(\bar{\omega}) = T_{g-ps}^{-1} \, \ddot{V}_{cp}(\bar{\omega}) \tag{5.2.13}$$

and further, the time history of the base acceleration can be obtained by the inverse Fourier transform applied to (5.2.12).

$$\ddot{v}_g(t) = \int_{-\infty}^{\infty} \ddot{V}_g(\bar{\omega}) \, e^{i\bar{\omega}t} \, d\bar{\omega} \tag{5.2.14}$$

where the fast Fourier transform is used in the computation of (5.2.14) above.

Once the base acceleration is known, the site amplification, given as the standard dynamic analysis problem, concludes the kinematic interaction phase of the analysis.

It is important to notice that we have solved the kinematic interaction problem *without* the assumed wave pattern. In addition, the model for the kinematic interaction is completely *consistent* with the model for the inertial interaction; hence, it is easily possible to recover the complete motion field in the foundation (superimposing free-field motion determined from kinematic interaction and added motion determined from inertial interaction), which is needed if the stress state in the foundation is of interest.

We presented the deconvolution process for the case where only one component of acceleration is measured at the control point. For the case when all 3 components are measured at the control point, the procedure given above is easily generalized. In that case, compliance $G(\bar{\omega})$ in the equation (5.2.7) is a 3×3 matrix $G(\bar{\omega})$, given as the inverse of the

3×3 impedance matrix, $H(\bar{\omega})$. For any particular frequency $\bar{\omega}$, 3×3 matrices would appear instead of scalar quantities in (5.2.8) to (5.2.13) above. The time history for the base motion acceleration $\ddot{v}_g(t)$ is obtained componentwise by the inverse Fourier transform of $\ddot{V}_g(\bar{\omega})$.

If the spatial variation of the free-field motion is known over the whole free surface (e.g. using the data from SMART array of measuring instruments), then we may abandon the assumption of the rigid base input $v_g(t)$, and obtain the spatial variation of the base motion (or, spatial distribution of the prescribed displacement over boundary Γ_u), consistent with the measured variation along the free surface.

5.3. Formulation for Inelastic Constitutive Equations for Structure-Foundation Interface

The equations (5.2.2) can be further reformulated if only the interface constitutive equations are considered as inelastic, while the structure and the foundation are governed by the linear viscoelastic constitutive equations. In this case, the total motion field for the interface dofs on the foundation side (Figure 5.3.1), according to formulation (5.2.2) is split into the free-field motion and the added motion field. By the solution of (5.2.2) only the added motion field in the foundation is obtained. However, for the inelastic constitutive equations of the interface, the total motion field is normally required.

Instead of recovering of the total motion field for the foundation, we propose the additive split of the added motion for the structure (equal to total motion of the structure) into the motion introduced by the structure interface motion identical to foundation interface free field motion and the remaining part (see Figure 5.3.1). If the assumption of a constant free-field motion over all interface dofs is introduced (equivalent to rigid base assumption), then the motion caused by the free-field motion represents the rigid body motion, and the corresp ..... stress field is zero for both the interface and the structure. In opposite, if the variation of the free-field motion along the structure-foundation interface is assumed, the stress field will be nonzero in both the structure and the interface. However, from the specified variation of the free-field motion, this stress field can be easily obtained (state determination), even for the inelastic interface constitutive equations, and further introduced

in the formulation (5.2.2) as the initial stress in the interface.

Practically, the split of the structure added motion is equivalent to the split of the total motion into the pseudo-static and the dynamic components for the linear structure-foundation system, although the motivation in the case currently discussed is different. The basic transformations that follow from the above discussion are:

-equality of the interface motion for the structure and the foundation

$$v_i^s(t) = v_i^f(t) \tag{5.3.1}$$

-additive split of the structure motion

$$u^t(t) = u(t) + u_{v_i}(t) \tag{5.3.2}$$

-where by definition

$$u_{v_i}(t) = -K_{ss}^{-1} K_{si} v_i^s(t) = R \, v_i^f(t) \tag{5.3.3}$$

where (5.3.1) is introduced into (5.3.3).

For the linear viscoelastic constitutive equations for the structure, it also hold that

$$r_s(u(t),\dot{u}(t)) = K_{ss} \, u_s(t) + C_{ss} \, \dot{u}_s(t) + K_{si} \, u_i(t) + C_{si} \, \dot{u}_i(t) \tag{5.3.4}$$

Hence, by introducing (5.3.1) to (5.3.4) into the equations of motion (5.2.2), we can rewrite the equations of motion

$$M \, \ddot{u}(t) + C \, \dot{u}(t) + K \, u(t) + r(u(t),\dot{u}(t)) = \tilde{M} \, \ddot{v}_i^s(t) \tag{5.3.5}$$

Where the expanded form of the matrix and vector quantities in the equations of motion (5.3.5) for the complete structure-foundation system (for clarity) is given further:

-displacement vector (equivalent for velocity and acceleration)

$$u(t) = \begin{pmatrix} u_s(t) \\ u_i^s(t) \\ u_i^f(t) \\ u_f(t) \end{pmatrix}$$

-mass matrix of the complete system

$$
\mathbf{M} = \begin{bmatrix} \mathbf{M}_{ss} & \mathbf{M}_{si} & \mathbf{0} & \mathbf{0} \\ \mathbf{M}_{is} & \mathbf{M}_{ii}^{s} & \mathbf{0} & \mathbf{0} \\ \mathbf{0} & \mathbf{0} & \mathbf{M}_{ii}^{f} & \mathbf{M}_{if} \\ \mathbf{0} & \mathbf{0} & \mathbf{M}_{fi} & \mathbf{M}_{ff} \end{bmatrix}
$$

-damping matrix of the complete system

$$
\mathbf{C} = \begin{bmatrix} \mathbf{C}_{ss} & \mathbf{C}_{si} & \mathbf{0} & \mathbf{0} \\ \mathbf{C}_{is} & \mathbf{C}_{ii}^{s} & \mathbf{0} & \mathbf{0} \\ \mathbf{0} & \mathbf{0} & \mathbf{C}_{ii}^{f} & \mathbf{C}_{if} \\ \mathbf{0} & \mathbf{0} & \mathbf{C}_{fi} & \mathbf{C}_{ff} \end{bmatrix}
$$

(5.3.6)

-stiffness matrix of the complete system

$$
\mathbf{K} = \begin{bmatrix} \mathbf{K}_{ss} & \mathbf{K}_{si} & \mathbf{0} & \mathbf{0} \\ \mathbf{K}_{is} & \mathbf{K}_{ii}^{s} & \mathbf{0} & \mathbf{0} \\ \mathbf{0} & \mathbf{0} & \mathbf{K}_{ii}^{f} & \mathbf{K}_{if} \\ \mathbf{0} & \mathbf{0} & \mathbf{K}_{fi} & \mathbf{K}_{ff} \end{bmatrix}
$$

-interface internal force

$$
\mathbf{r}(\mathbf{u}(t),\dot{\mathbf{u}}(t)) = \begin{pmatrix} \mathbf{0} \\ \mathbf{r}_{i}^{s}(\mathbf{u}_{i}(t),\dot{\mathbf{u}}_{i}(t)) \\ \mathbf{r}_{i}^{f}(\mathbf{u}(t),\dot{\mathbf{u}}(t)) \\ \mathbf{0} \end{pmatrix}
$$

-external force vector - "directional" mass

$$
\tilde{\mathbf{M}} = - \begin{bmatrix} \mathbf{M} \, \mathbf{R} + \begin{bmatrix} \mathbf{M}_{si} \\ \mathbf{M}_{ii}^{s} \\ \mathbf{0} \\ \mathbf{0} \end{bmatrix} \end{bmatrix}
$$

To enhance the computational efficiency, the dynamic substructuring concept discussed in section 2.3, is applied to the equations (5.3.5). The basic transformation for the dynamic substructure:

-structure

$$
\begin{pmatrix} \mathbf{u}_s(t) \\ \mathbf{u}_i^s(t) \end{pmatrix} = \begin{bmatrix} \mathbf{\Psi}_s & \mathbf{R}_s \\ \mathbf{0} & \mathbf{I}_i \end{bmatrix} \begin{pmatrix} \mathbf{y}_s(t) \\ \mathbf{u}_i^s(t) \end{pmatrix}
\tag{5.3.7}
$$

-foundation

$$
\begin{pmatrix} \mathbf{u}_f(t) \\ \mathbf{u}_i^f(t) \end{pmatrix} = \begin{bmatrix} \mathbf{\Psi}_f & \mathbf{R}_f \\ \mathbf{0} & \mathbf{I}_i \end{bmatrix} \begin{pmatrix} \mathbf{y}_f(t) \\ \mathbf{u}_i^f(t) \end{pmatrix}
\tag{5.3.8}
$$

where $\mathbf{\Psi}_s$ and $\mathbf{\Psi}_f$ are sets of Ritz vectors (subspace basis) for the structure and the foundation, respectively, $\mathbf{R}_s$ and $\mathbf{R}_f$ are the corresponding pseudo-static transformations, $\mathbf{I}_i$ is the identity matrix of the dimension equal to number of interface dofs, and $\mathbf{y}_s(t)$ and $\mathbf{y}_f(t)$ are sets of generalized Ritz coordinates for the structure and the foundation. Relations (5.3.7) and (5.3.8) are completely equivalent to $(4.3.1^3)$, if the appropriate dofs are recognized.

Introducing transformations (5.3.7) and (5.3.8) into the weak form of the equations of motion (5.3.5) and utilizing the additive split of the non-proportional damping matrix $\mathbf{C}_f = diag(2\xi_f\omega_f) + \hat{\mathbf{C}}_f$ (as discussed in section 4.2) we get new form of the equations of motion

$$
\mathbf{M}^* \ddot{\mathbf{u}}^*(t) + \mathbf{C}^* \dot{\mathbf{u}}^*(t) + \mathbf{K}^* \mathbf{u}^*(t) + \mathbf{r}^*(\mathbf{u}_i(t),\dot{\mathbf{u}}_i(t)) = \mathbf{T}^T \tilde{\mathbf{M}} \ddot{\mathbf{v}}_i^s(t) - \hat{\mathbf{C}}_f^* \dot{\mathbf{y}}_f(t) \tag{5.3.9}
$$

Where expanded forms of the matrix quantities in (5.3.9) are given further:

-displacement vector (equivalent for velocity and acceleration)

$$
\mathbf{u}^*(t) = \begin{pmatrix} \mathbf{y}_s(t) \\ \mathbf{y}_f(t) \\ \mathbf{u}_i^s(t) \\ \mathbf{u}_i^f(t) \end{pmatrix}
\tag{5.3.10}
$$

-mass matrix of the complete system

$$
\mathbf{M}^* = \begin{bmatrix}
\mathbf{I}_s & 0 & \Psi_s^T \mathbf{M}_{ss} \mathbf{R}_s + \Psi_s^T \mathbf{M}_{si} & 0 \\
0 & \mathbf{I}_f & 0 & \Psi_f^T \mathbf{M}_{ff} \mathbf{R}_f + \Psi_f^T \mathbf{M}_{fi} \\
\mathbf{R}_s^T \mathbf{M}_{ss} \Psi_s + \mathbf{M}_{si} \Psi_s & 0 & \mathbf{R}_s^T \mathbf{M}_{ss} \mathbf{R}_s + \mathbf{M}_{si} \mathbf{R}_s + \mathbf{R}_s^T \mathbf{M}_{is} + \mathbf{M}_{ii}^s & 0 \\
0 & \mathbf{R}_f^T \mathbf{M}_{ff} \Psi_f + \mathbf{M}_{fi} \Psi_f & 0 & \mathbf{R}_f^T \mathbf{M}_{ff} \mathbf{R}_f + \mathbf{M}_{fi} \mathbf{R}_f + \mathbf{R}_f^T \mathbf{M}_{if} + \mathbf{M}_{ii}^f
\end{bmatrix}
$$

-damping matrix of the complete system

$$
\mathbf{C}^* = \begin{bmatrix}
diag(2\xi_s \omega_s) & 0 & \Psi_s^T \mathbf{C}_{ss} \mathbf{R}_s + \Psi_s^T \mathbf{C}_{si} & 0 \\
0 & diag(2\xi_f \omega_f) & 0 & \Psi_f^T \mathbf{C}_{ff} \mathbf{R}_f + \Psi_f^T \mathbf{C}_{fi} \\
\mathbf{R}_s^T \mathbf{C}_{ss} \Psi_s + \mathbf{C}_{si} \Psi_s & 0 & \mathbf{R}_s^T \mathbf{C}_{ss} \mathbf{R}_s + \mathbf{C}_{si} \mathbf{R}_s + \mathbf{R}_s^T \mathbf{C}_{is} + \mathbf{C}_{ii}^s & 0 \\
0 & \mathbf{R}_f^T \mathbf{C}_{ff} \Psi_f + \mathbf{C}_{fi} \Psi_f & 0 & \mathbf{R}_f^T \mathbf{C}_{ff} \mathbf{R}_f + \mathbf{C}_{fi} \mathbf{R}_f + \mathbf{R}_f^T \mathbf{C}_{if} + \mathbf{C}_{ii}^f
\end{bmatrix}
$$

-stiffness matrix of the complete system

$$
\mathbf{K}^* = \begin{bmatrix}
\mathbf{\Omega}_s^2 & 0 & 0 & 0 \\
0 & \mathbf{\Omega}_f^2 & 0 & 0 \\
0 & 0 & \mathbf{R}_s^T \mathbf{K}_{ss} \mathbf{R}_s + \mathbf{K}_{si} \mathbf{R}_s + \mathbf{R}_s^T \mathbf{K}_{is} + \mathbf{K}_{ii}^s & 0 \\
0 & 0 & 0 & \mathbf{R}_f^T \mathbf{K}_{ff} \mathbf{R}_f + \mathbf{K}_{fi} \mathbf{R}_f + \mathbf{R}_f^T \mathbf{K}_{if} + \mathbf{K}_{ii}^f
\end{bmatrix}
$$

-interface internal force

$$
\mathbf{r}^*(\mathbf{u}_i(t), \dot{\mathbf{u}}_i(t)) = \begin{pmatrix}
0 \\
0 \\
\mathbf{r}_i^s(\mathbf{u}(t), \dot{\mathbf{u}}(t)) \\
\mathbf{r}_i^f(\mathbf{u}(t), \dot{\mathbf{u}}(t))
\end{pmatrix}
$$

-expanded form of force vector

$$
-\mathbf{T}^T \left[\mathbf{M} \, \mathbf{R} + \begin{bmatrix} \mathbf{M}_{si} \\ 0 \\ \mathbf{M}_{ii}^s \\ 0 \end{bmatrix} \right] \mathbf{v}_i^s(t) - \begin{bmatrix} 0 \\ \hat{\mathbf{C}}_f \\ 0 \\ 0 \end{bmatrix} \dot{\mathbf{y}}_f(t) \qquad \text{\textit{?} \ \text{\textit{is}}}
$$

where

$$T = \begin{bmatrix} \Psi_s & 0 & R_s & 0 \\ 0 & \Psi_f & 0 & R_f \\ 0 & 0 & I_i & 0 \\ 0 & 0 & 0 & I_i \end{bmatrix}$$

and I_s and I_f are identity matrices of the dimension equal to the number of generalized Ritz coordinates for the structure and the foundation, respectively (this follows from mass ortho-normalized subspace basis); Ω_s^2 and Ω_f^2 are approximations for the squares of the natural frequencies of the structure and the foundation components (this follows from the property of Lanczos algorithm); while the rest of the quantities have the same meaning as in (5.3.5) to (5.3.8).

The semidiscrete equations of motion (5.3.9) can be further solved by utilizing step-by-step methods, i.e. fully discretizing them. The implicit Newmark algorithm family is used for that purpose, as discussed in the next chapter, where we concentrate on the case of dynamic frictional contact. This requires the solution of the nonlinear set of equations at each time step. A possible way to avoid the need to solve the nonlinear equations is by the use of an explicit method. However, since the "mass" matrix in (5.3.9) does not have diagonal form, no big advantage is to be gained and unconditional stability is to be lost. The task of solving a set of nonlinear equations is greatly simplified by first reducing the size of the linear part of the complete system by employing generalized Ritz coordinates, and second by reducing the linear part to its Schur complement (see Duff et al [1986]), i.e. prior to the solution of the nonlinear equations set, the static condensation is performed on the effective stiffness matrix $\hat{K}$

$$\begin{bmatrix} \hat{K}_{11} & \hat{K}_{12} \\ \hat{K}_{21} & \hat{K}_{22} \end{bmatrix} \rightarrow \begin{bmatrix} \hat{K}_{22} - \hat{K}_{21}\hat{K}_{11}^{-1}\hat{K}_{12} \end{bmatrix} \tag{5.3.11}$$

where the static condensation is made trivial by the diagonal form of $\hat{K}_{11}$ of all matrices in (5.3.9), and consequently the effective stiffness matrix $\hat{K}$. For the step-by-step algorithm with variable step size (requirement of efficient solution for dynamic frictional contact), the linear part of the effective stiffness matrix has to be reformed and refactorized quite often.

Computation of Schur complement (5.3.11) of the linear part is much more efficient for the equations of the form (5.3.9) than for the complete set (5.3.5) where the linear part is represented in the finite element coordinates (Bathe&Gracewski [1981]). Hence, the initial cost of formulating the Ritz vector subspace for both the structure and the foundation is likely to be compensated for, especially for loading of long duration (e.g. earthquake loading). In addition, the number of operations used to form the effective load vector is also significantly reduced, since $dim(\mathbf{y}_s) \ll dim(\mathbf{u}_s)$ and $dim(\mathbf{y}_f) \ll dim(\mathbf{u}_f)$.

The formulation presented herein can be further expanded to account for large interface sliding of the structure over the foundation. We consider only the shape of interface that yields very small rotations of the sliding structure. Hence, the motion of the origin of the reference frame attached to the structure and the motion of the structure with respect to that reference frame are directly additive. In addition, the motion of the structure with respect to this reference frame is a small displacement gradient motion, so the concept of dynamic substructuring, as discussed in section 4.3, directly applies. The origin of the moving reference frame can be made to coincide with one of the interface nodes. Let us denote the motion of the origin (equal to the motion of that interface node) as $\mathbf{u}_i^0(t)$. With the assumptions we introduced, the structure equations of motion with respect to the moving reference frame are

$$\begin{bmatrix} \mathbf{M}_{ss} & \mathbf{M}_{si} \\ \mathbf{M}_{is} & \mathbf{M}_{ii}^s \end{bmatrix} \begin{pmatrix} \ddot{\mathbf{u}}_s(t) - \ddot{\mathbf{u}}_s^0(t) \\ \ddot{\mathbf{u}}_i(t) - \ddot{\mathbf{u}}_i^0(t) \end{pmatrix} + \begin{bmatrix} \mathbf{C}_{ss} & \mathbf{C}_{si} \\ \mathbf{C}_{is} & \mathbf{C}_{ii}^s \end{bmatrix} \begin{pmatrix} \dot{\mathbf{u}}_s(t) - \dot{\mathbf{u}}_s^0(t) \\ \dot{\mathbf{u}}_i(t) - \dot{\mathbf{u}}_i^0(t) \end{pmatrix} + \begin{bmatrix} \mathbf{K}_{ss} & \mathbf{K}_{si} \\ \mathbf{K}_{is} & \mathbf{K}_{ii}^s \end{bmatrix} \begin{pmatrix} \mathbf{u}_s(t) - \mathbf{u}_s^0(t) \\ \mathbf{u}_i(t) - \mathbf{u}_i^0(t) \end{pmatrix} =$$

$$\begin{pmatrix} \mathbf{f}_s(t) \\ \mathbf{f}_i(t) \end{pmatrix} - \begin{bmatrix} \mathbf{M}_{ss} & \mathbf{M}_{si} \\ \mathbf{M}_{is} & \mathbf{M}_{ii}^s \end{bmatrix} \begin{pmatrix} \ddot{\mathbf{u}}_s^0(t) \\ \ddot{\mathbf{u}}_i^0(t) \end{pmatrix} \qquad (5.3.12)$$

where $\mathbf{u}^0(t) = (\mathbf{u}_s^0(t) \ \mathbf{u}_i^0(t))^T$ is the rigid body motion of the structure introduced by the sliding interface motion equal at each node to the motion of a selected interface nodal point. Since $\mathbf{u}^0(t)$ represents rigid body motion, no internal force that corresponds to it appears in (5.3.12)

Since the motion of the structure with respect to the moving reference frame is governed by small displacement gradient theory, the dynamic substructuring transformation, adequate to the one from section 4.3, is given

$$
\begin{pmatrix} \mathbf{u}_s(t) - \mathbf{u}_s^0(t) \\ \mathbf{u}_i(t) - \mathbf{u}_i^0(t) \end{pmatrix} = \begin{bmatrix} \mathbf{\Psi}_s & \mathbf{R}_s \\ \mathbf{0} & \mathbf{I} \end{bmatrix} \begin{pmatrix} \mathbf{y}_s(t) \\ \mathbf{u}_r(t) \end{pmatrix} \tag{5.3.13}
$$

where the pseudo-static transformation matrix $\mathbf{R}_s$ and the Ritz vector basis $\mathbf{\Psi}_s$ are as given in (5.3.7); $\mathbf{y}_s(t)$ is set of generalized Ritz coordinates for the structure motion with respect to the moving reference frame; and $\mathbf{u}_r(t)$ is a set of the retained finite element dofs of the structure. The retained coordinates $\mathbf{u}_r(t)$ are related to the global interface coordinates through the rigid body transformation matrix $\mathbf{A}$ (see (4.3.4)). Hence, the complete transformation for the structure as a dynamic substructure under the large sliding is

$$
\begin{pmatrix} \mathbf{u}_s(t) \\ \mathbf{u}_i^s(t) \end{pmatrix} = \mathbf{A} \begin{bmatrix} \mathbf{\Psi}_s & \mathbf{R}_s \\ \mathbf{0} & \mathbf{I} \end{bmatrix} \begin{pmatrix} \mathbf{y}_s(t) \\ \mathbf{u}_g(t) \end{pmatrix} = \mathbf{T}_A \, \mathbf{u}_g^*(t) \tag{5.3.14}
$$

Introducing the transformation (5.3.14) into the weak form of the equations of motion (5.3.12) for the structure, the dynamic substructure version is obtained

$$
\mathbf{M}^* \, \ddot{\mathbf{u}}_g^*(t) + \mathbf{C}^* \, \dot{\mathbf{u}}_g^* + \mathbf{K}^* \, \mathbf{u}_g^*(t) = \mathbf{f}^*(t) \tag{5.3.15}
$$

where $\mathbf{M}^*$, $\mathbf{C}^*$ and $\mathbf{K}^*$ are again of the form (4.3.3), but the force vector $\mathbf{f}^*(t)$ now has an additional term that follows from the equations (5.3.12).

To facilitate implementation of large sliding within the context of the dynamic analysis of the structure-foundation system, a 2D segment dynamic contact element is described in the next chapter. However, it should be pointed out that if large sliding is allowed for, it is not likely that only limited (interface) nonlinearities will occur.

Remark 5.3.1 If we want to expand our considerations for large sliding along the interface such that the finite rotations of the structure are also possible, the equations of motion, in spite of the assumptions of small strains, will become nonlinear due to the coupled inertia terms in the presence of Coriolis acceleration. Hence, the concept of dynamic

substructuring as discussed in section 4.3 does not apply any more. An alternative approach of setting equations of motion in an inertia reference frame will uncouple the inertia terms to a standard linear form. However, the nonlinear coupling effect will remain in the internal force terms (see Simo&VuQuoc [1985]), which again eliminates the dynamic substructuring we used.
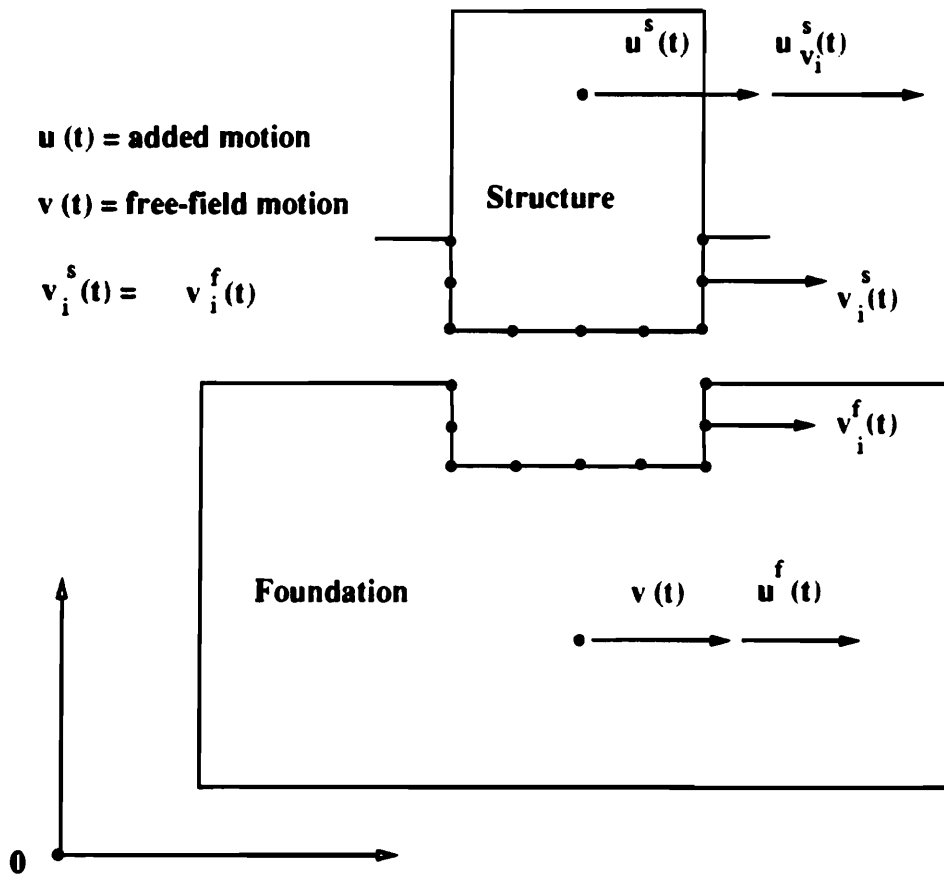
u (t) = added motion

v (t) = free-field motion

$v_i^s(t) = \quad v_i^f(t)$

Structure

$u^s(t)$ $u_{v_i}^s(t)$

$v_i^s(t)$

$v_i^f(t)$

Foundation v (t) u^f (t)

0

Figure 5.3.1 - Structure-foundation system with inelastic interface - additive split of total motion field

Chapter 6
Dynamic Frictional Contact

6.1. Variational Inequality

It has been long recognized that the natural way of vibration isolation, in the case of maximum credible earthquake, is achieved by permitting the uplifting of the structure (see Huckelbridge&Clough [1977]). To generalize such an isolation concept, the dynamic frictional contact is addressed as a model problem of nonlinearity which occurs at the structure-foundation interface, i.e. a structure can both uplift and slide. The uplifting (contact) phenomena are intrinsically *nonlinear* in nature (even if the contacting structure and the foundation are described by linear constitutive equations), since the contact area is changing in time; consequently they are not handled trivially. The first approach to the study of the uplifting phenomena utilized ad-hock simplified single dof models (Meek [1974]), or excluded the foundation interaction (Huckelbridge&Clough [1977]), both with the intent of getting manageable computational models. We, however, keep the consistency in formulating the reduced model which includes the foundation interaction effect by utilizing dynamic substructuring concept. The formulation is given as discussed in section 5.3, but the interface constitutive equations are specialized to the case of dynamic frictional contact. The general formulation is first cast as a *variational inequality* (in the spirit of Duvaut&Lions [1976]), and later, by a regularization procedure, recast into a *variational equality*. However, in our interpretation, the regularization procedure is put into proper continuum mechanics context, that correspond to transition from perfectly-plastic to elasto-plastic material. To account for energy dissipation that should supplement elastic power law for normal penetration interface, the simple nonlinear viscoelastic model is suggested.

Energy dissipation mechanism for tangential interface is governed by Coulomb law. The analysis is restricted to small displacement gradient theory, since for large sliding it is not reasonable to expect local nonlinearities only.

On the other hand, motivated by another class of contact problems in the large displacement motions, the finite element solution was considered by Hughes et al. [1976], Simo et al. [1984], Landers&Taylor [1985] and Ju et al. [1987]. The analysis is based on various versions of Lagrange multipliers method used to enforce *non-penetration* condition of the two bodies in contact, i.e. *perturbed Lagrangian* (Simo et al. [1984], Ju et al. [1987]) and *augmented Lagrangian* (Landers&Taylor [1985]). Application of Lagrange multipliers method to the solution of evolution equations for two contacting bodies leads to a system of differential algebraic equations (DAE), which are very difficult to solve. Some considerations of the solutions of DAE that rely strongly on the methods of nonlinear programming are given by Lotstedt [1984].

The common drawback of all non-penetration models, based on Lagrange multiplier techniques, is that they do not properly account for the reduction of the frictional force in dynamic versus static contact, i.e. ad-hoc reduction of coefficient of friction is normally used instead. It is a fundamental contribution of Tolstoi [1967] to point out that no distinction should be made between the *static* and the *kinematic* coefficient of friction. The reduction of the frictional force in dynamic frictional sliding is rather the consequence of the reduction of the normal force due to the interface high frequency vibrations in the normal direction, than of the reduction of the coefficient of friction. Hence, the penetration condition and the associated normal interface dof have to be incorporated in the model for dynamic frictional contact. This, in return, leads to *penalty method*, where non-penetration condition is enforced approximately by supplementing, essentially, very stiff spring to ensure diminishing of the relative displacement of contacting nodes (see Carey&Oden [1983]). The main difficulty associated with the penalty method is the proper choice of the penalty parameter, to prevent ill-conditioning of tangent operators (some considerations are given by Nour&Wriggers [1986]). Another approach to prevent ill-conditioning of tangent operators is suggested earlier by Wilson [1975], who introduced relative dofs for the contact

elements. It is important to note that relative dofs should be defined in possibly rotated coordinate system that yields the uncoupled form of tangent operators for the contact element. One way to incorporate the contact element with relative dofs into the mesh of standard finite elements (with absolute dofs) leads again to Lagrange multipliers methods. Instead, we adopt the approach of the penalty method for relative dofs of the contact element, where the penalty parameter has associated physical meaning of normal interface compliance. It should be emphasized that relative dofs fit naturally within the proposed split of structure total motion field (see (5.3.2)), since structure reference motion causes no contact stress.

By the experiments performed on the contacting machined surfaces, Burdekin et al. [1978] demonstrated that a good model for the normal interface compliance has the form of power law. This form of the normal interface compliance is furnished as the limit for the summation of elastic compliances of the individual asperities. If linear height distribution of asperities is assumed, quadratic relationship between penetration and normal stress is obtained. Similarly, different distribution of asperity heights results in different powers in constitutive law for the normal interface. The same model given by power law is adopted by Oden&Martins [1985] for the finite element analysis of stick-slip motion of machined interfaces. In this study, the same concepts are applied to dynamic contact of the structure and the foundations. Although the mechanical characteristics of the material for the structure and the foundation are generally quite different from those of the metals, the model for the interface under adequate range of stress can be expected to perform in a very similar fashion in both cases, since the same mechanism of asperities compression is triggered.

Initial-Boundary Value Problem

Since we adopt linear viscoelastic constitutive equations for both the structure a $\;\cdot\;$ foundation, the field equations of standard boundary value problem, discussed in section 2.1 directly apply. Namely, (2.1.1), (2.1.2) and (2.1.3) stand for kinematics, equilibrium and constitutive equations. Initial conditions, specified by the equations (2.1.6) are also unaffected. The only change is in the boundary conditions. The complete boundary Γ is

partitioned as $\Gamma = \Gamma_\sigma \cup \Gamma_u \cup \Gamma_c$. Prescribed displacement boundary conditions on Γ_u and prescribed traction boundary conditions on Γ_σ are again given by the equations (2.1.5). However, the boundary conditions on the contact boundary (*all* $\mathbf{x} \in \Gamma_c$) are now introduced as

$$\sigma_n = -C_n <u_n>^{m_n}$$

$$|\sigma_t| = C_t <u_n>^{m_t} \qquad \dot{u}_t = -\lambda \sigma_t \qquad\qquad (6.1.1)$$

$$|\sigma_t| < C_t <u_n>^{m_t} \qquad \dot{u}_t = 0$$

where $< . >$ is standard Macauley bracket (i.e. $<x> = x$ if $x > 0$, and $<x> = 0$ if $x < 0$), and u_n is normal interface deformation (approach), while $\dot{u}_t$ is the rate of tangential interface deformation. Normal interface deformation (approach) u_n is determined as the difference between the relative normal displacement Δ and the initial normal gap g (see Figure 6.1.1).

The equations (6.1.1) stand for penetration power law for normal interface and generalized Coulomb law for tangential interface, i.e. if $m_n = m_t$ standard Coulomb friction law is recovered with the coefficient of friction given as C_t/C_n.

The contact boundary Γ_c can be further divided into a part Γ_c^1 where the body is in contact with rigid media, and a part Γ_c^2 where two bodies (parts of the body) come in contact, as presented on Figure 6.1.2. However, if u_n and u_t on Γ_c^2 are defined with the difference of the adequate displacement components (relative displacement) of the two bodies in contact, the same methodology applies for both types of the boundary Γ_c.

Steps taken to derive the variational problem that is formally equivalent to the given boundary value problem are the ones that follow *virtual power method* derivation :

Multiply the equilibrium equation (2.1.2) by an admissible velocity function $(v_i - \dot{u}_i)$ $(v_i, \dot{u}_i \in V)$ and integrate over the domain Ω. As noted by remark 2.1.1, kinematically admissible velocity function is formed as the difference of two velocity fields that satisfy all prescribed boundary conditions, i.e. both $\dot{u}_i$ and $v_i \in V$ in the previously defined notation

(see section 2.1). In variational interpretation, since the solution space for this problem (due to inequality in (6.1.1)) is the convex set rather than the differentiable manifold (see Stakgold [1979]), the total variation is constructed by utilizing the convexity property. Namely, if $\dot{u}_i$, $v_i \in V$, then also $[\dot{u}_i + \varepsilon(v_i - \dot{u}_i)] \in V$. Weak form, (6.1.2) below, corresponds to the first variation $\frac{d}{d\varepsilon} J\mid_{\varepsilon=0} = 0$ of adequate functional J.

$$\int_\Omega \left(\sigma_{ij,j} + f_i - \rho\, \ddot{u}_i \right) \left(v_i - \dot{u}_i \right) d\Omega = 0 \tag{6.1.2}$$

Use Gauss divergence theorem on the first term on the left hand side in above and the constitutive equations (2.1.3), and get

$$\int_\Omega \sigma_{ij,j} \left(v_i - \dot{u}_i \right) d\Omega = - \int_\Omega D_{0\, ijkl}\, \varepsilon_{ij}\, \dot{\varepsilon}_{kl}\, d\Omega +$$

$$\int_\Omega D_{1\, ijkl}\, \dot{\varepsilon}_{ij}\, \dot{\varepsilon}_{kl}\, d\Omega + \int_\Gamma \sigma_{ij}\, n_j \left(v_i - \dot{u}_i \right) d\Gamma \tag{6.1.3}$$

And further

$$\int_\Omega D_{0\, ijkl}\, \varepsilon_{ij}\, \dot{\varepsilon}_{kl}\, d\Omega + \int_\Omega D_{1\, ijkl}\, \dot{\varepsilon}_{ij}\, \dot{\varepsilon}_{kl}\, d\Omega + \int_\Omega \rho\, \ddot{u}_i \left(v_i - \dot{u}_i \right) d\Omega =$$

$$\int_\Omega f_i \left(v_i - \dot{u}_i \right) d\Omega + \int_\Gamma \sigma_{ij}\, n_j \left(v_i - \dot{u}_i \right) d\Gamma \tag{6.1.4}$$

Let us consider the last term in the equation above; Integration can be split over the different portions of the boundary Γ and the specified boundary conditions utilized.

$$\int_\Gamma \sigma_{ij}\, n_j \left(v_i - \dot{u}_i \right) d\Gamma = \int_{\Gamma_u} \sigma_{ij}\, n_j \left(v_i - \dot{u}_i \right) d\Gamma + \int_{\Gamma_\sigma} \sigma_{ij}\, n_j \left(v_i - \dot{u}_i \right) d\Gamma$$

$$+ \int_{\Gamma_c} \sigma_{ij}\, n_j \left(v_i - \dot{u}_i \right) d\Gamma \tag{6.1.5}$$

We take a closer look at the terms on the right hand side of the equation above. The first term drops out because of admissibility of functions v_i and $\dot{u}_i$ (they both satisfy essential boundary conditions on Γ_u). The second term can be obtained from specified traction on Γ_σ

(with $\sigma_{ij} \, n_j = \bar{t}_i$). The third term we further split into the parts for normal penetration interface (p) and tangential friction interface (j)

$$\int_{\Gamma_c} \sigma_{ij} \, n_j \left(v_i - \dot{u}_i \right) d\Gamma = p + j \tag{6.1.6}$$

where

$$p = \int_{\Gamma_c} C_n <u_n>^{m_n} n_i \left(v_i - \dot{u}_i \right) d\Gamma$$

$$j \le -\int_{\Gamma_c} C_t <u_n>^{m_t} t_i \mid v_i \mid d\Gamma + \int_{\Gamma_c} C_t <u_n>^{m_t} t_i \mid \dot{u}_i \mid d\Gamma \tag{6.1.7}$$

and n_i and t_i are the components of normal and tangent vectors on the boundary Γ_c.

If we take p and j parts of the variational formulation to the left hand side of (6.1.4), we get *variational inequality*

$$\int_{\Omega} D_{0 \, ijkl} \, \varepsilon_{ij} \, \dot{\varepsilon}_{kl} \, d\Omega + \int_{\Omega} D_{1 \, ijkl} \, \dot{\varepsilon}_{ij} \, \dot{\varepsilon}_{kl} \, d\Omega + \int_{\Omega} \rho \, \ddot{u}_i \left(v_i - \dot{u}_i \right) d\Omega -$$

$$\int_{\Gamma_c} C_n <u_n>^{m_n} n_i \left(v_i - \dot{u}_i \right) d\Gamma + \int_{\Gamma_c} C_t <u_n>^{m_t} t_i \mid v_i \mid d\Gamma -$$

$$\int_{\Gamma_c} C_t <u_n>^{m_t} t_i \mid \dot{u}_i \mid d\Gamma \ge \int_{\Omega} f_i \left(v_i - \dot{u}_i \right) d\Omega + \int_{\Gamma_\sigma} \bar{t}_i \left(v_i - \dot{u}_i \right) d\Gamma \tag{6.1.8}$$

In order to simplify notation we introduce

$$a_0 \left(u, v - \dot{u} \right) = \int_{\Omega} D_{0 \, ijkl} \, \varepsilon_{ij} \, \dot{\varepsilon}_{kl} \, d\Omega$$

$$a_1 \left(u, v - \dot{u} \right) = \int_{\Omega} D_{1 \, ijkl} \, \dot{\varepsilon}_{ij} \, \dot{\varepsilon}_{kl} \, d\Omega$$

$$b \left(\ddot{u}, v - \dot{u} \right) = \int_{\Omega} \rho \, \ddot{u}_i \left(v_i - \dot{u}_i \right) d\Omega \tag{6.1.9}$$

$$j \left(u, v \right) = \int_{\Gamma_c} C_t <u_n>^{m_t} t_i \mid v_i \mid d\Gamma$$

$$p\left(u , v - \dot{u} \right) = \int_{\Gamma_c} C_n <u_n>^{m_*} n_i \left(v_i - \dot{u}_i \right) d\Gamma$$

Hence, the variational inequality can be restated as

$$a_0 \left(u, v-\dot{u} \right) + a_1 \left(u, v-\dot{u} \right) + b \left(\ddot{u}, v - \dot{u} \right) + j\left(u , v \right) - j\left(u , \dot{u} \right) -$$

$$p\left(u , v-\dot{u} \right) \geq \int_{\Omega} f_i \left(v_i - \dot{u}_i \right) d\Omega + \int_{\Gamma_\sigma} \bar{t}_i \left(v_i - \dot{u}_i \right) d\Gamma \qquad (6.1.10)$$

6.2. Regularization Procedure

One approach to obtain the solution to variational problem (6.1.10) leads to *regularization* of friction functional *j*. The regularization procedure uses a perturbed friction functional formulation with respect to (virtual) velocity field. Namely, *nondifferentiable* friction functional is substituted by *differentiable convex* friction functional (Figure 6.2.1).

Utilizing the property of convex function $j_\varepsilon(v) - j_\varepsilon(\dot{u}) \geq \dfrac{\partial j_\varepsilon(\dot{u})}{\partial \dot{u}} \left(v - \dot{u} \right)$, the variational *inequality* is transformed to the variational *equality*.

$$a_0 \left(u, v - \dot{u} \right) + a_1 \left(u, v - \dot{u} \right) + b \left(\ddot{u}, v - \dot{u} \right) + \left[\dfrac{\partial j_\varepsilon \left(u , \dot{u} \right)}{\partial \dot{u}} . \left(v - \dot{u} \right) \right] -$$

$$p\left(u , v - \dot{u} \right) = \int_{\Omega} f_i \left(v_i - \dot{u}_i \right) d\Omega + \int_{\Gamma_\sigma} \bar{t}_i \left(v_i - \dot{u}_i \right) d\Gamma \qquad (6.2.1)$$

and, if needed, kinematically admissible velocity function can be denoted as $w_i = v_i - \dot{u}_i$ (with $w_i = 0$ on Γ_u), so that the familiar form of virtual power method is recovered.

The regularization procedure is first introduced by Lions&Magenes [1972] in the study of elliptic problems. In the present context, the regu'. .̇∴∵·on procedure is used by Duvaut&Lions [1976] to prove the existence and the uniqueness of the dynamic frictional contact for the linear viscoelastic bodies and the regularized friction condition, under the prescribed time history of normal stress at the contact boundary Γ_c. Standard Feado-Galerkin procedure was used. Their proof is extended by Martins&Oden [1987] to account

for normal interface compliance given in the form of power law (6.1.1[1]). Klarbring et al. [1988] extended that work to the general implicit form of penetration compliance and adequate incremental and rate problems utilizing subgradient notion introduced by Moreau [1974].

For a particular choice of regularization procedure given by Oden&Martins [1985] (Figure 6.2.1), the regularization of friction functional with respect to sliding velocity is

$$
z(x) = \begin{cases} \varepsilon\left(\dfrac{x}{\varepsilon}\right)^2 (1-\dfrac{1}{3}\dfrac{|x|}{\varepsilon}) & \text{if } |x| \leq \varepsilon \\ \varepsilon(\dfrac{|x|}{\varepsilon}-\dfrac{1}{3}) & \text{if } |x| \geq \varepsilon \end{cases}
\tag{6.2.2}
$$

where ε is the regularization parameter.

By pairing of energy conjugate quantities (Lubliner [1989]), the derivative of the regularized friction functional gives the expression for tangential stress (Figure 6.2.2).

$$
y(x) = \begin{cases} (2-\dfrac{|x|}{\varepsilon})\dfrac{x}{\varepsilon} & \text{if } |x| \leq \varepsilon \\ sgn(x) & \text{if } |x| \geq \varepsilon \end{cases}
$$

or, in notation we introduced, friction stress in Oden&Martins [1985] model is

$$
\sigma_t = -C_t <u_n>^{m_t} \begin{cases} (2-\dfrac{|\dot{u}|}{\varepsilon})\dfrac{\dot{u}}{\varepsilon} & \text{if } |\dot{u}| \leq \varepsilon \\ sgn(\dot{u}) & \text{if } |\dot{u}| \geq \varepsilon \end{cases}
\tag{6.2.3}
$$

The regularization procedure, as introduced by Duvaut&Lions [1976], relies on the infinitesimal value of regularization parameter ε that the perturbed problem would approach the original problem. In practical computations, however, the value of regularization parameter ε has to be finite. Hence, the value of the just described regularization procedure as a computational tool is questionable. Two drawbacks can be pointed out :

(1) It corresponds to stating constitutive equations for the interface in the form of *non-linear elasticity (viscoelasticity)*, since the unique relationship between the *total* stress

and the *total* sliding velocity is given; dissipation and path-dependence properties of friction are not correctly represented.

(2)   Tangential friction stress depends on sliding velocity ("strain rates") only; hence, no transition to accommodate quasi-static problems is possible.

In our work we take more physical approach which relies on the equivalence of the interface constitutive equations (6.1.1) to *non-associated rigid* plasticity. In our interpretation, the regularization procedure then accounts for the elastic part of deformation, i.e. performs the transition from rigid plastic to elasto-plastic material. In other words, the regularization of the solution field is performed as opposed to the regularization of the variation field in previously described procedure.

If we follow the general *internal variable* theory (see Lubliner [1989]), we can recognize $(6.1.1^2)$ as the evolution equation for the internal variable u_t (with the physical meaning of being relative slip of two contacting bodies along the common tangential plane). Yield condition can be recovered by combination of $(6.1.1^1)$ and $(6.1.1^2)$ for the common case of $m_n = m_t$ as

$$f(\sigma_n, \sigma_t) = \mid \sigma_t \mid - \frac{C_t}{C_n} \mid \sigma_n \mid = 0 \qquad (6.2.4)$$

However, from the evolution equation of the internal variable u_t, it follows that flow potential is given as

$$g(\sigma_n, \sigma_t) = -\frac{1}{2} \, sgn(\sigma_t) \, \sigma_t^2 \qquad (6.2.5)$$

Since the yield criterion (6.2.4) and the flow potential (6.2.5) are of different form, the constitutive equations for the interface have the form of non-associated plasticity.

It is generally accepted (see Lubliner [   ]   that, for the small displacement gradient theory, an *additive split* of elastic and inelastic strain components holds. In our case, we defined u_t as an equivalent to the *inelastic* strain component $(u_t \rightarrow u_t^i)$. In addition, additive to it, we can define the *elastic* strain component of u_t^e, so that the *total tangential*

deformation is given as

$$\dot{u}_t = \dot{u}_t^e + \dot{u}_t^i \tag{6.2.6}$$

The existence of the elastic component is demonstrated by the experiments on machined surfaces (see Burdekin et al. [1978]). However, since in large interface sliding, the elastic component is very small compared to the inelastic one, the idealized Coulomb law is generally given in the form of (6.1.1). Here, as a regularization procedure of the idealized Coulomb law, the elastic part of the tangential interface compliance is furnished. To be consistent with the experimental results of Burdekin et al. [1978], a particular choice for the regularization procedure, i.e. a particular form of the constitutive law for the elastic part of deformation is given as

$$\sigma_t = - C_t <u_n>^{m_t} (2 - \frac{|u_t^e|}{\varepsilon}) \frac{u_t^e}{\varepsilon} \tag{6.2.7}$$

For clarity, we further summarize *regularized* constitutive equations for the contact interface

-constitutive equations for the elastic part

$$\sigma_n = - C_n <u_n>^{m_n} \tag{6.2.8}$$

$$\sigma_t = - C_t <u_n>^{m_t} (2 - \frac{|u_t^e|}{\varepsilon}) \frac{u_t^e}{\varepsilon}$$

-additive split of the elastic and the inelastic deformation components

$$u_t = u_t^e + u_t^i \tag{6.2.9}$$

$$u_n = u_n^e$$

-evolution equation for the inelastic deformation component

$$\dot{u}_t^i = \begin{cases} 0 & \text{if } f < 0 \\ -\lambda \, \sigma_t & \text{if } f = 0 \end{cases} \tag{6.2.10}$$

where f is "yield condition" given by (6.2.4).

The equations (6.2.9) and (6.2.10) in combination with yield condition (6.2.4) can be recognized as the constitutive equations of contact interface in the standard form of non-associated plasticity, as suggested by Michailowski&Mroz [1978]. However, the important difference is the *nonlinear compliance* for the elastic deformation part given by (6.2.8) for both the *normal* and the tangential interface dofs.

Once we defined the relationship of stress and deformation (6.2.8), we can formulate our problem completely in the strain space as suggested by Naghdi&Trapp [1975]. In particular, for $m_n = m_t$, yield criterion has a simple form

$$| u_t^e | = \varepsilon \tag{6.2.11}$$

The strain space formulation in our case, which is analogous to perfect plasticity (no hardening), has the computational advantages of providing the stability of the solution under displacement control. Displacement driven return mapping algorithm for integrating the constitutive equations is naturally fitted within the proposed model. This is elaborated in section 6.4.

6.3. Normal Interface Dissipation Law

The power law introduced as the constitutive model for normal penetration interface has one deficiency, which we propose to correct in this section. Namely, the material model does not account for energy dissipation that occurs in contact of two bodies due to permanent deformation of asperities. However, since this mechanism is too complex to be modeled accurately, the simpler approach is taken. In rigid body dynamics, energy dissipation in contact of two bodies is introduced by the *coefficient of restitution* (see Meriam [1966]), given by the ratio of the velocities of two bodies after and before the instant they come in contact. If the time of the contact of two bodies is much larger than the fundamental period of either of them, the contact problem solution of Hertz (see Love [1950]) is furnished, that considers only ideally elastic bodies. It is shown in many experiments (see Goldsmith [1960]) that the assumption of ideally elastic bodies in Hertz solution does

not apply, especially for the materials such as soil or concrete which one might consider when focusing on dynamic analysis of the structure-foundation systems. Hence, energy dissipation mechanism should be supplemented. For this we generalize the dissipative model of Hunt&Crossley [1975], which relies on measured data for the restitution coefficient of different materials. The experimental results for the coefficient of restitution, as given by Goldsmith [1960], show the linear dependence on relative velocities of two bodies in contact.

For the normal interface constitutive power law the proposed dissipation mechanism will have the form of nonlinear viscous damping. For contact constitutive equations (6.1.1) the dissipative term has the form

$$\sigma_n = B_n <u_n>^{l_n} \dot{u}_n \qquad (6.3.1)$$

where B_n and l_n are the constitutive coefficients, and u_n and $\dot{u}_n$ are the normal components of (relative) displacement and velocity at the point of contact. If l_n is chosen of the same value as m_n in (6.1.1[1]), then the simple relation for B_n is given as

$$B_n = \frac{3}{2} C_n \eta \qquad (6.3.2)$$

where η is the slope of the line that represents the relation between the coefficient of restitution and velocity.

The normal interface dissipative model (6.3.1), in return, introduces additional term in the variational inequality (6.1.10), and the same term in its regularized version, variational equality (6.2.1), since the regularization is not concerned with the normal interface dofs.

$$d\left(u_n, \dot{u}_n, w\right) = \int_{\Gamma_c} B_n <u_n>^{l_n} \dot{u}_n w_n d\Gamma \qquad (6.3.3)$$

The hysteresis loops produced by this dissipation law in free vibrations are presented on Figure 6.3.1, for different values of the initial relative velocity.

Remark 6.3.1 Motivated by Hertz solution of the contact problem, Hughes et al. [1976] have supplied impact condition within the discretized *non-penetration* model,

consistent with one-dimensional wave propagation. For that purpose, special impact and release conditions are incorporated within the framework of step-by-step Newmark algorithm. Further expansion of that model to explicit step-by-step algorithm and large displacements is performed by Hallquist et al. [1985]. Since the *penetration* contact model is proposed in this work, equivalent considerations are not necessary.

6.4. Discretization

For certain mesh (h) the approximate displacements, velocities and accelerations at each time t are the elements of the finite-dimensional approximation subspace $V_h \subset V$, constructed by the finite element method.

$$u_i^h(\mathbf{x},t),\ \dot{u}_i^h(\mathbf{x},t),\ \ddot{u}_i^h(\mathbf{x},t) \in V_h \tag{6.4.1}$$

The finite element version of the variational equality (6.2.1) then becomes : *Find the function* $t \rightarrow \mathbf{u}_\varepsilon^h(t)$ *of* [0,T] $\rightarrow V_h$ *such that*

$$a_0\left(\mathbf{u}_\varepsilon^h, \mathbf{w}^h\right) + a_1\left(\dot{\mathbf{u}}_\varepsilon^h, \mathbf{w}^h\right) + b\left(\ddot{\mathbf{u}}_\varepsilon^h, \mathbf{w}^h\right) + j_\varepsilon^h\left(\mathbf{u}_\varepsilon^h, \mathbf{w}^h\right) - p\left(\mathbf{u}_\varepsilon^h, \mathbf{w}^h\right)$$

$$= \int_\Omega \mathbf{f}\ \mathbf{w}^h\ d\Omega + \int_{\Gamma_\sigma} \bar{\mathbf{t}}\ \mathbf{w}^h\ d\Gamma \tag{6.4.2}$$

To simplify notation, we further drop the subscript ε (reminder of regularization process) and the superscript h (reminder of semidiscretization process).

Within each element Ω_e^h ($e = 1,2,...,N_{elem}$) the components of displacements, velocities and accelerations are expressed as

$$u_i^h(\mathbf{x},t) \qquad \sum \quad u_{iI}(t)\ N_I(\mathbf{x})$$

$$\dot{u}_i^h(\mathbf{x},t) = \sum_{I=1}^{N_{en}} \dot{u}_{iI}(t)\ N_I(\mathbf{x}) \tag{6.4.3}$$

$$\ddot{u}_i^h(\mathbf{x},t) = \sum_{I=1}^{N_{en}} \ddot{u}_{iI}(t) \, N_I(\mathbf{x})$$

where $i = 1,2,...N_{dof}$, and N_{en} is a number of element nodes.

If we introduce the approximation (6.4.3) in variational equality (6.4.2) and group equations for each component of variational velocity vector w_i, the problem is transformed to the standard finite element semidiscretized equations

$$\mathbf{M} \, \ddot{\mathbf{u}}(t) + \mathbf{C} \, \dot{\mathbf{u}}(t) + \mathbf{K} \, \mathbf{u}(t) + \mathbf{j}(\mathbf{u}(t)) - \mathbf{p}(\mathbf{u}(t)) = \mathbf{f}(t) \qquad (6.4.4)$$

with initial conditions given

$$\mathbf{u}(0) = \mathbf{u}_0 , \qquad \dot{\mathbf{u}}(0) = \dot{\mathbf{u}}_0$$

where we utilized again the matrix notation introduced in section 2.1, i.e. $\mathbf{u}(t)$, $\dot{\mathbf{u}}(t)$, $\ddot{\mathbf{u}}(t)$ are column vectors of nodal displacements, velocities and accelerations respectively; $\mathbf{M}$ is standard mass matrix given by (2.2.11); $\mathbf{C}$ is standard damping matrix given by (2.2.12); $\mathbf{K}$ is standard stiffness matrix given by (2.2.13); $\mathbf{f}(t)$ is consistent load vector given by (2.2.14); and $\mathbf{p}\left(\mathbf{u}(t)\right)$ is vector of consistent nodal normal residual on Γ_c, while $\mathbf{j}\left(\mathbf{u}(t)\right)$ is vector of consistent nodal tangential friction residual on Γ_c. The element contributions to nodal residual vectors for normal and tangential interface on Γ_c are given further in section 6.5 for 6-noded contact element.

Newmark Algorithm for Structural Dynamics

To fully discretize the finite element form of the variational equality on hand we choose Newmark family of algorithms. Let us partition the interval $[0,T]$ into M intervals of length Δt such that $0=t_0,t_1,....,t_k,....,t_M=T$. We make approximation to the velocities and accelerations at time t_k (same as in (2.2.17)) by expressing them as functions of the displacements, velocities and accelerations at time t_{k-1} and of the displacements at time t_k by the following relation

$$\dot{u}_k = \frac{\gamma}{\beta \Delta t} \left(u_k - u_{k-1} \right) + \left(1 - \frac{\gamma}{\beta} \right) \dot{u}_{k-1} + \Delta t \left(1 - \frac{\gamma}{2\beta} \right) \ddot{u}_{k-1} \qquad (6.4.5)$$

$$\ddot{u}_k = \frac{1}{\beta \Delta t^2} \left(u_k - u_{k-1} \right) - \frac{1}{\beta \Delta t} \dot{u}_{k-1} - \left(\frac{1}{2\beta} - 1 \right) \ddot{u}_{k-1}$$

where β and γ are so-called Newmark parameters and $u_k = u_c^h(t_k)$, etc. is used in foregoing if no confusion is likely to arise.

Introducing the above relation in variational equality we obtain variation equality at time t_k

$$\frac{1}{\beta \Delta t^2} M u_k + \frac{\gamma}{\beta \Delta t} C u_k + K u_k - p(u_k) + j(u_k) = \hat{f}_k \qquad (6.4.6)$$

where

$$\hat{f}_k = f_k + M \left(\frac{1}{\beta \Delta t^2} u_{k-1} + \frac{1}{\beta \Delta t} \dot{u}_{k-1} + \left(\frac{1}{2\beta} - 1 \right) \ddot{u}_{k-1} \right) +$$

$$C \left(\frac{\gamma}{\beta \Delta t} u_{k-1} + \left(\frac{\gamma}{\beta} - 1 \right) \dot{u}_{k-1} + \Delta t \left(\frac{\gamma}{2\beta} - 1 \right) \ddot{u}_{k-1} \right)$$

The discretized variational equality (6.4.6) above can be further put into the operator form

$$r_k(u_k) = \frac{1}{\beta \Delta t^2} M u_k + \frac{\gamma}{\beta \Delta t} C u_k + K u_k - p(u_k) + j(u_k) - \hat{f}_k = 0 \qquad (6.4.7)$$

Let $\hat{K}(u_k) = Dr_k(u_k) \in L(V_h, V_h')$ be derivative of the map r_k at $u_k \in V_h$. Then the Newton iteration method is

$$u_k^{(i+1)} = u_k^{(i)} - \left[\hat{K}(u_k^{(i)}) \right]^{-1} r_k(u_k^{(i)}) \qquad (6.4.8)$$

where : $i = 1, 2, \ldots, N_{iter}$ is the iteration counter. Thus, at each iteration i, the following system of linear equations has to be solved.

$$\left(\hat{K}(u_k^{(i)}) \right) \left(u_k^{(i+1)} - u_k^{(i)} \right) = -r_k(u_k^{(i)}) \qquad (6.4.9)$$

or, in a simplified notation (6.4.9) can be rewritten as

$$\hat{\mathbf{K}}_k^{(i)} \ \Delta \mathbf{u}_k^{(i)} = -\mathbf{r}_k^{(i)} \tag{6.4.10}$$

In order to ensure *quadratic convergence* properties of Newton method *consistent tangent* matrix has to be supplied at each iteration given as follows:

$$\hat{\mathbf{K}}_k^{(i)} = \frac{1}{\beta \ \Delta t^2} \ \mathbf{M} + \frac{\gamma}{\beta \ \Delta t} \ \mathbf{C} + \mathbf{K} + \frac{\partial \mathbf{p}(\mathbf{u}_k)}{\partial \mathbf{u}} |_k^{(i)} + \frac{\partial \mathbf{j}(\mathbf{u}_k)}{\partial \mathbf{u}} |_k^{(i)} \tag{6.4.11}$$

Return Mapping Algorithm

The linearization of contact residual requires that the solution algorithm for integrating constitutive equations provides a closed form expression for tangent moduli. Namely, it holds

$$\mathbf{K}_k^{c \, (i)} = \frac{\partial \mathbf{r}(\mathbf{u}_k)}{\partial \mathbf{u}} |_k^{(i)} = \int_{\Gamma_c} \mathbf{B}^T \ \frac{\partial \boldsymbol{\sigma}}{\partial \boldsymbol{\varepsilon}} |_k^{(i)} \ \mathbf{B} \ d\Gamma = \int_{\Gamma_c} \mathbf{B}^T \ \mathbf{C}_T |_k^{(i)} \ \mathbf{B} \ d\Gamma \tag{6.4.12}$$

where $\mathbf{r}$ is either normal interface residual $\mathbf{p}$ or tangential interface residual $\mathbf{j}$, $\mathbf{B}$ is appropriate strain-displacement matrix, and $\mathbf{C}_T$ is the tangent moduli.

Next, we present the derivation of tangent moduli for both normal penetration and tangential friction interface within the framework of return mapping algorithm, as well as the complete procedure for integrating constitutive equations of regularized Coulomb friction. The return mapping algorithm is operator split method (see Chorin et al. [1978], hence, it is first order accurate (since the splitted operator parts do not share the same set of eigenvectors). For the presentation of the logic of the return mapping algorithm, we refer to Figure 6.4.1. The return mapping algorithm is displacement driven: given the displacement (strain) increment (the best guess), one first computes the *elastic trial* state of stress (see Figure 6.4.1). The initial guess for displacement increment, within the framework of dynamic analysis, is given by the chosen predictor for the step-by-step integrating scheme (see Taylor [1988]). The first part of the operator split methodology is then performed, assuming that for the given displacement increment the trial state of stress is elastic. In our case, where the elastic compliance has nonlinear form, the tangent moduli are computed by

linearizing the equations (6.2.8) to obtain

$$
\begin{pmatrix} \Delta\sigma_n \\ \Delta\sigma_t \end{pmatrix} = \begin{bmatrix} C_n m_n <u_n>^{m_n-1} & 0 \\ C_t m_t <u_n>^{m_t-1}(2-\dfrac{|u_t^e|}{\varepsilon})\dfrac{u_t^e}{\varepsilon} & C_t <u_n>^{m_t}(1-\dfrac{|u_t^e|}{\varepsilon})\dfrac{2}{\varepsilon} \end{bmatrix} |_k^{(i)} \begin{pmatrix} \Delta u_n \\ \Delta u_t \end{pmatrix} \quad (6.4.13)
$$

If the trial state of stress satisfies the yield condition (6.2.4) then the trial is successful and the step is completed, with the tangent moduli for the next iteration given by (6.4.13) above. Note that, by this approach, unloading is automatically accommodated.

However, if the trial state of stress violates the yield condition (6.2.4), the return mapping algorithm is introduced to enforce consistency condition and bring the stress state down to the yield surface. In our case, consistency condition is easily enforced by keeping the same value of normal stress as in the trial state, while the tangential stress is obtained by vertically projecting the trial stress onto the yield surface (Figure 6.4.1). The tangent moduli for the next iterate is then obtained as

$$
\begin{pmatrix} \Delta\sigma_n \\ \Delta\sigma_t \end{pmatrix} = \begin{bmatrix} C_n m_n <u_n>^{m_n-1} & 0 \\ C_t m_t <u_n>^{m_t-1} sgn(u_t^e) & 0 \end{bmatrix} |_k^{(i)} \begin{pmatrix} \Delta u_n \\ \Delta u_t \end{pmatrix} \quad (6.4.14)
$$

A step-by-step procedure of return mapping algorithm is presented in Table 6.4.1 below.

Table 6.4.1 - Return Mapping Algorithm for Friction

----

1) Known state at t_{k-1}; elastic normal $u_n^e|_{k-1} = u_n|_{k-1}$ and tangential deformation $u_t^e|_{k-1}$ and inelastic tangential deformation $u_t^i|_{k-1}$

2) Given displacement increment $\Delta u^{(i)}$; where the first iterative value of $\Delta u^{(0)}$ is set by chosen predictor

3) Compute the total elastic and inelastic deformation, assuming the *elastic trial* step

$$u_n|_T = u_n|_{k-1} + \Delta u_n^{(i)}, \qquad \Delta u_n^{(i)} = \Delta \mathbf{u}^{(i)} \cdot \mathbf{n}$$

$$u_t^e|_T = u_t^e|_{k-1} + \Delta u_t^{(i)}, \qquad \Delta u_t^{(i)} = \Delta \mathbf{u}^{(i)} \cdot \mathbf{t}$$

$$u_t^i|_T = u_t^i|_{k-1}$$

and compute the trial values for stress

$$\sigma_n|_T = - C_n <u_n|_T>^{m_n}$$

$$\sigma_t|_T = - C_t <u_n|_T>^{m_t} \left(2 - \frac{|u_t^e|_T|}{\varepsilon} \right) \frac{u_t^e|_T}{\varepsilon}$$

4) If $|\sigma_t|_T| < C_t/C_n <u_n|_T>^{m_t-m_n} |\sigma_n|_T|$ then

    accept trial for final values

$$u_n|_k = u_n|_T$$

$$u_t^e|_k = u_t^e|_T$$

$$u_t^i|_k = u_t^i|_T$$

    and supply elastic tangent matrix for the next iterative step from (6.4.13)

else

    perform return mapping algorithm to enforce consistency condition

$$u_n|_k = u_n|_T$$

$$u_t^e|_k = \varepsilon \, sgn(\Delta u_t^{(i)})$$

$$u_t^i|_k = \Delta u_t^{(i)} - (u_t^e|_k - u_t^e|_{k-1}) + u_t^i|_{k-1}$$

    compute stress values for residual computation

$$\sigma_n|_k = \sigma_n|_T$$

$$\sigma_t|_k = -C_t/C_n \; \sigma_n|_k \; sgn(u_t^e|_k)$$

and supply inelastic tangent matrix for the next iterative step from (6.4.14)

endif

5) Check convergence; if necessary go to step 2) and repeat.

Remark 6.4.1 Within the context of quasi-static fully nonlinear contact problem, the return mapping algorithm was proposed by Ju et al. [1987]. The solution procedure was based on perturbed Lagrangian formulation.

6.5. Dynamic Frictional Contact - 2D Isoparametric 6-noded Element

The geometry and the kinematics of 6-noded contact element are described by the same *quadratic polynomial* (isoparametric element). Higher order interpolation for the contact element is selected to better approximate different boundary shapes. For the setting presented on Figure 6.5.1, the geometry of the contact element is given as

$$\mathbf{x} = \sum_{I=1}^{3} N_I \, \mathbf{x}_I \qquad\qquad (6.5.1)$$

where N_I are standard shape functions in the form of Lagrange polynomials

$$N_I = \begin{cases} 0.5\,(1-\xi) - 0.5\,(1-\xi^2) & \text{for } I=1,4 \\ (1-\xi^2) & \text{for } I=2,5 \\ 0.5\,(1+\xi) - 0.5\,(1-\xi^2) & \text{for } I=3,6 \end{cases} \qquad (6.5.2)$$

The set of three nodes $\{\mathbf{x}_I, \, I=1,2,3\}$ that supports geometry interpolation (6.5.1), can be chosen to belong to one or the other body in contact, or to be a linear combination of corresponding nodes dependent upon the relative stiffness of the bodies in contact. For small displacement gradient theory, the choice of the nodes is immaterial.

The components of the normal vector n and tangential vector t are then computed

$$dx_1 = \sum_{I=1}^{3} N_{I,\xi} \, x_{1I} \, d\xi \qquad dx_2 = \sum_{I=1}^{3} N_{I,\xi} \, x_{2I} \, d\xi \qquad dx = \sqrt{dx_1^2 + dx_2^2}$$

$$\mathbf{n} = \begin{pmatrix} n_1 \\ n_2 \end{pmatrix} \qquad n_1 = -\frac{dx_2}{dx} \qquad n_2 = \frac{dx_1}{dx} \qquad (6.5.3)$$

$$\mathbf{t} = \begin{pmatrix} t_1 \\ t_2 \end{pmatrix} \qquad t_1 = \frac{dx_2}{dx} \qquad t_2 = \frac{dx_2}{dx}$$

If we further introduce the nodal vectors $\mathbf{N}_I$ and $\mathbf{T}_I$

$$\mathbf{N}_I = \begin{pmatrix} n_1 \, N_I \\ n_2 \, N_I \end{pmatrix} , \qquad \mathbf{T}_I = \begin{pmatrix} t_1 \, N_I \\ t_2 \, N_I \end{pmatrix} \qquad (6.5.4)$$

the element contribution to the nodal residual for normal and tangential interface on Γ_c are

$$\mathbf{p}_I^{(e)} = \int_{\Gamma_c} \mathbf{N}_I \, \sigma_n \, d\Gamma \qquad (6.5.5)$$

$$\mathbf{j}_I^{(e)} = \int_{\Gamma_c} \mathbf{T}_I \, \sigma_t \, d\Gamma \qquad (6.5.6)$$

Utilizing consistent linearization procedure (see Hughes&Pister [1978]) for both penetration (6.5.5) and friction residual (6.5.6), the consistent stiffness matrices can be written

$\mathbf{K}_k^{n \, (i)}$ is tangent stiffness matrix resulting from the linearization of penetration contact residual

$$\mathbf{K}_{IJ}^{n(i)} = \int_{\Gamma_c} C_n \, m_n \, <u_n^{(i)}>^{m_n-1} \, \mathbf{N}_I \, \mathbf{N}_J^T \, d\Gamma \qquad (6.5.7)$$

$\mathbf{K}_k^{t \, (i)}$ is tangent stiffness matrix resulting from the linearization of friction residual, for elastic

$$\mathbf{K}_{IJ}^{t(i)} = \int_{\Gamma_c} C_t \, m_t \, <u_n^{(i)}>^{m_t-1} \, (2 - \frac{| u_t^{e \, (i)} |}{\varepsilon}) \, \frac{u_t^{e \, (i)}}{\varepsilon} \, \mathbf{T}_I \, \mathbf{N}_J^T \, d\Gamma +$$

$$\int_{\Gamma_c} C_t <u_n^{(i)}>^{m_t} \left(1 - \frac{|\dot{u}_t^{e\,(i)}|}{\varepsilon} \right) \frac{2}{\varepsilon} \, T_I \, T_J^T \, d\Gamma \tag{6.5.8}$$

and inelastic phase

$$K_{IJ}^{t\,(i)} = \int_{\Gamma_c} C_t \, m_t <u_n^{(i)}>^{m_t-1} \, sgn(u_t^{e\,(i)}) \, T_I \, N_J^T \, d\Gamma \tag{6.5.9}$$

Due to the nature of the Coulomb friction law employed in the constitutive equations for frictional contacte, the tangent stiffness matrix for tangential interface is *non-symmetric*. For the class of problems with the linearized kinematics we are confined to, all the contact tangent operators have *rank-one* matrix form, inherent in plasticity problems. This is quite natural consequence of the equivalence between the regularized constitutive friction law employed and the non-associated perfect plasticity.

For the normal interface dissipation model, discussed in section 6.3, the tangent operators have the additional terms given as

$K_k^{n\,(i)}$ is the tangent stiffness matrix resulting from the linearization of the normal interface dissipation residual with respect to displacements

$$K_{IJ}^{n\,(i)} = \int_{\Gamma_c} B_n \, l_n <u_n^{(i)}>^{l_n-1} \, \dot{u}_n^{(i)} \, N_I \, N_J^T \, d\Gamma \tag{6.5.10}$$

$C_k^{n\,(i)}$ is the tangent damping matrix resulting from the linearization of the normal interface dissipation residual with respect to velocities

$$C_{IJ}^{n\,(i)} = \frac{\gamma}{\beta \Delta t} \int_{\Gamma_c} B_n <u_n^{(i)}>^{l_n} \, N_I \, N_J^T \, d\Gamma \tag{6.5.11}$$

Numerical Examples

Example 6.5.1 - Forced membrane vibrations of elastic slab

Forced vibrations under harmonic excitation ($\bar{\omega}$ = 30000 rad/sec) of axially loaded homogeneous elastic slab are studied in the first example. Young's modulus of the slab is 1.4×10^6 kN/cm^2, Poisson ratio 0.3, mass density 7×10^{-6}, and the dimensions of prismatic slab are $16 \times 4 \times 1$ cm. Taking advantage of symmetry, only half of the slab is modeled by the finite elements. The finite element model of the slab and the imposed boundary conditions are presented on Figure 6.5.2. Frictional contact boundary, with $C_n = 10^8$, $C_t = 3 \times 10^7$ and $m_n = m_t = 2$, is imposed by precompressing the slab along the length with initial approach $u_n = 0.0005$ cm. This example is adopted from Oden&Martins [1985] to compare the performance of here proposed model versus there proposed regularization procedure. To match approximately the elastic compliance to Oden&Martins [1985] case, the regularization parameter is given value $\varepsilon = 10^{-5}$.

Tangential displacements at the contact boundary are presented on Figure 6.5.3 for the midpoint and the free end point, for the cases where the normal interface force is kept constant and where the normal dof is considered. The adequate Oden&Martins [1985] model performance is presented as well. It is evident (fig. 6.5.3) that Oden&Martins [1985] model does not correctly represent the dissipative properties of friction, while here presented model is characterized by asymptotically quadratic amplitude decay during the sliding phase, which is the property of Coulomb damping mechanism for this model problem.

The time history of the normal interface stress at the free end point (Figure 6.5.4) corroborates experimental findings of Tolstoi [1967]. The tangential interface stress (Figure 6.5.4) also exhibits fast oscillation trend observed in experiments. The fast interface vibrations can be eliminated by introducing the normal interface damping. Consequently, the tangential stress smoothing is achieved the same way. Distribution of the normal interface stress along the slab is given on Figure 6.5.5 at different instants, together with adequate distribution of the tangential frictional stress.

Hysteresis loops of the tangential frictional stress for here proposed regularized frictional contact model are plotted on Figure 6.5.6 for both the constant and the variable

normal contact force. The same loops are produced for Oden&Martins model and presented on Figure 6.5.7. Since the analysis is performed for harmonic excitation with the frequency very close to resonance with the first mode of the slab, displacement and velocity at any point are 90 degrees out of phase. Consequently, the results obtained by Oden&Martins model are of acceptable accuracy. If the excitation has the general form, so that all the frequencies are excited, the disagreement would be much more pronounced.

Example 6.5.2 - Uplifting of the dam

The analysis of the dam-foundation model presented on Figure 3.2.1 is extended for the case when the uplifting of the dam occurs. Only the uplifting effect is considered; the tangential sliding is assumed to be restricted either by embedment or otherwise. Material properties for the dam and the foundations are again those described in section 3.2. Material properties for the contact boundary are specified as $C_n = 10^6 MN/m^2$ and $m_n = 2$. To model maximum credible earthquake, Taft earthquake record, already used in section 3.2, is arbitrarily scaled by 3. In addition, since we are considering nonlinear problem, all the load cases are considered simultaneously, starting from the deformed configuration under the influence of dead load. In this study only *hydrostatic* water pressure is considered, while hydrodynamic effects are completely disregarded. Both the dam and the foundations are represented by a set of 10 Ritz vectors, which by the previous analysis (see section 4.2), proved to carry most of the information. The non-proportional damping, which arises from the paraxial approximation to radiation condition, is accounted for by the iterative procedure discussed in previous chapters. The equilibrium position of the dam-foundation system under the static load only is determined from the analysis of the complete system represented in FE coordinates (1154 dofs). It is interesting to point out that the computational effort for this analysis is almost the same as for the dynamic nonlinear analysis on consistently reduced model (approximately 8000 CPU sec. on VAX II/GPX workstation).

The displacements at the dam top and the bottom are plotted in Figure 6.5.8 for both cases where the uplifting of the dam is permitted and prevented. Over the certain range of frequencies response amplification occurs due to the uplifting, but in the part of strong

shaking beneficial isolation effects of the uplifting are evident. To asses the stress field in the dam, the difference of the horizontal displacement at the dam top vs. the bottom as well as the vertical stress time history at the dam bottom are plotted on Figure 6.5.9. If we assume that the dam is made of low quality concrete, say MB20 (which is consistent with the choice for Young'c modulus for the dam material), then the allowable compressive stress is 8 MPa (8000 kN/m^2) and the allowable tensile stress is 0.8 MPa (800 kN/m^2). Hence, if the uplifting of the dam is allowed for, no cracking of the dam body would occur. That is not the case if the uplifting is prevented (see Figure 6.5.9)

6.6. Dynamic Frictional Contact - 2D Segment Element

As discussed in closure of Chapter 5, here presented model for the frictional contact can be expanded to accommodate large sliding of the structure across the foundation. However, to be able to retain the reduced representation of the structure by generalized Ritz coordinates, we limit our consideration to the shape of the interface that yields only small rotations of the sliding structure (e.g. flat interface). Motion of the structure is then again small displacement gradient motion, if moving reference frame is used for its description.

The constitutive model for the normal penetration interface and the local Coulomb friction law for the tangential interface are retained in this consideration. Moreover, for large sliding, Coulomb friction is more realistic constitutive model.

However, for large sliding, node-to-node contact element (such as the one presented in section 6.5) can not be used to properly describe kinematics. Instead, the contact segment element is defined by generalizing the approach suggested by Simo et al. [1984] to higher order elements. For the implementation of this segment element into the finite element computer program, *slideline logic*, such as the one given by Hallquist et al. [1985], should be developed. Namely, the program should be able to identify the current position of the contact boundary Γ_c, and reformulate the profiles of the tangent matrices accordingly.

Hence, beside the slideline logic computational algorithm, the only thing needed for implementation of segment element is reformulating kinematics. For that we refer to Figure 6.6.1, where a part of the contact boundary Γ_c is depicted, together with a typical segment

element. The segment element is defined by 2 edges of 2D, say 9-noded, elements with quadratic variation of displacement field which is specified by nodes x_I^1 and x_I^2, and their adequate orthogonal projections $\bar{x}_I^1$ and $\bar{x}_I^2$, as shown on Figure 6.6.1. To clarify our notation, we state that superscript relates to the body in contact (e.g. 1 for foundations, and 2 for the structure), and subscript relates to the node number.

The new nodal points $\bar{x}_I^1$ and $\bar{x}_I^2$ are given as the intersection of the orthogonal projection of the nodes x_I^2 and x_I^1 (respectively) onto the straight line joining the corresponding nodes on the bodies 1 and 2 with the corresponding edges of the bodies 1 and 2 (see Figure 6.6.1). The choice of particular projection is motivated exclusively by resulting simplifications of computational algorithm. Essentially, any choice for $\bar{x}_I^1$ and $\bar{x}_I^2$ that results in unique partition of the contact boundary Γ_c into the contact segments, is eligible.

The position of new nodal points $\bar{x}_I^1$ and $\bar{x}_I^2$ can be found by the algorithm given below

(i) $\bar{x}_I^1 \in \Gamma_c^1$

$$\bar{x}^1 = \sum_{I=1}^{3} N_I(\bar{\xi}) \, x_I^1, \qquad \bar{y}^1 = \sum_{I=1}^{3} N_I(\bar{\xi}) \, y_I^1 \tag{6.6.1}$$

(ii) $\bar{x}_I^1$ on the line through x_J^2

$$\bar{y}_I^1 - y_J^2 = \alpha \, (\bar{x}_I^1 - x_J^2) \tag{6.6.2}$$

where N_I are Lagrange polynomials given by (6.5.2) and α is determined by the pair of nodes which enclose the projected node $\bar{x}_I$ (e.g. $\alpha = (y_2^1 - y_1^1)/(x_2^1 - x_1^1)$ for the setting on Figure 6.6.1).

The equations (6.6.1) and (6.6.2) represent determinate system of 3 equations with 3 unknowns ($\bar{x}_I^1$, $\bar{y}_I^1$, $\bar{\xi}$). However, if we substitute (6.6.1) into (6.6.2) only one quadratic equations in $\bar{\xi}$ needs to be solved. The closed form solution for different cases can be

easily found, e.g. for the node $\bar{x}_1^1$ on Figure 6.6.1 it holds $\bar{\xi} = (b+\sqrt{b^2-4ac})/2a$; where

$$a = (y_1^1 - 2y_2^1 + y_3^1) - \alpha(x_1^1 - 2x_2^1 + x_3^1), \qquad\qquad b = (y_1^1 - y_3^1) - \alpha(x_1^1 - x_3^1) \qquad\qquad \text{and}$$

$$c = 2(y_2^1 - y_1^2) - 2\alpha(x_2^1 - x_1^2).$$

Once, all the $\bar{x}_I^1$ and $\bar{x}_I^2$ are known, segment element nodes can be determined as

$$x_I^s = (1-\beta)\, x_I^1 + \beta\, \bar{x}_I^2 \qquad\qquad\qquad\qquad (6.6.3)$$

or

$$x_I^s = (1-\beta)\, x_I^2 + \beta\, \bar{x}_I^1 \qquad\qquad\qquad\qquad (6.6.4)$$

where choice of $\beta \in [0,1]$ depends on relative stiffness of two contacting bodies.

The contact segment element is now completely determined by the choice of its three nodal points, and usual quadratic interpolation can be defined

$$\mathbf{x}^s = \sum_{I=1}^{3} N_I(\xi)\, \mathbf{x}_I^s \qquad\qquad\qquad\qquad (6.6.5)$$

which provides smooth contact between two bodies.

Further definition of kinematics, (normal and tangent, initial gap and current gap), follows exactly the development presented in section 6.5 for node-on-node contact element.

Remark 6.6.1 We defined kinematics for the contact segment with the quadratic displacement field, which is probably the highest order dictated by the efficiency of the computations. For the linear displacement field (2-noded segment element), considerations of Simo et al. [1984] can be used.

Reference configuration

Body B $_1$

t_0 - initial asperities height
t - height of compressed asperities
u_n - approach
$\triangle$ - relative normal displacement
g - initial gap
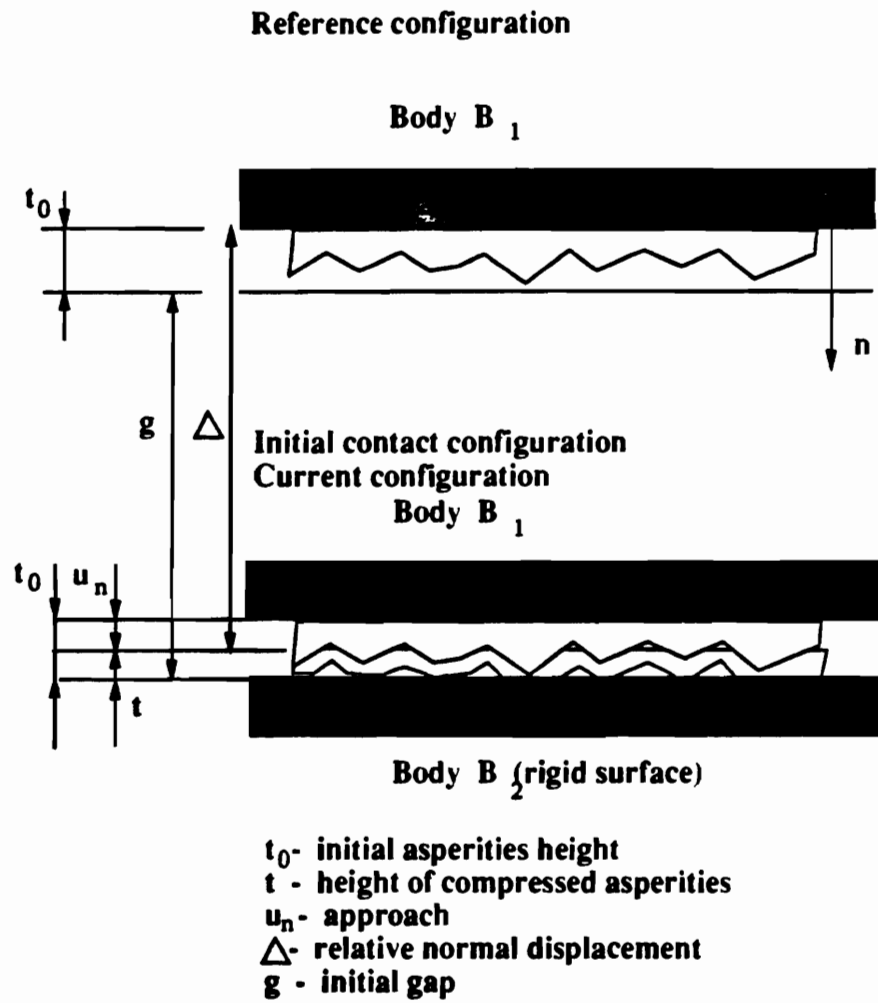
Figure 6.1.1 - Initial gap, normal displacement and penetrating approach

contact boundary
Γ_c^2

Γ_u

body Ω_2

Γ_c

Γ_u

body Ω_1

x_3

x_2

x_1

Rigid Foundation

contact boundary Γ_c^1
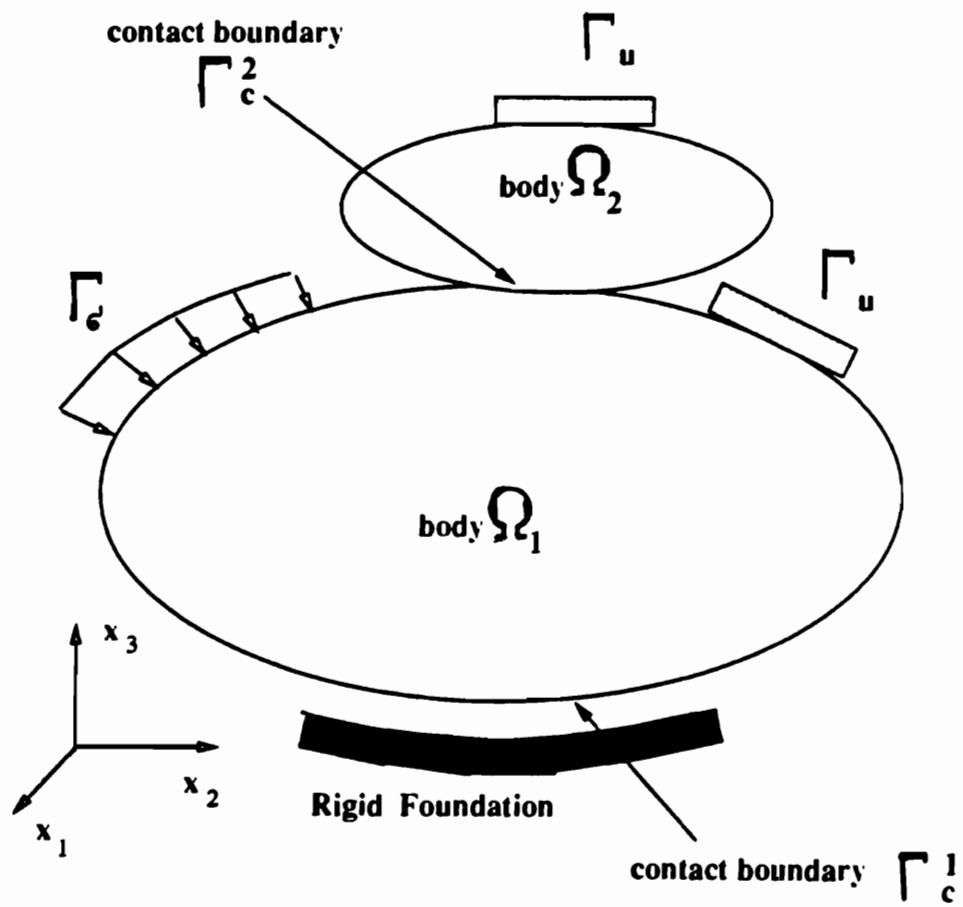
Figure 6.1.2 - Geometry of elastic bodies in contact

Friction functional $j(x)$

$j(x) = |x|$

Regularized friction
functional $z(x)$

$$z(x) = \begin{cases} x^2(3\,eps - |x|)/3\,eps^2 & \text{if } |x| < eps \\ (3|x| - eps)/3 & \text{if } |x| > eps \end{cases}$$

$j(x)$
$z(x)$

$j(x)$

$z(x)$

- eps   0|0   eps

Relative velocity x
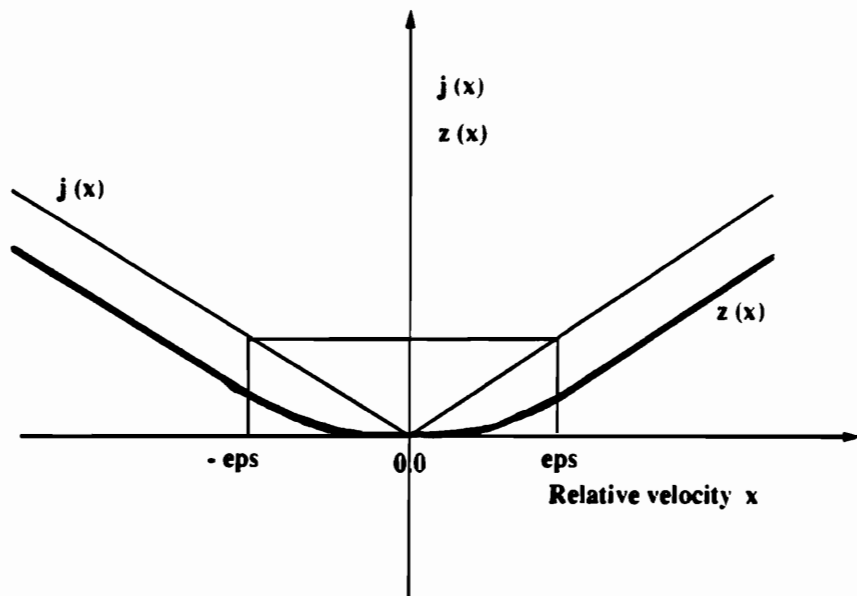
**Figure 6.2.1 - Regularization of friction functional
(Oden&Martins [1985])**

Derivative of regularized friction functional y (x)

$$y (x) = \begin{cases} x (2 \, eps - |x|) / eps & \text{if } |x| < eps \\ sgn (x) & \text{if } |x| > eps \end{cases}$$
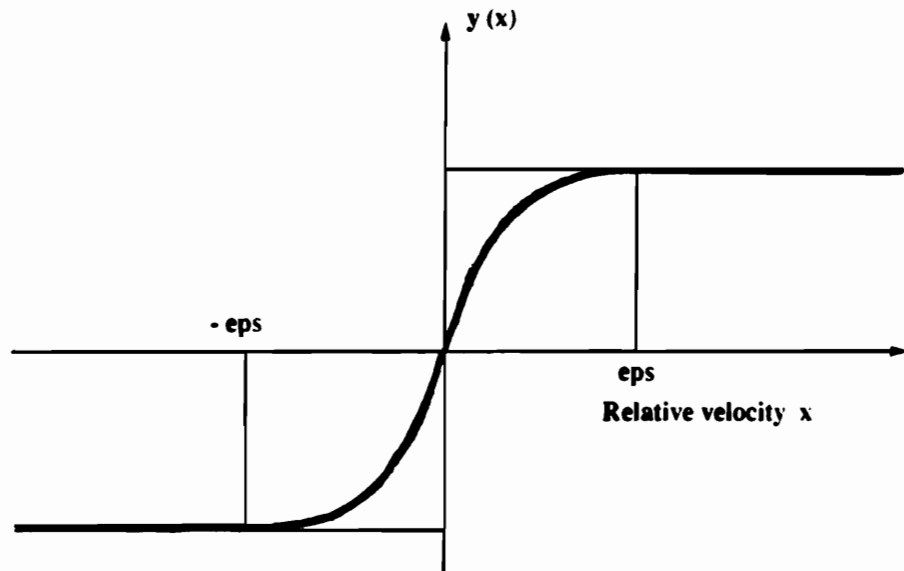
**Figure 6.2.2 - Derivative of regularized friction functional
(regularized friction stress)**
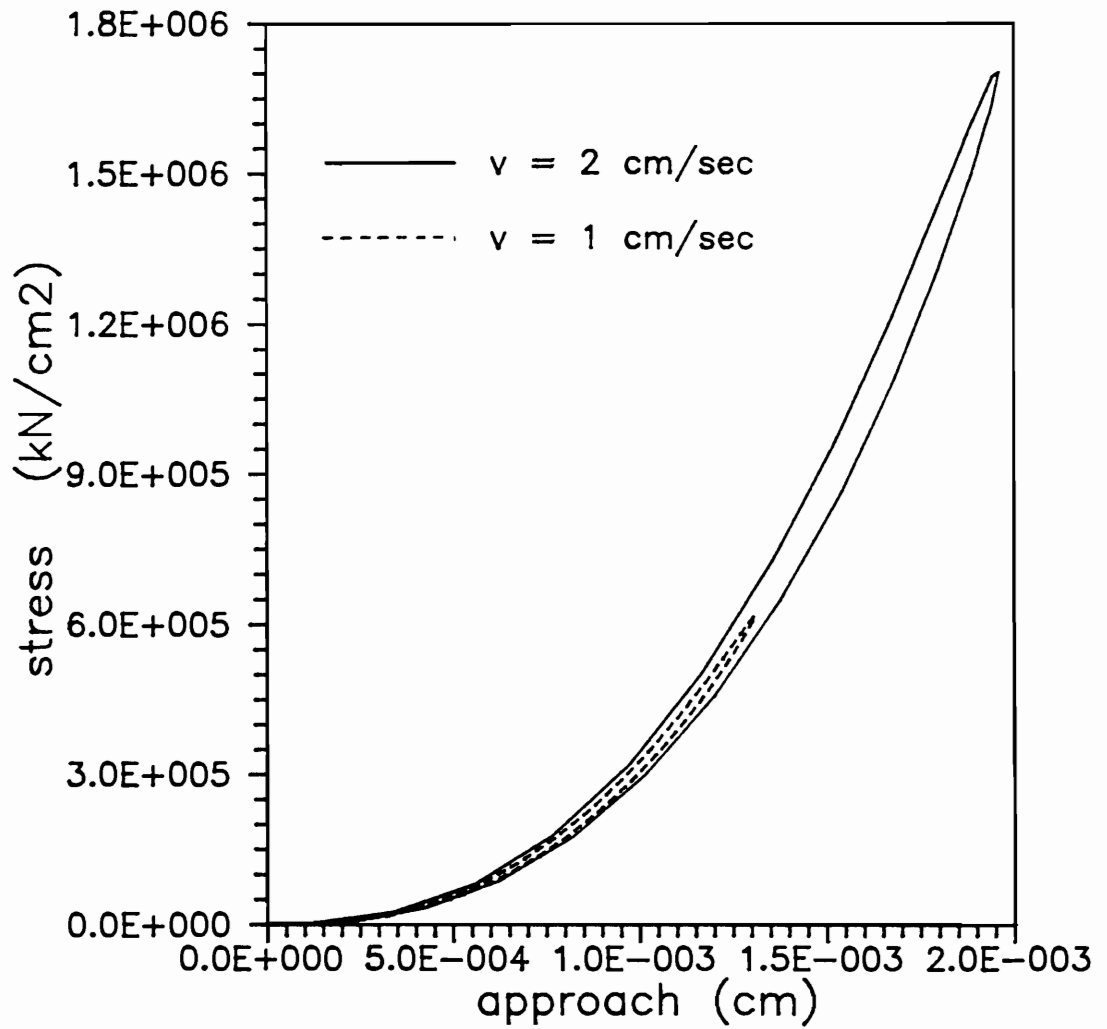
Figure 6.3.1 - Hysteresis loops of normal stress

(i) - elastic trial

(ii) - plastic corrector
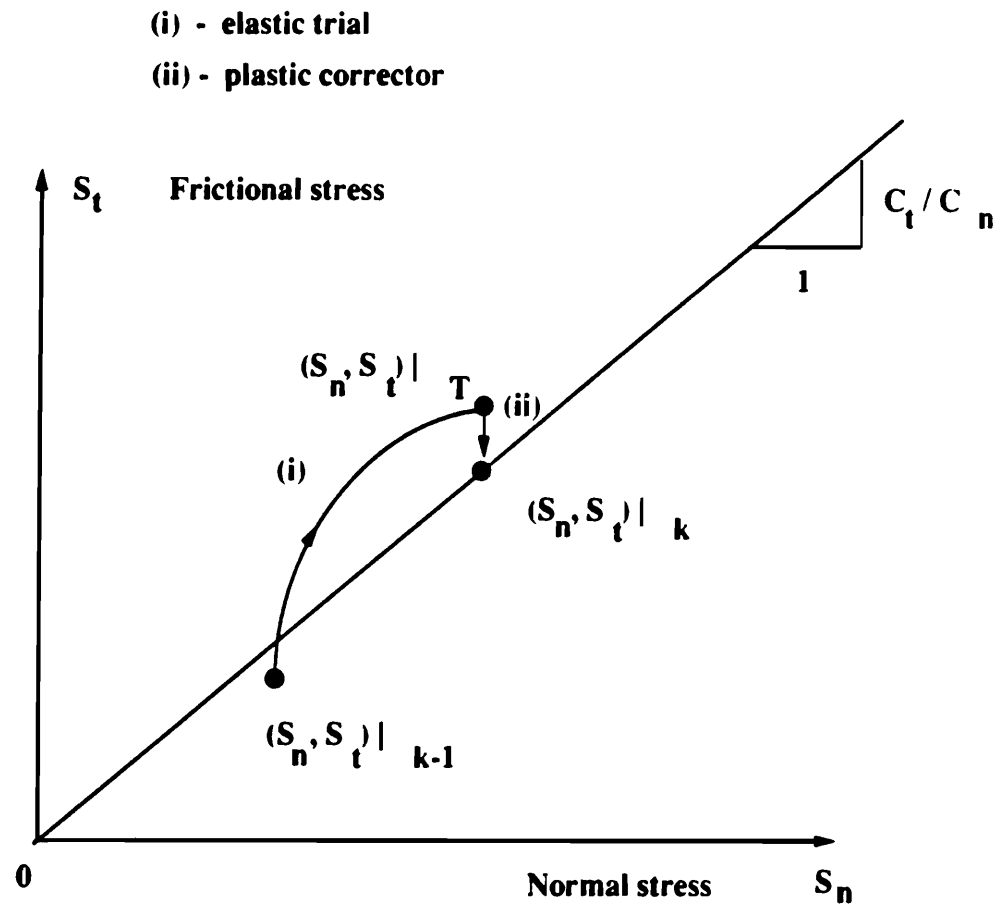
Figure 6.4.1 - Return mapping algorithm for integrating
regularized friction constitutive equations
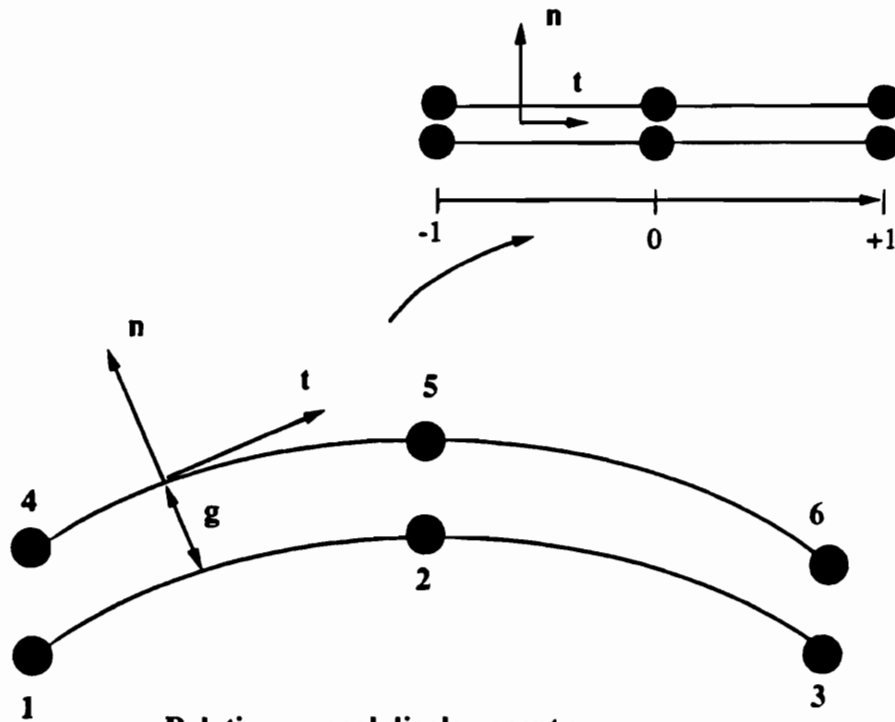
Relative normal displacement :

$$u_n = (u_i - u_j) @ n - g$$

$$i - 1, 2, 3$$

$$j - 4, 5, 6$$

n - normal vector
t - tangent vector
g - initial gap

Figure 6.5.1 - 6-noded isoparametric contact element
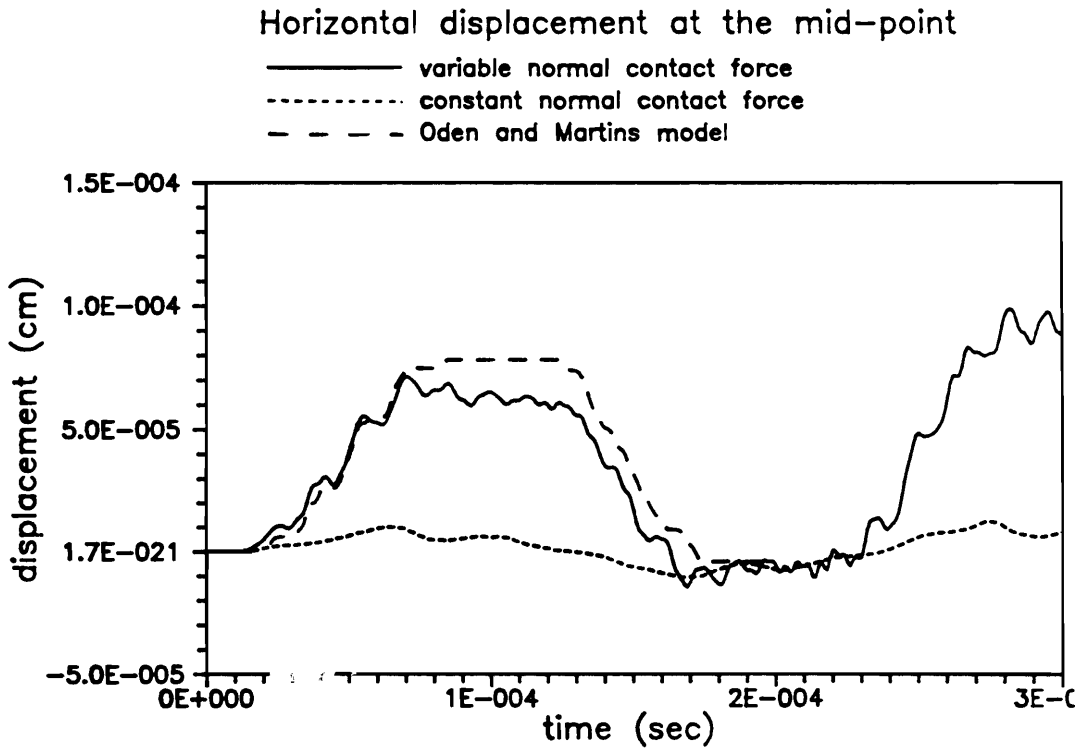
finite element mesh

PCFEAP

boundary conditions

PCFEAP
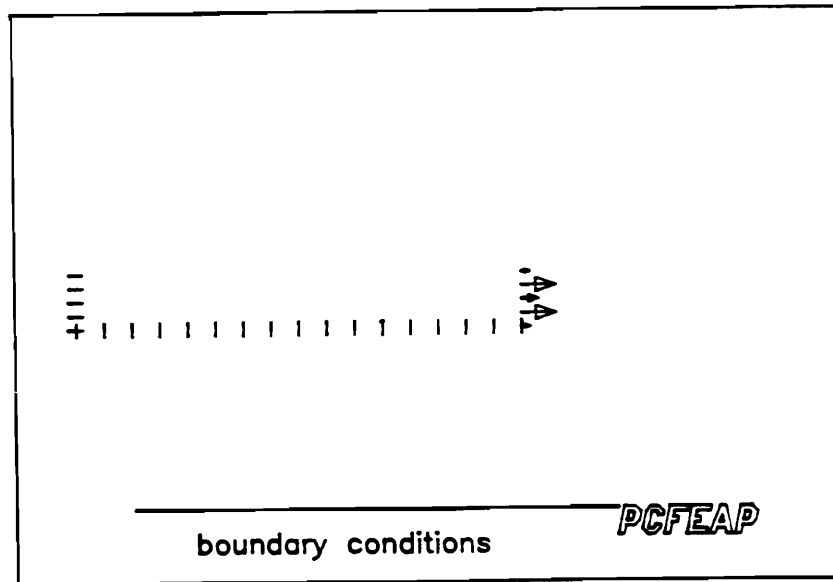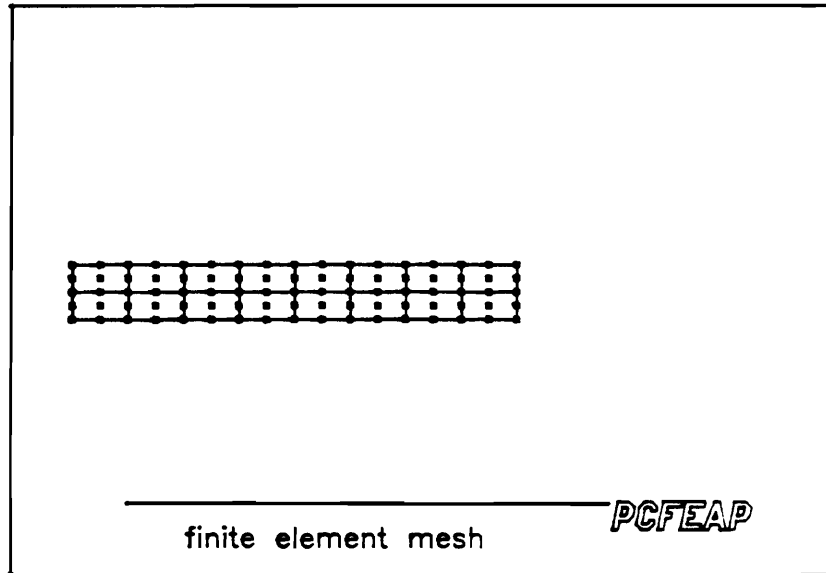
Figure 6.5.2 - Finite element model of elastic slab

Horizontal displacement at the free end

————————— variable normal contact force
·········· constant normal contact force
— — — — Oden and Martins model

Horizontal displacement at the mid—point

————————— variable normal contact force
·········· constant normal contact force
— — — — Oden and Martins model
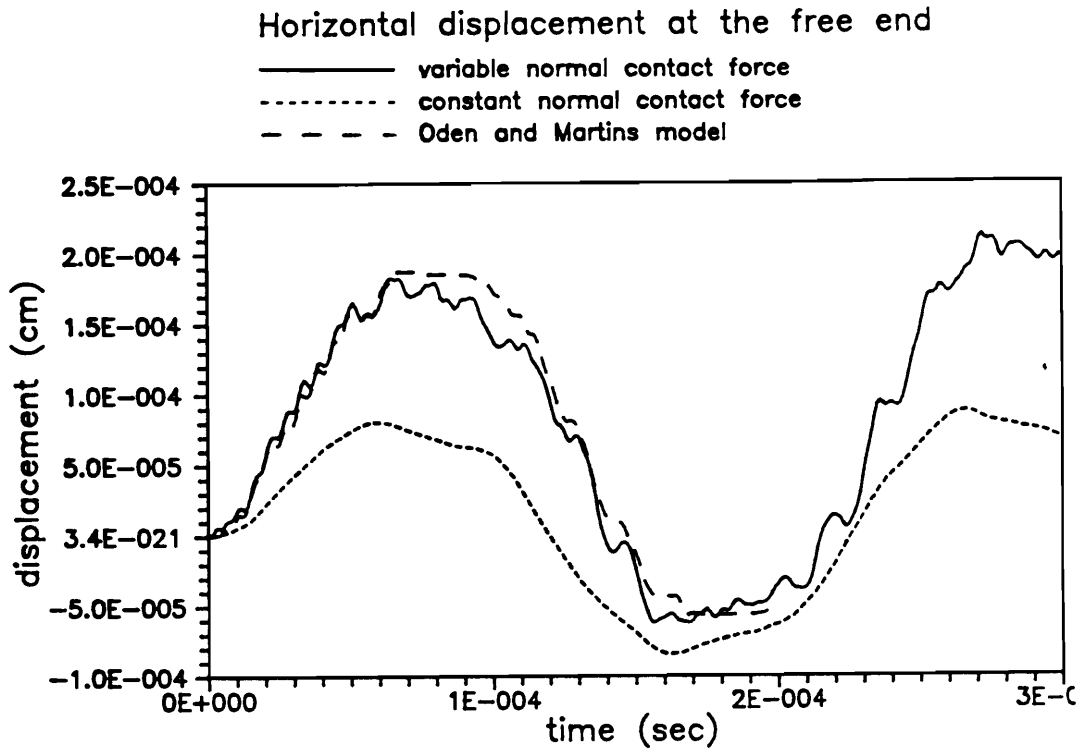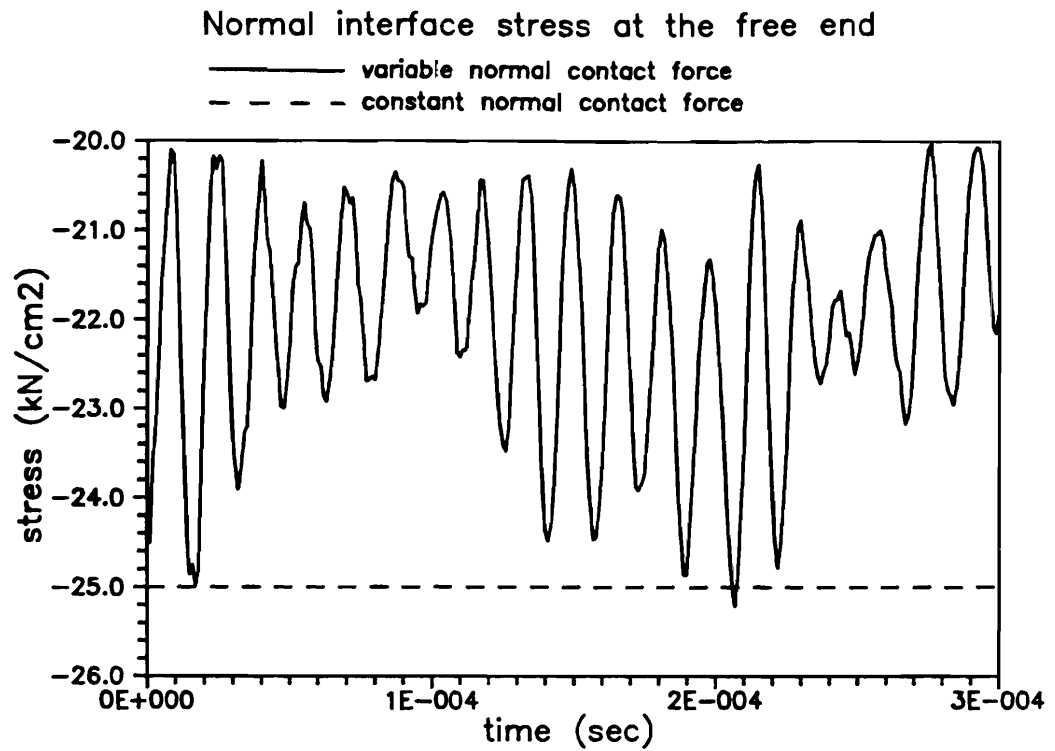

Figure 6.5.3 - Horizontal displacement at free end and mid-point

Normal interface stress at the free end

——————— variable normal contact force

— — — — constant normal contact force

Tangential friction stress at the free end

——————— variable normal contact force

·········· constant normal contact force
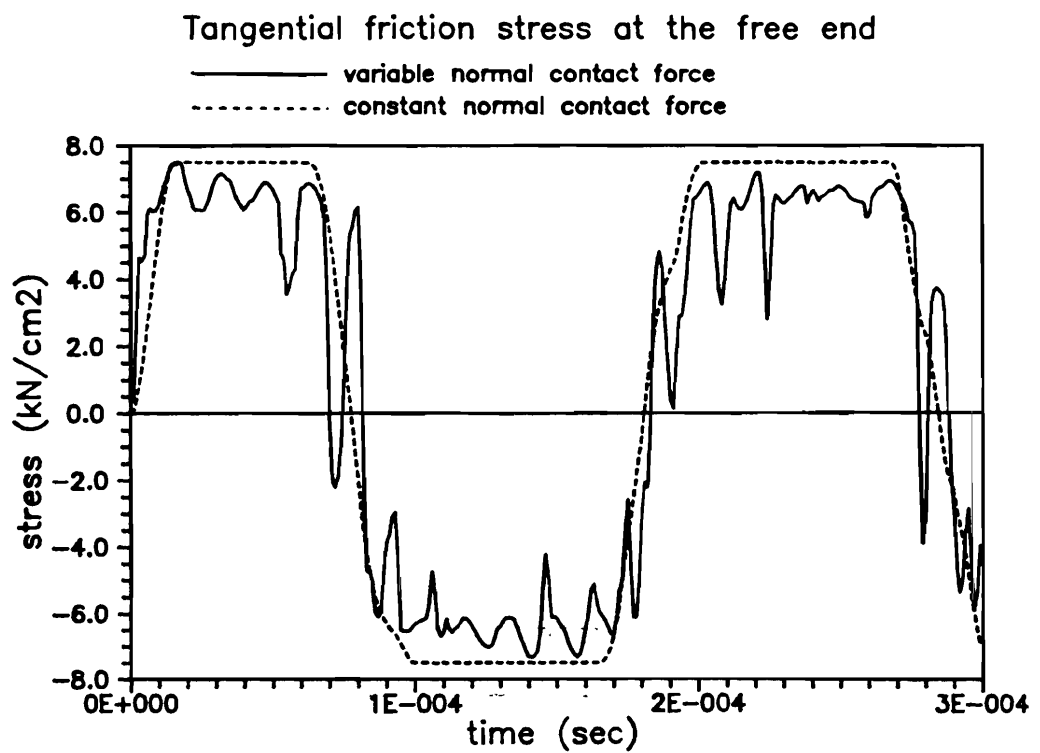
Figure 6.5.4 - Normal and tangential stress at the free end

Normal contact stress along the length
——————— at time t = 0.00005 sec
——————— at time t = 0.0001 sec
················· at time t = 0.00015 sec
— — — — at time t = 0.0002 sec

Tangential friction stress along the length
(variable normal force)
——————— at time t = 0.00005 sec
——————— at time t = 0.0001 sec
················· at time t = 0.00015 sec
— — — — at time t = 0.0002 sec

Tangential friction stress along the length
(constant normal force)
——————— at time t = 0.00005 sec
——————— at time t = 0.0001 sec
················· at time t = 0.00015 sec
— — — — at time t = 0.0002 sec

**Figure 6.5.5 - Distribution of normal and tangential interface
stress along the contact boundary**
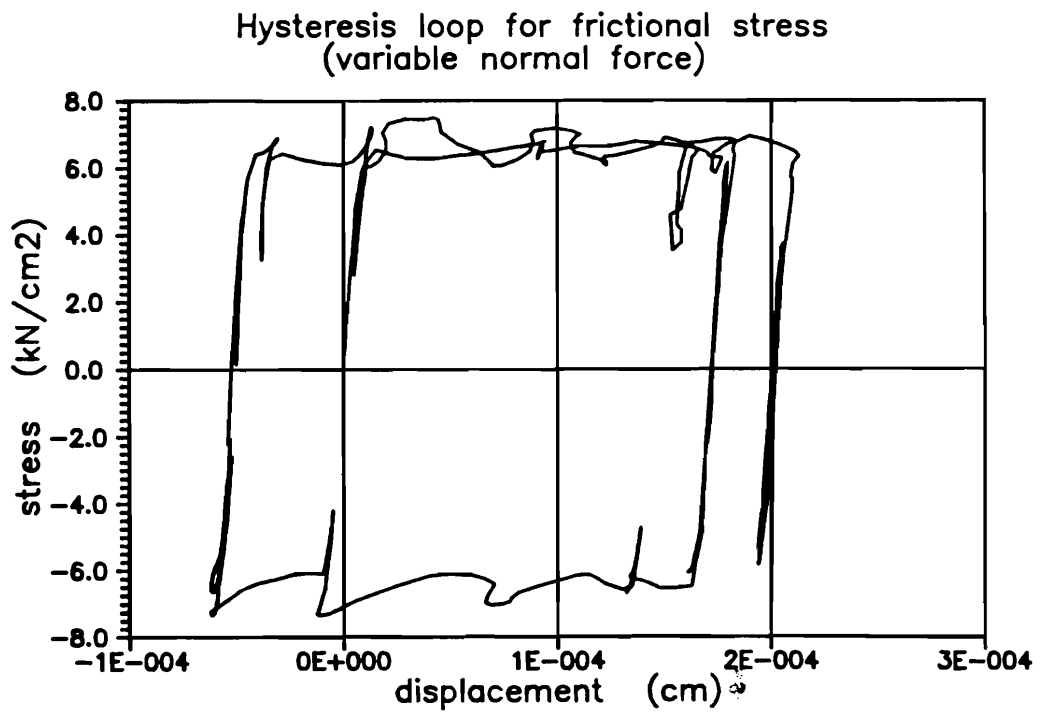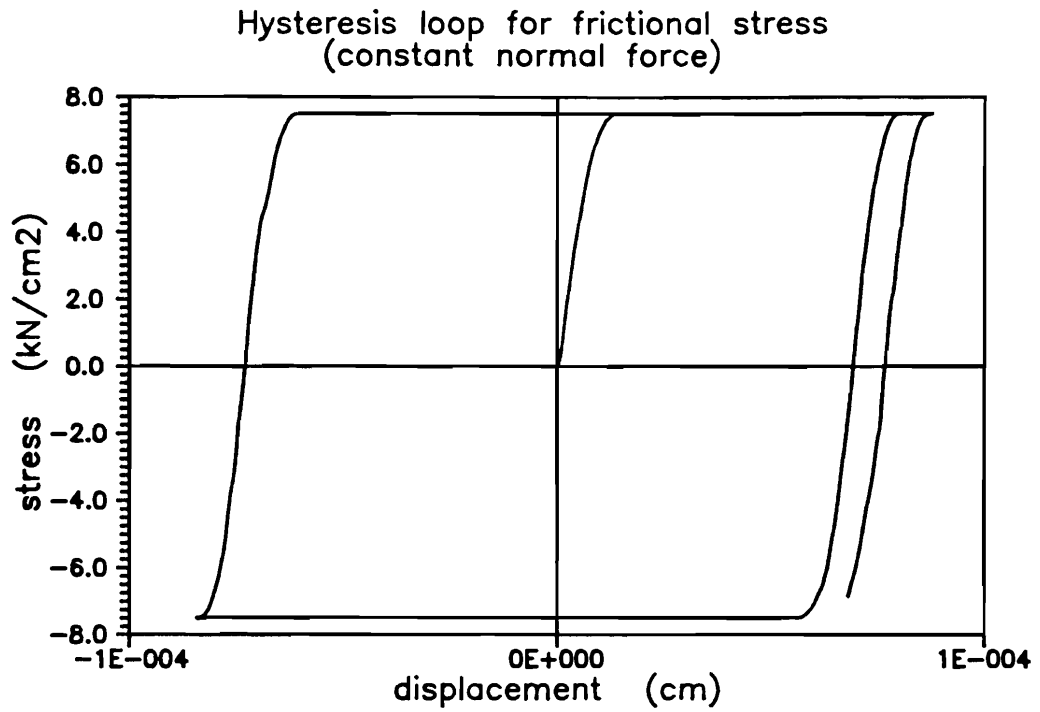
Figure 6.5.6 - Hysteresis loops of frictional stress for
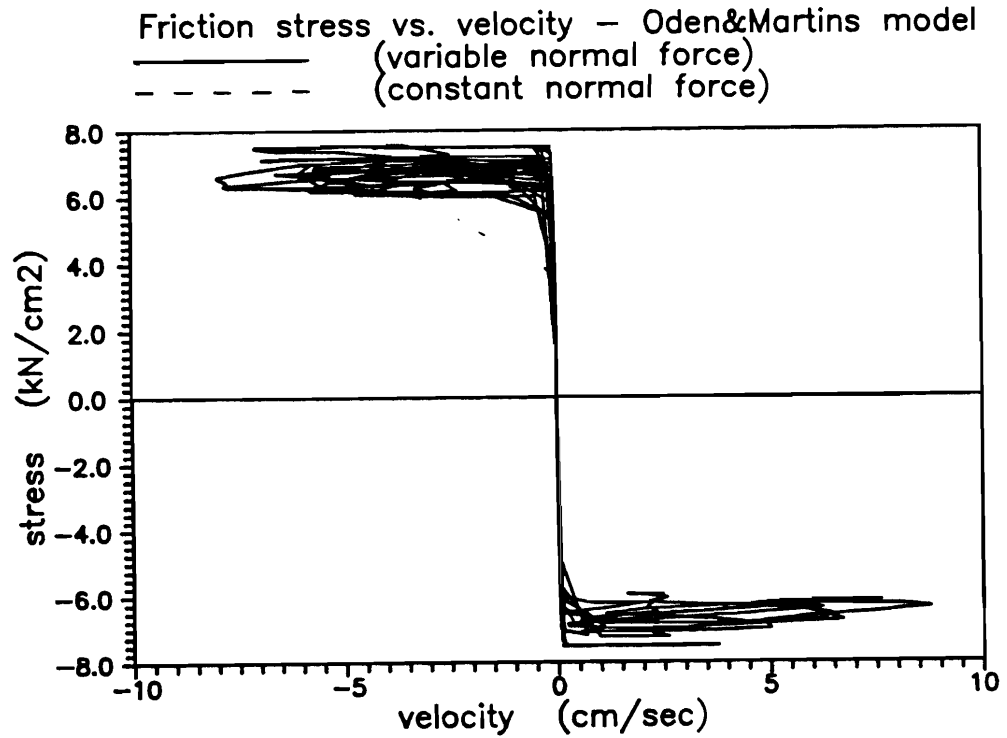constant and variable normal contact force

Friction stress vs. displac. — Oden&Martins model
——————————— (variable normal force)
— — — — — (constant normal force)

Friction stress vs. velocity — Oden&Martins model
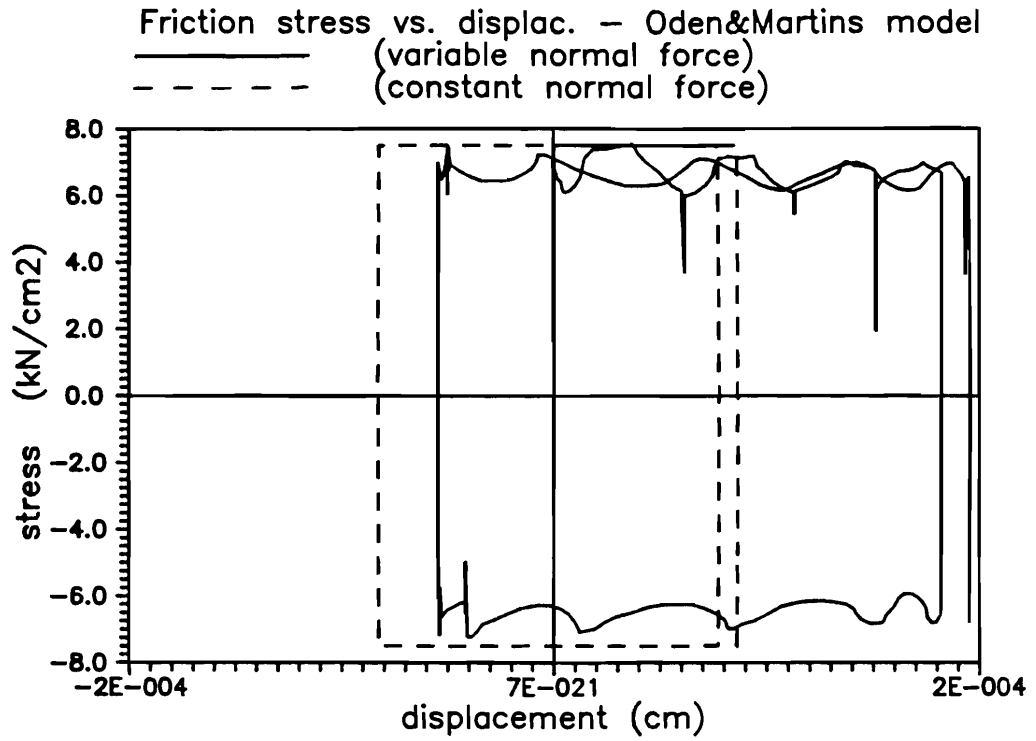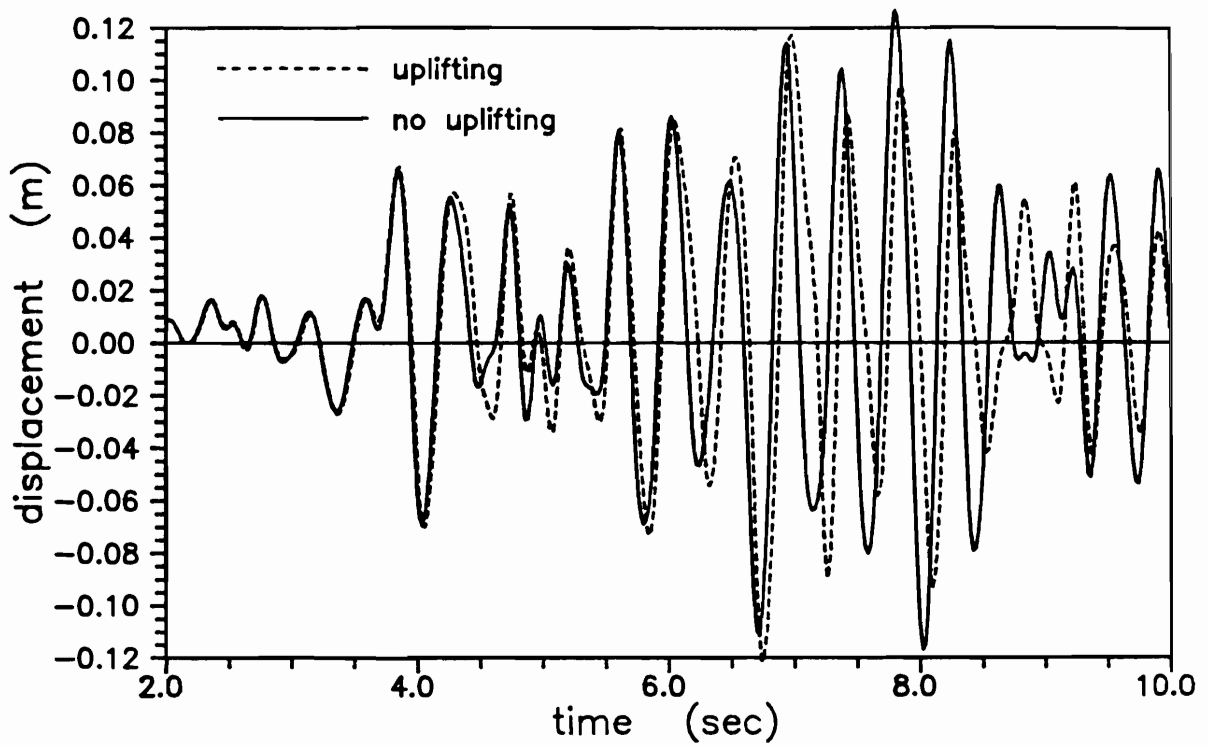——————————— (variable normal force)
— — — — — (constant normal force)

Figure 6.5.7 - Hysteresys loops of frictional stress for Oden&Martins model

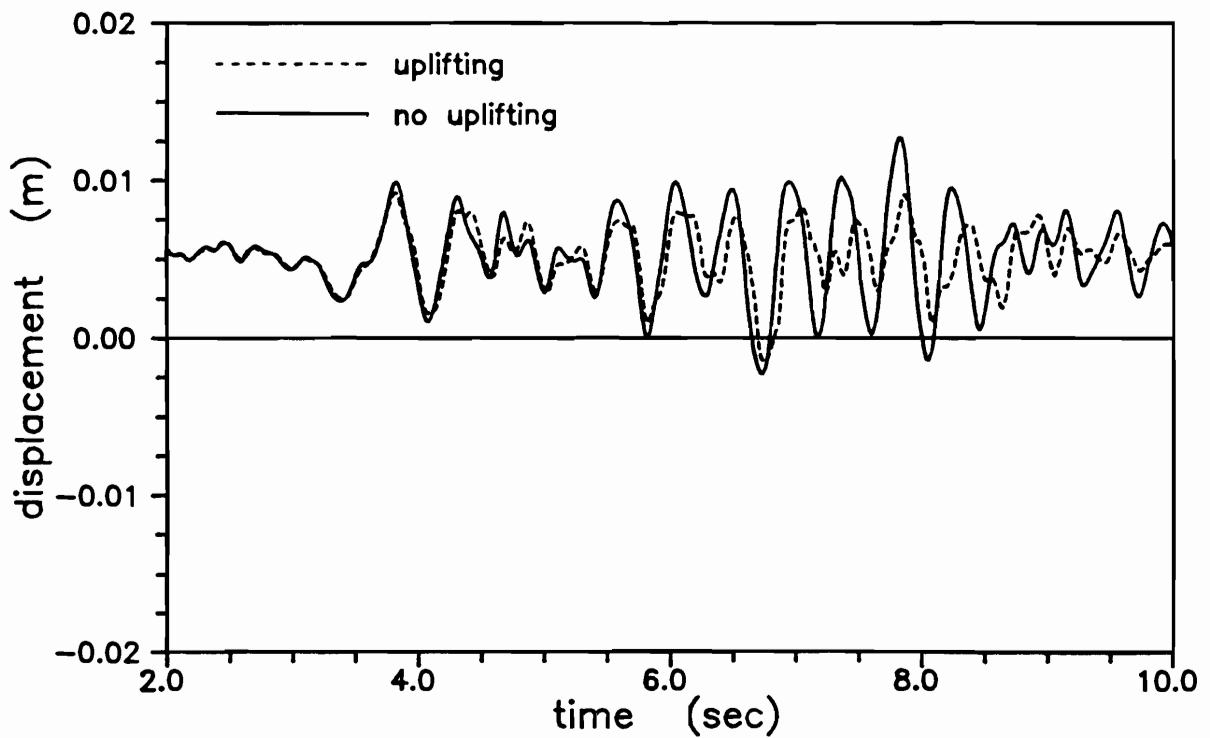## Horizontal displacement at dam tip

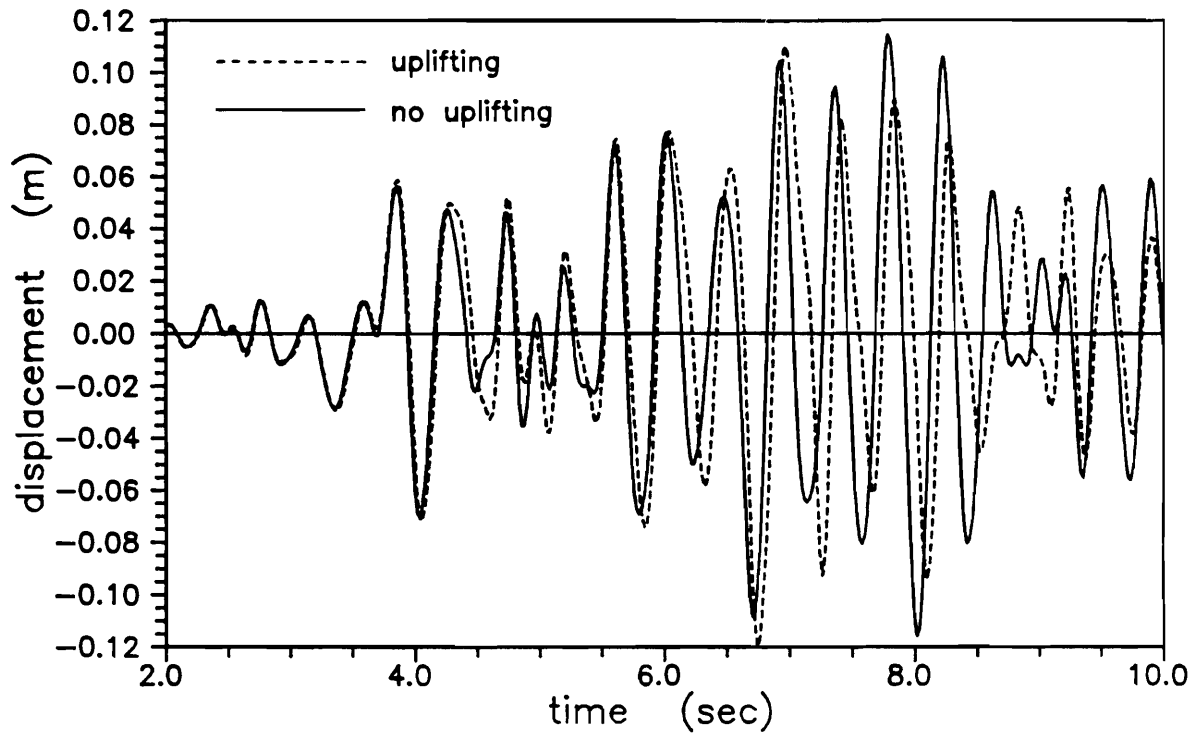## Horizontal displacement at dam bottom

Figure 6.5.8 - Horizontal displacements at dam tip and dam bottom

Difference in horizontal displacement — top vs. bottom
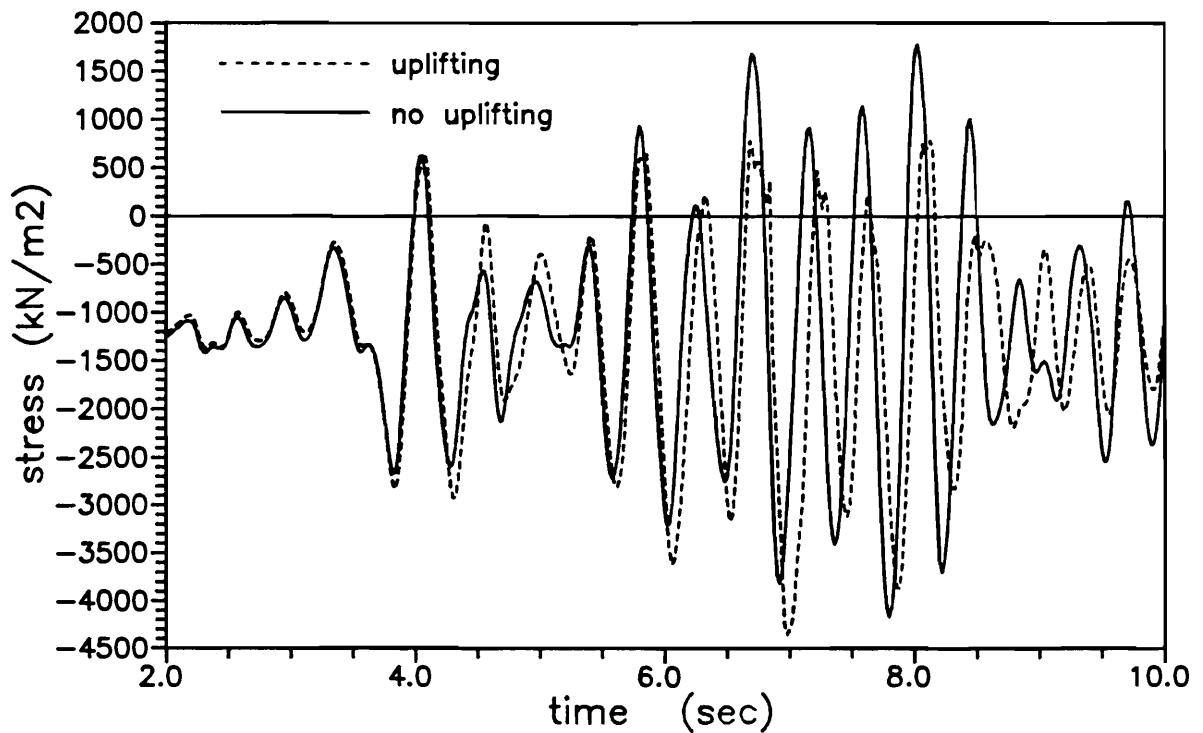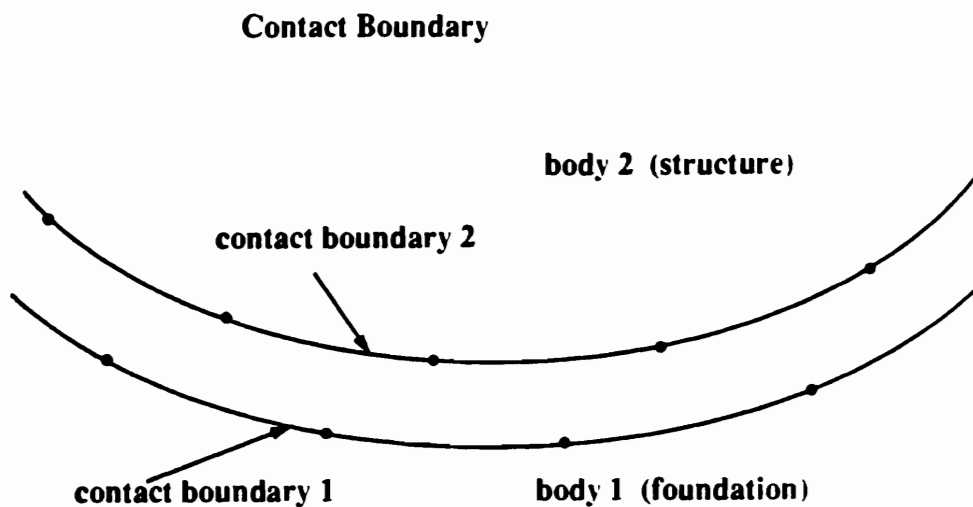

Vertical stress at dam bottom (at node 141)

Figure 6.5.9 - Difference in horizontal displacement - top vs. bottom and vertical stress at dam bottom

Contact Boundary

body 2 (structure)

contact boundary 2

contact boundary 1   body 1 (foundation)

Typical segment element

○ projected nodes
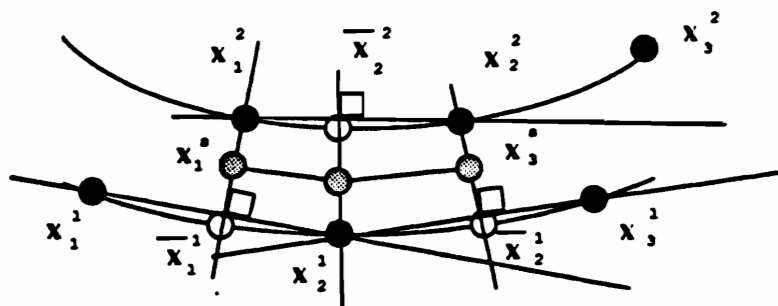
● body nodes

◉ segment el. nodes

Figure 6.6.1 - Segment contact element - planar case

Chapter 7
Closure

The consistently reduced model for the dynamic analysis of large linear system with local nonlinearities provides the rational approach to the earthquake-resistant design of structure-foundation systems. In addition, the efficiency of the method gives a solid basis to place the design procedure into the context of random vibrations theory, which accounts properly for the stochastic nature of earthquake excitation. However, more experimental results (along the directions pointed by Huckelbridge&Clough [1977]) should be obtained for verification of both deterministic and stochastic computational model.

Beside the non-deterministic nature of excitation, one should also consider the different probability distributions of contact asperities to devise stochastic constitutive model for the frictional contact, whose deterministic model is presented in this work. Some work in this area is already initiated by Oden&Pires [1984] for quasi-static contact problem. Any computation in non-deterministic framework requires enormous effort. For that reason only oversimplified models are mostly studied. However, based on the efficiency of here presented formulation, the extension of stochastic dynamic analysis to more elaborate models seems feasible.

Motivated by the remarkable convergence properties of the approximate solution obtained within reduced Ritz vector subspace and the low computational cost of load dependent vector algorithm used for its generation, one is tempted to expand the same concepts to fully nonlinear problems. Projection subspace in that case would change form step to step. However, an efficient update procedure could be devised, which carry over the information form the previous steps to the current time. Some work in this area is initiated in the

context of static problems with the nonlinear kinematics (see Noor&Peters [1980]), utilizing the notion of path derivative to provide the update of the projection subspace.

Within the proposed framework for dynamic analysis of large linear structure-foundation system with local nonlinearities, a different nonlinearity source other than the dynamic frictional contact can be addressed. In particular, the performance of some of the base isolation devices could be examined within the proposed framework.

References

Agnostopoulos S. A. [1982], Wave and Earthquake Response of Offshore Structure : Evaluation of Modal Solution, ASCE J. Sruct. Div. 108, 2175-2191

Bathe K. J. and E. L. Wilson [1976], Numerical Methods in Finite Element Analysis, Prentice-Hall

Bathe K. J. and S. Gracewski [1981], On Nonlinear Dynamic Analysis Using Substructuring and Mode Superposition, Comput. Struct., 13, 699-707

Bayo E. P. and E.L. Wilson [1984], Finite Element and Ritz Vector Technique for the Solution to Three-Dimensional Soil-Structure Interaction Problem in the Time Domain, Eng. Comput., 1, 311-324

Belytschko T. and T.J.R. Hughes [1983], Computational Methods for Transient Analysis, Elsevier Science Publisher

Bielak J. and P. Cristiano [1984], Effective Seismic Input for Nonlinear Soil-Structure Interaction Systems, Earthq. Engng. Struct. Dynam., 12, 107-121

Borino G. and G. Muscolino [1986], Mode-Superposition Methods in Dynamic Analysis of Classically and Non-Classically Damped Linear Systems, Earthq. Engng. Struct. Dynam., 14, 705-718

Brebbia C. [1978], The Boundary Element Method for Engineers, John Wiley

Burdekin M., A. Cowley and N. Back [1978], Experimental Study of Normal and Shear Characteristics of Machined Surfaces in Contact, J. Mech. Engng. Sci., 20, 129-132

Carey G.F. and J.T. Oden [1983], Finite Elements : A Second Course, Prentice-Hall

Caughey T. K. [1960], Classical Normal Modes in Damped Linear Dynamic Systems, J. Appl. Mech., 27, 269-271

Chadwick P. [1976], Continuum Mechanics, John Wiley

Chakrabarti P. and Chopra A. K. [1973], Earthquake Analysis of Gravity dams Including Hydrodynamic Interaction, Earthq. Engng. Struct. Dynam., 2, 143-160

Chen H. C. and Taylor R. L. [1988], Solution of Viscously Damped Linear Systems Using a Set of Load-Dependent Vectors, Report no. UCB/SEMM 88/16, UC Berkeley

Chew Y. K. [1985], Accuracy of Consistent and Lumped Viscous Dampers in Wave Propagation Problems, Int. J. Numer. Methods Eng., 52, 721-732

Chorin A., T.J.R. Hughes, M.F.McCracken and J.E. Marsden [1978], Product Formulas and Numerical Algorithms, Commun. Pure Appl. Math., 31, 205-256

Claret A.M. and F.V. Filho, Modal Superposition-Pseudo-Force Method for Dynamic Analysis with Non-Proportional Damping, Earthq. Engng. Struct. Dynam., to appear

Clough R.W. and J. Penzien [1975], Dynamics of Structures, McGraw-Hill

Clough R. W., and S. Mojtahedi [1976], Earthquake Response Analysis Considering Non-Proportional Damping, Earthq. Engng. Struct. Dynam. 4, 489-496

Clough R.W. and E. L. Wilson [1979], Dynamics Analysis of Large Structural Systems With Local Nonlinearities', Comp. Methods Appl. Mech. Eng., 18, 107-129

Clough R.W., K.T. Chang, H.Q. Chen, R.M. Stephen, G.L. Wang and Y. Ghanaat [1984], Dynamic Response Behavior of Xiang Hong Dian Dam, Report no. EERC 84/02, UC Berkeley

Cohen M., and P.C. Jennings [1983], Silent Boundary Methods for Transient Analysis, in 'Computational Methods for Transient Analysis' ed. T. Belytschko, T. J. R. Hughes, 302-360

Cornwell R.E., R. R. jr Craig and C. P. Johnson [1983], On the Application of the Mode-Acceleration Method to Structural Engineering Problems', Earthq. Engng. Struct. Dynam., 11, 679-688

Craig R.R.jr [1981], Structural Dynamics : An Introduction to Computer Methods, John Wiley

Duff I.S., A.M.Erisman and J.K. Reid [1986], Direct Methods for Sparse Matrices, Oxford University Press

Duvaut G. and J.L. Lions [1976], Inequalities in Mechanics and Physics, Springer-Verlag

Enquist B. and A. Majda [1977], Absorbing Boundary Conditions for the Numerical Simulation of Waves, Math. Comput., 31, 629-651

Foss K.A. [1958], Coordinates Which Uncouple the Equations of Motion of Damped Linear Dynamic System, J. Appl. Mech., 25, 361-364

Frazer R.A., W.J. Duncan and A.R. Collar [1960], Elementary Matrices and Some Applications to Dynamics and Differential Equations, Cambridge University Press

Gears I. [1971], Initial Value Problem, Prentice-Hall

Goldsmith W. [1960], Impact, Edward Arnold

Guyan R.J. [1965], Reduction of Stiffness and Mass Matrices, AIAA J., 3, 380-383

Hallquist J.O., G.L. Goudreau and D.J. Benson [1985], Sliding Interface with Contact-Impact in Large-Scale Lagrangian Computations, Comp. Methods Appl. Mech. Eng., 51, 107-137

Hansten O.E. and K. Bell [1979], 'On the Accuracy of Mode Superposition Analysis in Structural Dynamics', Earthq. Engng. Struct. Dynam. 7, 405-411

Herrera I [1984], Boundary Methods : An Algebraic Theory, Pitman Advanced Publishing Program

Hill R. [1950], The Mathematical Theory of Plasticity, Oxford Eng. Science Series

Huckelbridge A.A. and R.W. Clough [1977], Seismic Response of Uplifting Building Frame, ASCE J. Struct. Div., 104, 1222-1229

Hudson D.E. [1979], 'Reading and Interpreting Strong Motion Accelerograms' Report Earthquake Engng. Res. Instit . California Inst. Tech.

Hughes T.J.R., R.L. Taylor, J.L. S. .an, A. Cournier and W. Kanoknukulchai [1976], A Finite Element Method for a Class of Contact-Impact Problems, Comp. Methods Appl. Mech. Eng., 8, 249-276

Hughes T.J.R. and K.S. Pister [1978], Consistent Linearization in Mechanics of Solids and Structures, Comput. Struct., 391-397

Hughes T.J.R. [1987], The Finite Element Method, McGraw-Hill

Hunt K.H. and F.R. Crossley [1975], Coefficient of Restitution Interpreted as Damping in Vibroimpact, J. Appl. Mech., 42, 440-445

Ibrahimbegovic A. [1988], Soil-Structure Interaction : A Method for Linear Analysis, Individual Research Report, Civil Eng./SEMM, UC Berkeley

Ibrahimbegovic A. and E.L. Wilson [1988], Simple Numerical Algorithms for the Mode Superposition Analysis of Discrete Linear Systems with Non-Proportional Damping, Comput. Struct., to appear

Igusa T. and A. DerKiureghian [1983], Response Spectrum Method for System with Non-Classical Damping, Proceedings ASCE EMD Specialty Conf. 'Recent Advances in Engineering Mechanics and Their Application on Civil Engineering', 380-384

Inman D.J. and A.N.J. Andry [1980], Some Results on the Nature of Eigenvalues of Discrete Damped Linear Systems, J. Appl. Mech., 47, 927-930

Ju J., R.L. Taylor and L.Y. Cheng [1987], A Consistent Finite Element Formulation of Numerical Frictional Contact Problems, Proceedings NUMETA 87

Klarbring A, A. Mikelic and M. Shillor [1988], Frictional Contact Problems With Normal Compliance, Int. J. Engng. Sci., 8, 811-832

Kreiss H.O. [1970], Initial Boundary Value Problem for Hyperbolic Systems, Commun. Pure Appl. Math., 23, 277-298

Lanczos C. [1950], An Iteration Method for the Solution of the Eigenvalue Problem of Linear Differential and Integral Operator', J. Res. Nat. Bur. Standards, 45, 255-282

Landers J. and R.L. Taylor [1985], An Augmented Lagrangian Formulation for the Finite Element Solution of Contact Problem, Report, no. UCB/SEMM 85/09, UC Berkeley

Leger P. and E. L. Wilson [1987], 'Generation of Load Dependent Ritz Transformation Vectors in Structural Dynamics', Eng. Comput., 4, 309-318

Lysmer J. and R.L. Kuhlemeyer [1969], Finite Dynamic Models for Infinite Media, ASCE J. Eng. Mech. Div., 95, 859-877

Lysmer J. [1978], Analytical Procedures in Soil Dynamics, Report no. UCB/EERC 78/29, UC Berkeley

Lin Y.K. [1967], 'Probabilistic Theory of Structural Dynamics', McGraw-Hill

Lions J.L. and E. Magenes [1972], Non-Homogeneous Boundary Value Problems and Applications, Springer-Verlag

Lotstedt P. [1984], Numerical Simulation of Time Dependent Contact and Friction Problems in Rigid Body Mechanics, SIAM J. Sci. Statist. Comput., 5, 370-393

Love A.E.H. [1944], A Treatise on the Mathematical Theory of Elasticity, Cambridge University Press

Lubliner J. [1989], Plasticity Theory, McMillan, to be published

Madox N.R. [1975], 'On the Number of Modes Necessary for Accurate Response and Resulting Forces in Dynamic Analysis', J. Appl. Mech., 42, 516-517

Martins J.A.C. and T.J. Oden [1987], Existence and Uniqueness Results for Dynamic Contact Problems With Nonlinear Normal and Friction Interface Laws, Nonlinear Anal.,

11, 407-428

Meek J.W. [1974], Effects of Foundation Tipping on Dynamic Response, ASCE J. Struct. Div. 101, 1297-1311

Meriam J.L. [1966], Dynamics, John Wiley

Michalowski R. and Z. Mroz [1978], Associated and Non-Associated Sliding Rules in Contact Friction Problems, Arch. Mech., 30, 259-276

Moreau J.J. [1974], On Unilateral Constraints, Frction and Plasticity, in New Variational Techniques in Math. Physics, ed. G. Capri and G. Stampachia

Mote C.D.jr. [1971], Global-local Finite Element, Comp. Methods Appl. Mech. Eng., 3, 565-574

Naghdi P.M. and J.A.Trapp [1975], The Significance of Formulating Plasticity Theory with Reference to Loading Surfaces in Strain Space, Int. J. Mech. Appl. Math., 28, 25-46

Noor. A.K. and J.M. Peters [1980], Reduced Basis Technique for Nonlinear Analysis of Structures, AIAA J., 18, 455-462

Nour-Omid B. and R.W. Clough [1984], Dynamic Analysis of Structures Using Lanczos Coordinates', Earthq. Engng. Struct. Dynam., 12, 565-577

Nour-Omid B. and R.W. Clough [1985], 'Block Lanczos Method for Dynamic Analysis of Structures', Earthq. Engng. Struct. Dynam., 13, 271-275

Nour-Omid B. and P. Wriggers [1986], A Two-Level Iteration Method for Solution of Contact Problem, Comp. Methods Appl. Mech. Eng., 54, 131-144

Oden J.T. and E.B. Pires [1984], Signorini Problem With Non-local Friction, in 'Numerical Methods in Coupled Systems' ed. R.W. Lewis et al., 217-229

Oden T.J. and J.A.C. Martins [1985], Models and Computational Methods for Dynamic Friction Phenomena, Comp. Methods Appl. Mech. Eng., 52, 527-634

Paige C.C. [1971], 'The Computation of Eigenvalues and Eigenvectors of Very Large Sparse Matrices', PhD thesis, University of London

Parlett B.N. [1980], 'The Symmetric Eigenvalue Problem', Prentice-Hall

Parlett B.N. [1982], 'Two Monitoring Schemes for the Lanczos Algorithm' in 'Computing Methods in Appl. Science and Eng.' ed. R.Glowinski and J.L.Lions, 27-34

Parlett B.N. and B. Nour-Omid [1985], 'The Use of a Refined Error Bound When Updating Eigenvalues of Tridiagonal', Linear Algebra Appl., 68, 179-219

Roesset J.M. and J.S. Kim [1987], Specification of Control Point for Embedded Foundations, Proceedings 5th Canadian Conf. Earthq. Engng., 63-86

Simo J. C., P. Wriggers and R.L. Taylor [1984], A Perturbed Lagrangian Formulation for the Finite Element Solution of Contact Prᵒᵇˡᵉm, Report, no. UCB/SEMM 84/14, UC Berkeley

Simo J.C. and R.L. Taylor [1985], Consistent Tangent Operators for Rate-Independent Elastoplasticity, Comp. Methods Appl. Mech. Eng., 48, 101-118

Simo J.C. and L. Vu Quoc [1985], A Novel Approach to the Dynamic of Flexible Beams Under Large Overall Motion : The Planar Case, Report no. UCB/ERL 85-63, UC Berkeley

Stakgold I. [1979], Green's Function and Boundary Value Problem, John Wiley

Taylor R.L. [1977] 'Computer Procedures for Finite Element Analysis ', in O. C. Zienkiewicz 'The Finite Element Method', chapter 24, 677-757

Taylor R.L. [1989], Analysis of Non-linear Problems in Inelasticity, ASME Engng. Mech. Div., to appear

Tolstoi D.M. [1967], Significance of the Normal Degree of Freedom and Natural Normal Vibrations in Contact Friction, Wear, 10, 199-213

Veletsos A.S. and C.E. Ventura [1986], Modal Analysis of Non-Classically Damped Linear Systems, Earthq. Engng. Struct. Dynam., 14, 217-243

Warburton G.B. and S.R. Soni [1977], Errors in Response Calculations for Non-Classically Damped Systems, Earthq. Engng. Struct. Dynam., 5, 365-376

Washizu K. [1982], Variational Methods in Elasticity and Plasticity, Pergamon Press

Wilson E.L., and J. Penzien [1972], Evaluation of Orthogonal Damping Matrices, Int. J. Numer. Methods Eng., 4, 5-10

Wilson E.L. [1975], Finite Elements for Foundations, Joints and Fluids, Int. Proceedings Symposium Numer. Meth. Soil Rock Mech., Karlruhe, West Germany

Wilson E.L. [1977], Numerical Methods for Dynamic Analysis', Proceedings Int. Symposium Numer. Meth. Offshore Engng., Swansea, Great Britain

Wilson E.L. [1980], SAP80 - Structural Analysis Program for Small or Large Computer Systems, Proc. CEPA Fall Conference

Wilson E.L., A. DerKiureghian and E.P. Bayo [1981], A Replacement for the SRSS Method in Seismic Analysis, Earthq. Engng. Struct. Dynam., 9, 187-194

Wilson E.L., M.W. Yuan and J.M. Dickens [1982], Dynamic Analysis by Direct Superposition of Ritz Vectors', Earthq. Engng. Struct. Dynam., 10, 813-821

Wilson E.L. and T. Itoh [1983], 'An Eigensolution Strategy for Large Systems', Comput. Struct., 16, 259-265

Wilson E.L. and E.P. Bayo [1986], 'Use of Special Ritz Vectors in Dynamic Substructure Analysis', ASCE J. Struct. Div., 112, 1944-1953

Wolf J.P. [1985], Dynamic Soil-Structure Interaction, Prentice-Hall

Wolf J.P. [1986], A Comparison of Time-Domain Transmitting Boundaries, Earthq. Engng. Struct. Dynam., 14, 655-673

Zienkiewicz O.C., P. Bettes, T.C. Chiam and C. Eruson [1986], Numerical Methods for Unbounded Field Problems and a New Infinite Element Formulation, in 'Computational Methods for Infinite Domain Media-Structure Interaction' AMD ,vol.46